letnik/volume **53** - št./no. **5/07** - str./pp. **269 - 352**
Ljubljana, maj/May 2007, zvezek/issue **505**

STROJNIŠKI VESTNIK

JOURNAL OF MECHANICAL ENGINEERING

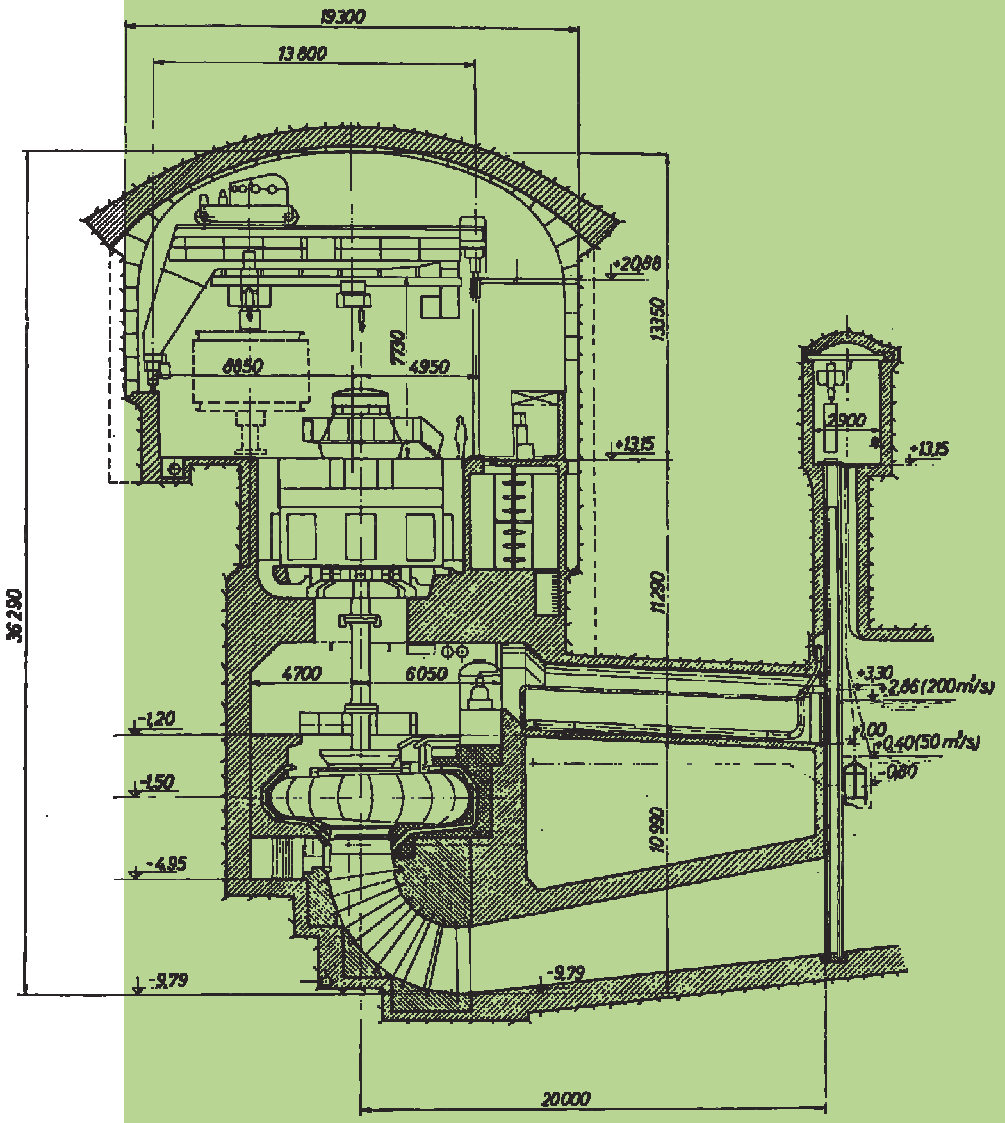

cena 3,34 EUR

9 770039 248001

ISSN 0039-2480

Vsebina - Contents

Strojniški vestnik - Journal of Mechanical Engineering
letnik - volume 53, (2007), številka - number 5
Ljubljana, maj - May 2007
ISSN 0039-2480

Izhaja mesečno - Published monthly

Strojniški vestnik - Journal of Mechanical Engineering 53(2007)5, 270-284
UDK - UDC 536.7:66.045.5:621.311.22
Izvirni znanstveni članek - Original scientific paper (1.01)

Izboljšanje termodinamičnih lastnosti hladilnih stolpov na naravni vlek

Improvement of the Thermodynamic Properties in a Natural-Draft Cooling Tower

Brane Širok - Maja Rotar - Marko Hočevar - Matevž Dular - Jure Smrekar - Tom Bajcar
(Fakulteta za strojništvo, Ljubljana)

Z uporabo metode CTP (Cooling Tower Profiler) v hladilnem stolpu na naravni vlek elektrarne Doel-3 (Belgija) smo določili hitrostna in temperaturna polja zraka nad izločevalniki kapljic. Meritve so pokazale, da so na obodu prečnega prereza stolpa področja z velikimi hitrostmi in nizkimi temperaturami zraka, kar ima za posledico manjšo učinkovitost v prenosu toplote in snovi. Postavljene pojavne povezave omogočajo rešitev problema s spremembo višine polnila in prerazporeditvijo masnega toka vode. Vpliv omenjenih parametrov smo preverili s simulacijo. Narejena je bila trirazsežna numerična simulacija enofaznega turbulentnega toka zraka. Lokalne izmerjene vrednosti hitrosti in temperature zraka so bile v model vključene prek izvirnih členov. Rezultati prikazujejo analizo vpliva lokalnih nepravilnosti na skupno značilko hladilnega stolpa. Predstavljeni so rezultati meritev, simulacija hitrostnega in temperaturnega polja po prerezu stolpa. Podani so ukrepi za odpravo nepravilnosti v delovanju stolpa, ki vključujejo povečanje višine polnil na obodu stolpa in ustrezno prerazporeditev celotnega masnega pretoka vode po prerezu stolpa. V numeričnem modelu smo ti dve spremenljivki opisali z lokalno spremembo izvirnih členov, kar vodi k ustreznejši porazdelitvi aerotermodinamičnih značilk in posledično k večji učinkovitosti hladilnega stolpa.

Na primeru izbranega hladilnega stolpa Doel-3 je v prispevku predstavljena celovita diagnostična metoda lokalnih anomalij, ki temelji na eksperimentalnem in numeričnem modeliranju prenosnih pojavov v hladilnem stolpu. Opisana metoda omogoča povečevanje učinkovitosti delovanja hladilnih stolpov. Izračunana povprečna gostota toplotnega toka se je v tem dejanskem primeru povečala za 2,8 odstotka.

(Ključne besede: hladilni stolpi, naravni vlek, termodinamične lastnosti, numerične analize)

The velocity and temperature fields above droplet eliminators inside a natural-draft cooling tower of the Doel-3 powerplant (Belgium) were determined using the CTP (Cooling Tower Profiler) method. The measurements show regions of high velocities and low temperatures of air at the cooling tower circumference, leading to locally impaired heat and mass transfer. The established phenomenological relations enable the solution of this problem, which can be achieved by a variation of the fill height and the water mass-flow rate. The influence of these two parameters was analysed numerically. A 3D numerical simulation of a single-phase turbulent airflow was performed. Local values of the air velocity and air temperature were included in the numerical model through source terms. The numerical results present the analysis of local irregularities and their influence on the overall cooling-tower characteristics. Experimental and numerical results for the velocity and temperature fields in a cooling tower's transverse section are presented, followed by a procedure for reducing irregularities in the cooling tower's operation. This procedure includes the increase of the fill height and the rearrangement of the local cooling-water mass-flow rate in the cooling tower's transverse section. In the numerical model these two parameters were modelled by a local modification of the source terms. Modified source terms of the model lead to more uniform aero-thermodynamic properties in the tower and consequently to a higher cooling-tower efficiency.

The paper presents a complete diagnostic method of local anomalies, based on the case of a representative Doel-3 cooling tower. The method is based on experimental and numerical modelling of the transport phenomena inside the cooling tower. It makes it possible to increase the efficiency of the cooling tower's operation. The calculated mean heat-flux density was increased by 2.8% in this particular case.

(Keywords: cooling towers, natural draft, thermodynamic properties, numerical analysis)

0 UVOD

V termoenergetskih sistemih se v kondenzatorju prenaša toplota iz parnega krožnega postopka na hladilno sredstvo. Le-ta je običajno voda, ki se jo lahko črpa iz reke ali jezera oz. se jo zaradi okoljevarstvenih razlogov neprekinjeno uporablja v zaprtih sistemih - ohlajevanje vode in njena ponovna uporaba. V tem primeru toplo vodo, ki zapušča kondenzator, hladimo v hladilnem stolpu. Ker delovanje hladilnega stolpa vpliva na temperaturo vode na vstopu v kondenzator, je njegov učinek bistvenega pomena za izkoristek celotnega sistema (delovanje kondenzatorja pri tem nižji temperaturi ima za posledico višji podtlak na parni strani, kar zagotavlja več pridobljenega dela iz turbine in večji izkoristek celotnega sistema).

Hladilni stolp na naravni vlek deluje na podlagi prenosa toplote in snovi med vodo in zrakom, ki sta v neposrednem stiku. Voda se hladi tako v področju polnil kakor tudi v področju prhe. V protitočnem hladilnem stolpu je opazen protitok med vodo in zrakom. Zrak vstopa na vznožju stolpa in teče skozi polnila ter področje prhe. Voda, ki teče v nasprotni smeri, se z uporabo šob razprši in steče v obliki plasti skozi polnila. Bistvenega pomena za učinkovit prenos toplote in snovi v hladilnem stolpu je velika stična površina med zrakom in vodo ter velik količnik prenosa toplote in snovi.

Prispevek prikazuje analizo delovanja hladilnega stolpa elektrarne Doel-3 z močjo 2040 MW. Možni problemi, ki se pojavljajo v hladilnih stolpih, so: omejen tlak prh, ki ga povzročajo odprti kanali, možnost prenapolnitve ob prehodnih pojavih – tveganje poškodbe polnil, poškodovanje polnil s peskom - zamašitev cevovodov in nalaganje nečistoč na polnilih, nerazprševanja hladilne vode zaradi odpadlih pršilnih glav, polomljene cevi in netesnosti razvodnih kanalov.

Opravljene so bile standardne meritve celostnih parametrov hladilnega stolpa [1] in tudi dodatne meritve temperature in hitrosti zračnega toka z metodo CTP [2] nad izločevalniki kapljic. Raziskava lokalnega delovanja hladilnega stolpa je bila osredotočena na lokalni prenos toplote in snovi ter na lokalne količnike izgub v polnilih. Hitrost zraka nad izločevalniki kaplic je odvisna od geometrijske oblike hladilnega stolpa (na primer

0 INTRODUCTION

In power-generation units (e.g., thermal and nuclear power plants) a circulating-water system supplies cooling water to a turbine condenser and thus acts as an instrument by which heat is extracted from the steam cycle to the environment. The turbine condenser is usually cooled with water from lakes or rivers, but often the use of cold, fresh water is limited for ecological reasons. Therefore, the continuous re-cooling and re-use of water in a closed system is necessary. In this case the warm water leaving the condenser is cooled in a cooling tower. The cooling tower's operation influences the water temperature at the condenser inlet, so its performance is vital for the efficiency of the entire system, because a condenser operating at the lowest temperature possible results in a higher sub-pressure on the steam side, which in turn makes possible a higher turbine work output and overall cycle efficiency.

The natural-draft cooling tower's operation is based on a principle whereby energy is removed from hot water in direct contact with relatively cool and dry air. The water is cooled in both the fill and rain regions. In a counterflow cooling tower a gaseous phase (air) flows upwards and a liquid phase (water), in variously sized droplets, falls downwards. The airflow enters the cooling tower at the bottom and flows through the fill and the rain regions. The water is sprayed through nozzles and flows as a film down the sheets of the fill. The key factors required for intensive heat and mass transfer in the cooling tower are a large air-to-water interface area and high heat- and mass-transfer coefficients.

In this study the operation of a Doel-3 (2040 MW) cooling tower was analysed. The problems that occur in the cooling tower are as follows: limited pressure of the sprayers caused by open channels, possible overflow during transients – risking fill damage and the fouling of fills by sand – clogging of the piping and deposit formation in fills, by-pass leaks due to lost end-caps, broken pipes, sprayers which have fallen off, and leaking baffles/distribution channels.

Accordingly, in order to establish the operation of a particular cooling tower's parts, standard integral measurements [1] as well as additional measurements of airflow temperature and velocity distribution above the droplet eliminators according to the CTP method [2] were performed. The investigation of the local operation of the cooling tower's parts was focused on a determination of locally transferred heat between the water and the air and the local value of the fill-loss coefficient. The air velocities above the drift eliminators depend on the cooling tower's geometry (e.g., the supporting walls, the water-distribution channels, etc.), on the local loss coefficient of the fill as well as on the difference between the air density inside and

sten, porazdelitvenih kanalov itn.), tlačnih izgub v polnilih ter od razlike gostot zraka v stolpu in okolici. Količnik izgub polnil je funkcija masnih tokov vode in zraka ter gostote in višine polnil. Lokalni količnik izgub je bil določen posredno iz padca statičnega tlaka in lokalne hitrosti nad izločevalniki kapljic. Temperatura zraka nad izločevalniki kapljic je odvisna od lokalnega prenosa toplote in snovi med vodo in zrakom. Lokalna vrednost prenesene toplote in snovi je bila izračunana iz masnega toka zraka in sprememb njegove temperature in vlažnosti.

Glede na izmerjeni hitrostni in temperaturni polji zraka smo podali nekatere predloge za spremembe, ki bi se kazale v učinkovitejšem prenosu toplote in snovi med zrakom in vodo. Spremembe bi bilo mogoče doseči z zmanjšanjem tlačnih izgub v polnilih in z ustreznejšo porazdelitvijo vode po prerezu stolpa. Vpliv teh sprememb na lastnosti toka zraka je predmet tega prispevka.

1 PRENOS TOPLOTE IN SNOVI V HLADILNEM STOLPU

Prenos toplote in snovi v določenem delu hladilnega stolpa je v veliki meri odvisen od lokalnih masnih tokov vode in zraka. Predstavljeni so osnovni modeli prenosa toplote in snovi v opazovanem sistemu, dobljene zakonitosti pa so vključene v enofazni trirazsežni model turbulentnega toka zraka skozi hladilni stolp na naravni vlek.

Postopek hlajenja vode se odvija v območju pršil in polnil. Prenos toplote in snovi je v obeh primerih dosežen z neposrednim stikom med vodo in okolišnim zrakom. Mehanizem prenosa toplote in snovi je razlika delnim tlakov vodne pare v mejni plasti in obtekajočim zrakom ter v manjši meri razlika temperatur med vodo in zrakom ([1] in [3]). Ker se večina toplote prenese v območju polnil ([4] in [5]), lahko območje pršil in polnil obravnavamo kot eno območje.

Za ustaljene adiabatne pogoje zapišemo enačbo ohranitve energije v nadzorni prostornini dV [6]:

outside the cooling tower. For a particular fill the fill-loss coefficient is a function of the air and water mass-flow rates as well as of the density and the height of the fills. The airflow rate through the fill could be additionally obstructed because of broken or blocked fills and the mass-flow rate could be reduced because of sealed spray nozzles and broken or damaged splash-cups. The local loss coefficient was determined indirectly from the static pressure drop and the local velocity value above the droplet eliminators. The air temperatures above the droplet eliminators depend on the local transferred heat and mass between the water and the air. The local value of the transferred heat and mass was calculated from the air mass-flow rate and its temperature and humidity change.

According to the obtained air velocity and temperature field some corrections are suggested to achieve a more efficient heat and mass transfer between the water and the air. This could be achieved by decreasing the air resistance in the fill system and by appropriately rearranging the water mass-flow rate in the cooling tower's transverse section. The influence of these changes on the air-flow properties is reported in this paper.

1TRANSFER PHENOMENA IN A COOLING TOWER

Transfer phenomena in particular segments of a cooling tower largely depend on the local water and air mass-flow rates. Basic models of heat and mass transfer in the observed system are presented later and the obtained relations are included in a single-phase 3D model of the turbulent airflow through the natural-draft cooling tower.

The process of water cooling takes place in the cooling tower's rain and fill region. In each of them the heat and mass transfer is accomplished by a direct contact between the water and the surrounding air. The heat and mass transfer is mostly driven by the difference between the partial pressures of the water vapour in the boundary layer and of the airflow, but the temperature difference between the water and the air also plays a role ([1] and [3]). Because the main heat exchange takes place in the fill region ([4] and [5]), the rain and fill regions are treated together as a fill system.

For stationary adiabatic conditions the conservation-of-energy equation for the differential control volume, dV, can be written in the following form [6]:

$$\dot{m}_{da} dh_a = \dot{m}_w c_{pw} dT_w + c_{pw} T_w d\dot{m}_w \quad (1).$$

Iz enačbe 1 vidimo, da je toplotni tok, ki ga prejme zrak, enak toplotnemu toku, ki ga odda voda.

Eq. 1 states that the heat flux received by the air is equal to the heat flux delivered by the water.

Lokalno preneseni toplotni tok med vodo in zrakom je odvisen od masnih tokov vode in zraka skozi določeno področje hladilnega stolpa ter od lokalnih vrednosti količnikov prenosa toplote in snovi. Krajevna masna tokova vode in zraka skozi hladilni stolp sta odvisna tudi od konstrukcijskih in okoliščnih razmer.

Različne predhodno navedene tehnične napake, ki se pojavijo po večletnem obratovanju hladilnega stolpa, vodijo k neustrezni omočenosti polnil ter k motenemu toku zraka skozi polnila. Značilnost teh anomalij je ta, da se pojavljajo na različnih mestih hladilnega stolpa in da jih je moč določiti le s krajevnimi meritvami temperaturnega in hitrostnega polja hladilnega zraka v stolpu. Prenos toplote in snovi ter tlačni padci v polnilih po prerezu hladilnega stolpa so bili analizirani z numerično simulacijo. Izmerjene vrednosti padca tlaka v polnilih in lastnosti zraka nad izločevalniki kapljic so bile uporabljene za izvirne člene v prenosnih in energijskih enačbah numeričnega modela.

Določitev prenosa toplote in snovi v določenem delu hladilnega stolpa temelji na toplotnem toku, ki ga prejme zrak. Izračunamo ga po enačbi [6]:

The locally transferred heat flux between the water and the air depends on the water and air mass flow through the particular segment of the cooling tower and on the local values of the heat- and mass-transfer coefficients. The water and airflow rates through a cooling tower also depend on the structural and surrounding conditions.

Various previously mentioned technical defects that occur in a cooling tower after years of operation lead to inappropriate fill-system moistening as well as to a disturbed airflow through the fill system. These anomalies can occur at various locations inside the cooling tower and can only be detected by the local measurements of velocity and temperature field of the cooling air across the cooling-tower area. The heat and mass transfer as well as the pressure drop in the fills across the cooling tower's transverse section were analysed numerically. The measured values of the pressure drop in the fill region and the properties of the air above the droplet eliminators were used as source terms in the transport and energy equations of the numerical model.

The determination of heat and mass transport in a certain segment of the cooling tower is based on the heat flux received by the air. The latter is calculated using the following equation [6]:

$$d\dot{Q}_a = \dot{m}_{da} dh_a \tag{2}.$$

Za rešitev enačbe (2) moramo poznati vstopno in izstopno temperaturo zraka, vlažnost zraka in masni tok zraka.

Vstopna temperatura zraka in njegova vlažnost sta bili izmerjeni v bližini stolpa – predpostavili smo, da se vrednosti na vstopu v stolp ne spreminjata. Na podlagi izkušenj prejšnjih meritev na različnih hladilnih stolpih [5] in priporočil standarda DIN-1947 [5] smo privzeli tudi, da je relativna vlažnost zraka nad polnili 100 odstotna. Temperatura zraka na izstopu iz polnil je bila izmerjena. Masni tok vlažnega zraka na krajevni ravni hladilnega stolpa je bil določen posredno z merjenjem hitrosti zraka. Entalpija vlažnega zraka je podana z vsoto entalpije suhega zraka in entalpije vodne pare:

The solution of Eq. 2 requires the inlet and outlet air temperatures, the air humidity and the air mass flow to be known.

The inlet temperature and the air humidity were measured in the vicinity of the cooling tower, supposing that these parameters remain constant over the inlet area of the cooling tower. It is also presumed that the relative humidity of the air that exits the fill system is 100%. This presumption is based on experience and from experimental results on various cooling towers [5], and is also in accordance with the standard DIN-1947 [5]. The temperature of the air exiting from the fill system was measured. The local mass flow of the humid air through the respective cooling-tower segment was determined indirectly by measuring the air velocity at the respective measurement points. The enthalpy of the humid air equals the sum of the dry-air enthalpy and the water-vapour enthalpy:

$$h_a = c_{pa} T_a + x(c_{pv} T_a + r) \tag{3}.$$

Če uporabimo znane izraze $\dot{m}_{da} = \dot{m}_a/(1+x)$, $\dot{m}_a = \dot{V}_a \rho_a$ in $\dot{V}_a = S\, v_a$, lahko gostoto toplotnega toka iz vode na zrak izrazimo z:

Using the common relations $\dot{m}_{da} = \dot{m}_a/(1+x)$, $\dot{m}_a = \dot{V}_a \rho_a$ and $\dot{V}_a = S\, v_a$ the heat-flux density from water to air can be expressed as:

$$\dot{q} = \frac{v_a \rho_a (h_{a1} - h_{a2})}{1 + x_1} \quad (4).$$

Gostota vlažnega zraka je izračunana glede na izmerjeno temperaturo in predpostavko, da je relativna vlažnost zraka nad izločevalniki kapljic 100 odstotna. Izmerili smo lokalne vrednosti temperature zraka in njegove hitrosti, gostoto toplotnega toka v polnilih pa smo izračunali po enačbah (3) in (4).

The density of humid air is calculated with respect to the measured temperature and the assumption that the relative humidity of the air above the droplet eliminators is equal to 100%. The measurements were performed to obtain local values of the heat-flux density in the fill system. The air temperatures and velocity were measured and the heat-flux density was calculated using Eqs. (3) and (4).

2 KOLIČNIK IZGUB V POLNILIH

Količnik izgub v polnilih hladilnega stolpa je odvisen od padca tlaka v polnilih, ki ga lahko določimo s preizkusi. Količnik izgub je tudi odvisen od masnih tokov zraka in vode in je zato odvisen od vleka skozi hladilni stolp [7].

Padec statičnega tlaka v polnilih in količnik izgub sta povezana z [7]:

2 LOSS COEFFICIENT OF A FILL SYSTEM

The loss coefficient of the cooling tower's fill system depends on the air-pressure drop across the fill, and this can be determined experimentally. The loss coefficient is also correlated with the air and water mass-flow rates and is therefore a function of the draft through the natural-draft cooling tower [7].

The static pressure drop through the fill system is coupled to the loss coefficient by the following relation [7]:

$$\Delta p_{fi} = k_{fi} \cdot \frac{\rho v^2}{2} \quad (5).$$

3 POSTOPEK MERITEV

Hitrostna in temperaturna polja zračnega toka se v okviru metode CTP merijo z uporabo razvite daljinsko upravljane premične enote (sl. 1), s katero je mogoče izmeriti hitrosti in temperature izstopnega

3 MEASURING PROCEDURE

In a CTP method, the velocity and temperature fields of the airflow are measured by a remotely controlled mobile unit (Fig. 1), developed to enable the air velocity and the temperature of the exit air mapping meas-

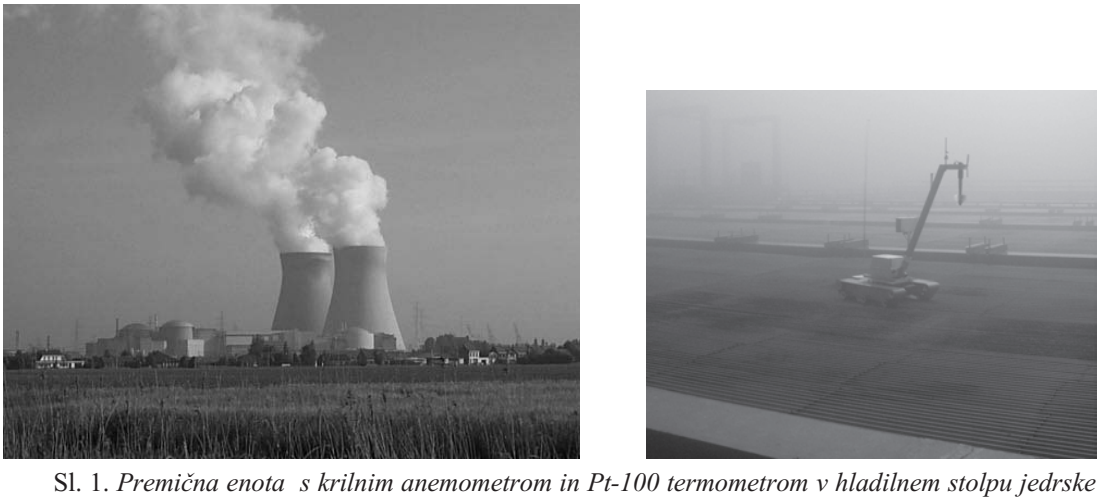

Sl. 1. *Premična enota s krilnim anemometrom in Pt-100 termometrom v hladilnem stolpu jedrske elektrarne Doel - Belgija*

Fig. 1. *Mobile unit with a vane anemometer and a Pt-100 thermometer inside the Doel nuclear powerplant cooling tower (Belgium)*

zračnega toka po celotni površini hladilnega stolpa v poljubni točki nad izločevalniki kapljic.

Premična enota se giblje po površini izločevalnikov kapljic (sl. 2 (1)). Zaznavala so nameščena na premično enoto v skladu z zahtevami standarda DIN 1947 [7]. Na premično enoto sta nameščena krilni anemometer, prirejen za delovanje v okolju nasičene vlažnosti ter Pt-100 temperaturno zaznavalo. Premična enota izvaja meritve obeh parametrov med vožnjo.

Zunanji del (sl. 2 (8)) sestavljajo: računalnik, ki vsebuje strojno opremo za povezavo z računalnikom premične enote (sl. 2 (7)) in programska oprema za obdelavo dobljenih podatkov. Lega premične enote se določa z merjenjem radialne razdalje in kota od referenčne točke v merni ravnini (sl. 2 (2)).

Hkrati z izvedbo zgoraj opisanih meritev se izvajajo meritve celostnih parametrov po standardu DIN 1947 [7]. : vstopna in izstopna temperatura hladilne vode (sl. 2 (4) in (5)), pretok hladilne vode, parametri okolice (sl. 2 (6)) in izstopna moč termoenergetskega sistema.

Z uporabo merjenih hitrostnih in temperaturnih polj v merni ravnini hladilnega stolpa

urements over the entire cooling tower area at an arbitrary measurement point above the droplet eliminators.

The mobile unit (Fig. 2 (1)) moves gradually over the entire measuring plane – the droplet eliminator surface. A vane-anemometer, designed to operate in 100% humidity, and Pt-100 thermometer sensor are mounted on the mobile unit according to the standard DIN 1947 [7]. The mobile unit measures both quantities simultaneously during its movement.

The external part of the equipment (Fig.2 (8)) comprises a PC with the appropriate hardware for the communications with the computer, mounted on the mobile unit (Fig. 2 (7)), and the software for processing the acquired data. The position of the mobile unit is determined by measuring the radial distance and the angle from a reference point in the measurement plane (Fig. 2 (2)).

Simultaneously, measurements of the integral parameters are carried out according to the DIN 1947 standard [14]: the inlet and outlet temperatures of the cooling water (Fig. 2 (4) and (5)), the cooling-water mass flow, the parameters of the surroundings (Fig. 2 (6)) and the output power of the thermo-energetic system.

The results of the velocity and temperature fields' measurements in the measurement plane of

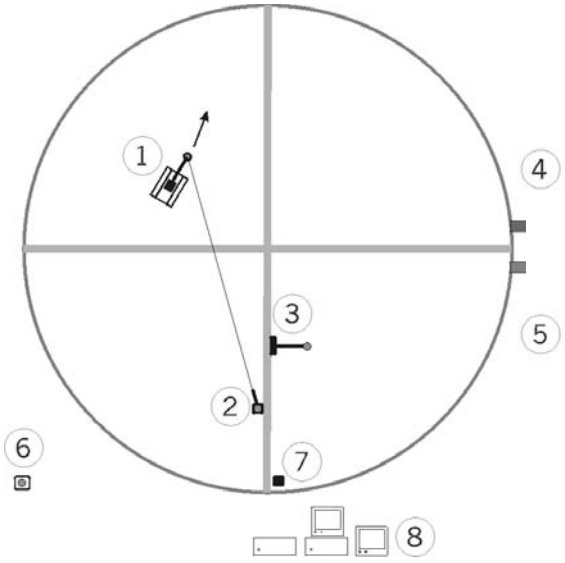

Sl. 2. *Shema elementov meritev: (1) premična enota, (2) enota za merjenje položaja, (3) položaj merilnikov referenčnih meritev, (4) meritve temperature vstopne vode, (5) meritve temperature izstopne vode, (6) meritve parametrov okolice, (7) sistem za povezavo, (8) nadzorna meritev, obdelava podatkov in shranjevanje*

Fig. 2. *Schematic view of the measurement elements: (1) mobile unit, (2) position-measurement unit, (3) position of the measurement equipment for reference measurements, (4) inlet-water temperature measurement, (5) outlet-water temperature measurement, (6) measurement of surroundings parameters, (7) communication system, (8) measurement control, data processing and saving*

dobimo trirazsežne topološke porazdelitve hitrosti in temperature izstopajočega vlažnega zraka nad izločevalniki pri znanih celostnih parametrih elektrarne. Rezultati so osnova za določitev učinkovitosti prenosa toplote iz hladilne vode na okolišni zrak.

Merilna negotovost merjenja temperature na premični enoti je znašala 1,5 odstotka, merilna negotovost anemometra pa 2 odstotka. Za merjenje lege premične enote pa je bila ključnega pomena merilna negotovost koračnega merilnika kota, ki je znašala 0,5° in je pri večjih oddaljenostih premične enote od izhodiščne točke značilno vplivala na določitev lege premične enote.

Podrobnosti o merilni opremi, njeni kalibraciji in merilnem sistemu so opisane v [8]. Pretok hladilne vode je bil merjen z ultrazvočnim merilnikom. Vlažnost in temperaturo okolišnega zraka smo merili v bližini hladilnega stolpa.

Ker se obratovalni režim elektrarne med meritvami spreminja, smo hitrost in temperaturo zraka merili tudi v stalni točki. Te meritve so bila skupaj s celostnimi parametri, namenjene za popravo meritev na krajevni ravni.

Sliki 3 in 4 prikazujeta rezultate meritev hitrosti in temperature vlažnega zraka. Iz diagramov lahko razberemo očitno nehomogenost hitrostnega in temperaturnega polja, kar kaže na to, da prenesena toplota po prerezu hladilnega stolpa ni nespremenljiva. Neenakomeren prenos toplote in snovi vodi k manjši učinkovitosti hladilnega stolpa in slabšemu izkoristku celotnega postrojenja [9].

Iz rezultatov meritev lahko sklepamo, da je ugodna rešitev težav prerazporeditev toplotnega toka v hladilnem stolpu. Povečana hitrost pretakanja hladilnega zraka na obodu stolpa (zunanje področje kolobarja s prekinjeno črto na sliki 3) in razmeroma nizka temperatura zračnega toka (zunanje področje kolobarja s prekinjeno črto na sliki 4) navaja na potrebo po povečani količini polnil odnosno na povišano plast polnil, ter hkrati povečanje dotoka vstopne hladilne vode v to področje. Nasprotno bi bilo treba dotok vstopne hladilne vode v osrednjem delu stolpa (notranje področje omejeno s sklenjeno neprekinjeno krivuljo s slik 3 in 4) sorazmerno zmanjšati ob hkratnemu zmanjšanju aerodinamičnega upora strujanja skozi osrednji del stolpa. Navedeni predlogi so v nadaljevanju prispevka ocenjeni z numeričnim modeliranjem, ki vključuje predstavljene

the cooling tower provide essential data for obtaining 3D topological structures of the velocity and temperature distribution of the moist air above the droplet eliminators at known integral parameters of the powerplant. These results represent the basis for a determination of the heat-transfer efficiency between the cooling water and the surrounding air.

The measurement uncertainty for the temperature measurements on the mobile unit was in the range of 1.5%, whereas the uncertainty of the anemometer amounted to 2%. The measurement uncertainty of the increment-angle measurement system was crucial for the measurement of the mobile unit's position. Its value was 0.5°, and it significantly influenced the determination of the mobile unit's position at greater distances from the origin point.

The details of the equipment, its calibration and the measurement system operation are described in [8]. The cooling-water flow rate was measured with an ultrasonic flowmeter. The air humidity and the air temperature were measured in the vicinity of the cooling tower.

The power plant's operating properties change during the measurements. For this reason the air velocity and the temperature at a stationary point were measured. The stationary data, together with the integral parameters and the power plant's operating data, serve as correction elements for the measurements on the local level.

Figs. 3 and 4 show the results of the moist-air velocity and temperature measurements. From the diagrams in Figs. 3 and 4 the non-uniform velocity and temperature field is obvious, which suggests that the transferred heat over the area of the cooling tower is not uniform. The non-uniform field of the heat-flux density indicates that the cooling tower does not operate equally well over the entire area. The non-uniformity of the heat and mass transfer leads to a lower efficiency of the cooling tower and thus to a lower efficiency of the entire powerplant [9].

It can be concluded from the measurement results that the problem of the mentioned non-uniformity could be solved by rearranging the heat flux inside the cooling tower. Higher cooling-air velocities at the cooling tower's peripheral region (i.e., the region radially outwards of the dashed curve in Fig. 3) and the relatively low temperatures of the airflow (i.e., the region radially outwards of the dashed curve in Fig. 4) address the need to increase the fill height and to increase simultaneously the amount of the inlet mass flow of the cooling water in this specific region. The other solution is to decrease the amount of cooling water in the central region of the cooling tower (i.e., the region radially inwards of the solid closed curve in Figs. 3 and 4) as well as to simultaneously decrease the aerodinamic drag in this central region. These suggestions are assessed later on by

izmerjene vrednosti na slikah 3 in 4 kot dejanske robne pogoje v numerično shemo. V primeru drugih krajevnih anomalij, ki se kažejo kot naključne - krajevne nehomogenosti temperaturnega in hitrostnega polja na slikah 3 in 4, bi le-te morali odpraviti s krajevnim pregledom posameznih področij, npr. z uporabo pred kratkim razvite termovizijske metode za hitro odkrivanje anomalij [10], in ugotovitvijo dejanskih vzrokov, kakor so polomljeni razpršilniki kapljic, netesnosti razvodnih kanalov, zamašenih pretočnih kanalov polnil in izločevalnikov kapljic.

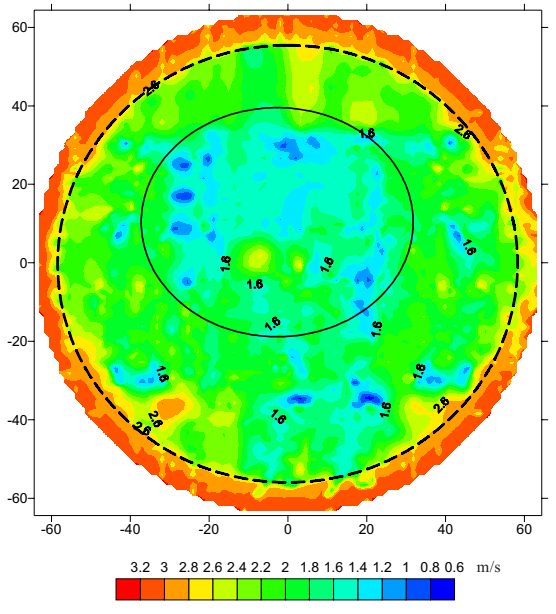

Sl. 3. *Hitrostno polje zraka nad izločevalniki kapljic*
Fig. 3. *Airflow velocity field above the droplet eliminators*

4 NUMERIČNA ANALIZA

Predstavljen je numerični model aero- in termodinamičnih značilnosti toka zraka v hladilnem stolpu. V model smo vključili vrednosti količnikov izgub v polnilih in gostoto toplotnega toka na krajevni ravni. Z analizo rezultatov numerične simulacije smo prišli do nekaterih sklepov o vplivu spremembe višine polnil in porazdelitve vode po prerezu stolpa. Numerična analiza tokovnih razmer v hladilnem stolpu je bila narejena s paketom za računalniško dinamiko tekočin CFX-5.6, ki uporablja numerične metode za reševanje Reynoldsovo povprečenih enačb ohranitve mase (enačba 6),

the numerical modelling, which introduces the presented measured values in Figs. 3 and 4 as real boundary conditions into the numerical scheme. The other local anomalies, which act as coincidental local inhomogeneities of the velocity and temperature fields in Figs. 3 and 4, should be suppressed through local inspections of particular regions, e.g., by applying the recently developed thermovision method for the rapid detection of anomalies [10], and through a determination of the actual causes, such as broken spray nozzles, leakages in dividing channels, clogged fill and droplet-eliminator passages.

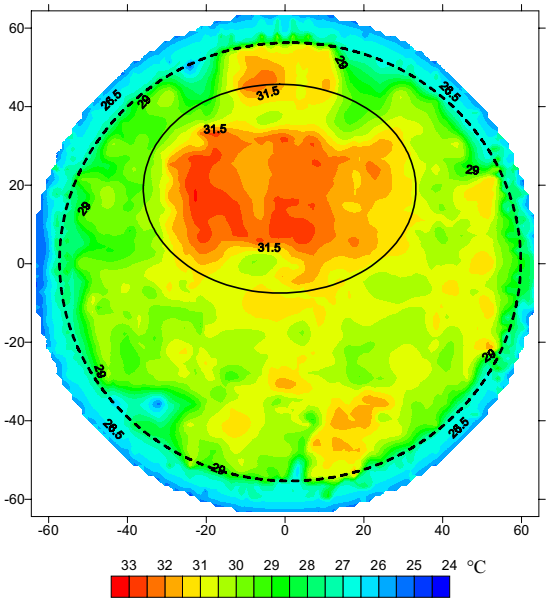

Sl. 4. *Temperaturno polje zraka nad izločevalniki kapljic*
Fig. 4. *Airflow temperature field above the droplet eliminators*

4 NUMERICAL ANALYSIS

A numerical model of the thermo- and aero-dynamic characteristics of the air flow in a cooling tower is presented. Real fill-loss coefficients and heat-flux densities in the particular segments of the cooling tower are included in the numerical model. An analysis of the numerical results led to certain conclusions about the influence of the fill-height alterations and the distribution of water across the cooling tower's transverse section. A numerical analysis of the flow properties in the cooling tower was performed using the CFD software package CFX-5.6. Its solver uses numerical methods for solving the Reynolds Averaged equations, includ-

momenta (enačba 7) in energije (enačba 8) [11]. Vse simulacije so bile opravljene v časovno neodvisnem stanju, kar pomeni, da nismo upoštevali odvodov spremenljivk po času.

ing continuity (Eq. 6), momentum (Eq. 7), and energy (Eq. 8) equations, [11]. All the simulations were performed for steady-state cases only, so the terms with time derivatives can be omitted.

$$\frac{\partial\left(\rho\bar{u}_j\right)}{x_j}=0 \tag{6},$$

$$\frac{\partial\left(\rho\bar{u}_j\bar{u}_i\right)}{\partial x_j}=-\frac{\partial\bar{p}}{\partial x_i}+\frac{\partial}{\partial x_j}\left[\mu\left(\frac{\partial\bar{u}_i}{\partial x_j}+\frac{\partial\bar{u}_j}{\partial x_i}\right)-\rho\overline{u_i'u_j'}\right]+S_M \tag{7},$$

$$\frac{\partial\left(\rho\bar{u}_j c_p T\right)}{\partial x_j}=\frac{\partial}{\partial x_j}\left(\lambda\frac{\partial T}{\partial x_j}\right)+S_E \tag{8}.$$

Zaprtje sistema enačb je poenostavljeno na določitev turbulentne viskoznosti [12]:

The closure of the set of equations is simplified to the determination of the turbulent viscosity [12]:

$$\mu_t=C_\mu\rho\frac{k^2}{\varepsilon} \tag{9}$$

ki je podana z enačbami turbulentnega modela. V danem primeru smo uporabili standardni turbulentni model k-ε[11]:

This is determined by the introduction of equations of the turbulence model. For the present case a two-equation standard k-ε turbulence model was applied [11]:

$$\bar{u}_i\frac{\partial\left(\rho k\right)}{\partial x_j}=\frac{\partial}{\partial x_j}\left[\frac{\mu_{eff}}{\sigma_k}\frac{\partial k}{\partial x_j}\right]+P_k-\rho\varepsilon \tag{10},$$

$$\bar{u}_i\frac{\partial\left(\rho\varepsilon\right)}{\partial x_j}=\frac{\partial}{\partial x_j}\left[\frac{\mu_{eff}}{\sigma_\varepsilon}\frac{\partial\varepsilon}{\partial x_j}\right]+\frac{\varepsilon}{k}\left(C_{1\varepsilon}P_k-C_{2\varepsilon}\rho\varepsilon\right) \tag{11}.$$

Dejanska viskoznost μ_{eff} je vsota stvarne in turbulentne viskoznosti, $\mu+\mu_t$; P_k je hitrost nastajanja turbulentne kinetične energije, ki nastane zaradi turbulence [11].

Člen S_M v enačbi 7 pomeni vir oziroma ponor gibalne količine v nadzorni prostornini. S tem členom smo popisali padec tlaka v območjih polnil in prh, ki ju tu obravnavamo kot porozno plast, ta pomeni določen upor za tok zraka skozi hladilni stolp. Padec statičnega tlaka lahko izračunamo iz enačbe (5). Za sistem polnil znane višine L izračunamo izkustveni količnik izgub po enačbi [11]:

The effective viscosity μ_{eff} is the sum of the real and turbulent viscosities, $\mu+\mu_t$; P_k is the production rate of the turbulent kinetic energy as a result of turbulence [11].

The term S_M in Eq. 7 represents the momentum source/loss in a control volume. This term was used to simulate the pressure loss within the fill and rain region. The fill and rain region could be regarded as a porous layer, which offers certain resistance to the airflow through the cooling tower. The resulting static pressure drop can be calculated using Eq. 5. For a fill system of known height L the empirical loss coefficient is calculated according to the following equation [11]:

$$k_{loss}=\frac{2\Delta p}{\rho v^2 L} \tag{12}.$$

Padec tlaka smo modelirali z uporabo izvirnega člena $S_{M,i}$ v momentni enačbi (7) za vsako od treh koordinatnih osi:

The pressure loss was modelled by using an additional source term in the momentum Eq. 7 for each of the three coordinate axes, in the form of:

$$S_{M,i}=-C_{R2}\left|u_j\right|u_j \tag{13}$$

C_{R2} je količnik kvadratičnega upora in je za porozno snov podan z:

where C_{R2} denotes the quadratic resistance coefficient and is expressed for porous media as:

$$C_{R2}=k_{loss}\rho \tag{14}.$$

Upoštevali smo vpliva težnosti in konvekcije, ki igrata pri toku zraka skozi hladilni

The influences of gravitation and convection, both of which play an important role regarding the air-

stolp pomembno vlogo. V enačbi (7) upoštevamo vzgonske sile z uporabo izvirnega člena, ki je podan z [11]:

flow through the cooling tower, were taken into account as well. The buoyancy forces in Eq. (7) are expressed via the source term, which can be calculated as [11]:

$$S_{M,buoy} = \rho\beta(T - T_{ref})g \tag{15}.$$

Izvirni člen $S_{M,buoy}$ v momentni enačbi je odvisen od toplotne razteznosti tekočine in krajevne temperaturne razlike glede na vzgon pri referenčni temperaturi.

Člen S_E v enačbi (8) pomen izvir/ponor energije v nadzorni prostornini. Z njim smo popisali toplotni tok z vode na zrak v območjih polnil in prhe. Izvirni člen se spreminja glede na mesto v hladilnem stolpu in je izračunan iz gostote toplotnega toka (enačba 4). Za območji polnil in prhe znane višine L je vir energije *WATT* izračunan z:

The source term $S_{M,buoy}$ in the momentum equation is a function of the thermal expansivity of the fluid as well as of the local temperature difference with regard to the buoyancy at the reference temperature.

The term S_E in Eq. (8) represents the energy source/loss in a control volume. This term was used to simulate the heat flux from the water to the air within the fill and rain region. The value of the source term changes over the transverse section of the cooling tower and is calculated from the heat-flux density (Eq. 4). For fill and rain regions of known height L the energy source *WATT* is calculated according to the following equation:

$$WATT = \frac{\dot{q}}{L} \tag{16}.$$

Vir energije v enačbi (8) lahko zapišemo z:

The energy source in Eq. (8) can be written as:

$$S_E = WATT \tag{17}.$$

5 ROBNI POGOJI

Računsko območje smo diskretizirali s tremi različno gostimi mrežami. Na podlagi analize rezultatov (opazovali smo hitrostno polje zraka nad izločevalniki kapljic) smo se odločili, da območje diskretiziramo z nestrukturirano mrežo z 1 017 000 elementi, ki je v območju polnil zgoščena. Obravnavali smo tudi okolico v bližini vstopa in izstopa iz hladilnega stolpa. Diskretizacijsko napako smo ocenili na manj ko 0,8 odstotka. Ker je bila simulacija narejena za primer enofaznega suhega zraka, so bile vrednosti količine toplote, ki jo prejme vlažen zrak v hladilnem stolpu izračunane za tok suhega zraka. Simulirali smo tri primere zračnega toka skozi hladilni stolp. V vseh primerih smo definirali naslednje robne pogoje:

- Vstop v domeno smo definirali kot robni pogoj "vhod", s tlakom okolice 100 kPa, temperaturo 282,6 K in masnim tokom zraka 29 700 kg/s.
- Na izstopu iz območja smo uporabili robni pogoj "odprtine". Glede na tlak okolice na vstopu v stolp je relativni tlak znašal 0 Pa.
- Stene stolpa so bile obravnavane kot hidravlično gladke.

5 BOUNDARY CONDITIONS

The calculation domain was discretized with three meshes of different density. According to the results of the analysis (the velocity field of the air above the droplet eliminators) a decision was made to discretize the domain of the calculation with an unstructured mesh of 1,017,000 elements, which was refined in the region of the fill system. At the cooling tower's inlet and outlet the surrounding was also modelled. The discretization error was assessed to be less than 0.8%. The simulation was executed for the case of single-phase dry air. Therefore, the amount of heat, which is received by the humid air inside the cooling tower, was calculated for the dry air. Three different cases of airflow through a cooling tower were calculated. In all cases the following boundary conditions were defined:

- The air inlet was modelled in the vicinity of the tower and was an "inlet" boundary condition, the ambient pressure was 100 kPa, the temperature was 282.6 K and the mass flow of the air was set at 29 700 kg/s.
- The air outlet was also modelled in the vicinity of the tower and was an "opening" boundary condition. According to the atmospheric pres-

- Zračni tok je bil turbulenten. Uporabili smo turbulentni model k-ε.
- Upoštevali smo naravno konvekcijo.
- Raven konvergence ostankov RMS je znašal 10^{-4}.
- Višina polnil je bila 2 m.
- Vrednost količnika izgub k_{loss} je po prerezu stolpa variirala med 4.8 in 151. Vrednosti smo dobili z meritvami.
- Izmerjene in uporabljene vrednosti *WATT* so se po prerezu stolpa gibale med 1 290 in 32 930.

Konvergenco smo določili na podlagi opazovanja različnih parametrov toka (hitrost zraka nad izločevalniki kapljic in temperatura nad izločevalniki kapljic). Parametra sta vedno konvergirala, ko je vsota razlik med iteracijami prenosnih enačb dosegla vrednost (ostanki spremenljivk: tlak, hitrost, turbulentna kinetična energija in hitrost raztrosa turbulentne kinetične energije) pod 10^{-3} (ko so se ostanki zmanjšali za tri velikostne rede). Preizkusili smo več kriterijev za konvergenco na koncu pa smo za rešitev vzeli stanje, ko je vsota ostankov padla pod 10^{-4}. Za skonvergirano rešitev je bilo potrebnih približno 350 iteracij. Iteracijsko napako smo ocenili na manj ko 0,08 odstotka [13].

6 REZULTATI NUMERIČNE SIMULACIJE

Najprej smo izvedli simulacijo v dejanskih razmerah. Vrednosti količnika izgub in prenesene toplote smo dobili iz rezultatov meritev. Sliki 5 in 6

- The walls of the tower were considered as smooth.
- the airflow was considered as turbulent, the k-ε model was used to model the turbulent flow.
- The natural convection was considered.
- The level of convergence for the RMS residual was 10^{-4}.
- The fill system height was 2 m.
- The values of the loss coefficient k_{loss} changed over the area of the cooling tower and varied between 4.8 and 151. These values were obtained experimentally.
- The experimentally obtained values of *WATT* changed over the area of the tower and varied between 11290 and 32930.

The convergence was determined by observing different flow parameters (the air velocity and the temperature above the droplet eliminators). These parameters always converged in the case where the sum of the differences between the iterations of the transport equations (residua of p, v, k and ε) amounted less than 10^{-3}, i.e., the residua dropped by three orders of magnitude. Several convergence criteria were tested. The chosen solution was the state where the sum of the residua dropped below 10^{-4}. For such a converged solution, approximately 350 iterations were needed. The iteration error was assessed to be less than 0.08% [13].

6 RESULTS OF THE NUMERICAL SIMULATION

In the first case the real conditions in the cooling tower were simulated. The values of the loss coefficient and the transferred heat were obtained

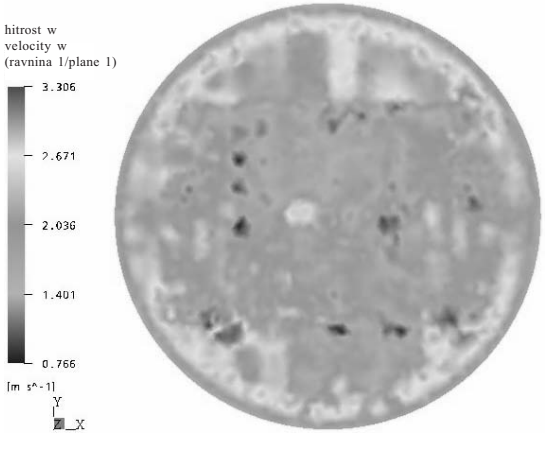

Sl. 5. *Numerična napoved hitrostnega polja zraka nad izločevalniki kapljic*
Fig. 5. *Numerically obtained air-velocity field above the droplet eliminators*

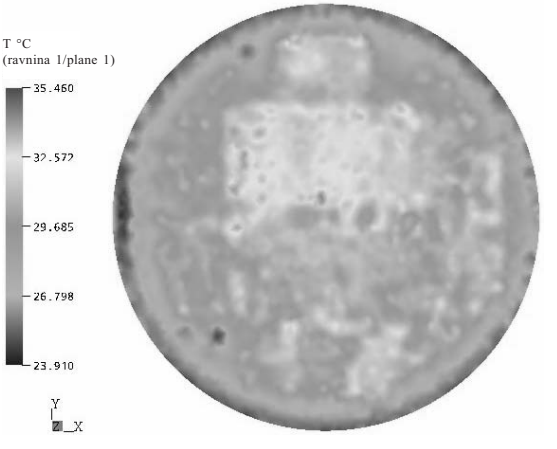

Sl. 6. *Numerična napoved temperaturnega polja zraka nad izločevalniki kapljic*
Fig. 6. *Numerically obtained air-temperature field above the droplet eliminators*

prikazujeta numerične napovedi stanja v hladilnem stolpu v sedanjih razmerah.

Napovedani hitrostno in temperaturno polje zraka nad izločevalniki kapljic (sl. 5 in 6) se nekoliko razlikujeta od rezultatov meritev (sl. 3 in 4), kar lahko razlagamo z numeričnimi napakami (napako konvergence, napako diskretizacije in napako modela), pa tudi kot posledico uporabljene merilne metode, saj meritve niso potekale zvezno po prostoru, pač pa v diskretnih merilnih točkah. Kljub temu pa so jasno vidna območja velikih hitrosti in nizkih temperatur na obodu stolpa. Nasprotni pojav (majhne hitrosti in visoke temperature) simulacija pravilno napove v srednjem zgornjem delu stolpa (sl. 5 in6). Glede na te rezultate smo v drugi simulaciji spremenili količnike izgub v srednjem delu in ob obodu stolpa. Da bi dobili večji toplotni tok na obodu stolpa, smo višino polnil povečali za 0,5 m. Količnik izgub v polnilih k_{fi} se spreminja linearno z višino polnil [8], torej se za naš primer poveča za 25 odstotkov. Med meritvami smo ugotovili, da so izločevalniki kapljic v zgornjem srednjem delu hladilnega stolpa poškodovani, kar povzroča povečan upor zraka. Ocenili smo, da bi se zračni upor z zamenjavo poškodovanih izločevalnikov zmanjšal za 10 %. Da bi dobili še

from the experimental data. Figs. 5 and 6 depict the numerical prediction of a state inside the cooling tower for particular conditions.

The air velocity and the temperature fields above the droplet eliminators obtained with the numerical simulation (Figs. 5 and 6) differ slightly from the experimental results (Figs. 3 and 4). The difference is due to numerical errors (convergence error, discretization error and model error), but is a consequence of the measurement method as well, because the measurements were carried out at discrete measurement points rather than being continuous. However, the regions of high velocities and low temperatures of air at the cooling tower's circumference can be perceived. The opposite phenomenon (lower velocities, higher temperatures of air) was correctly predicted by the numerical simulation in the upper central part of the cooling tower (Figs. 5 and 6). After considering these effects in the second study case the loss coefficients at the circumference and in the upper central part of the cooling tower were changed. The fill height was increased for 0.5 m in order to achieve a greater heat flux at the cooling tower's circumference. The fill system loss coefficient, k_{fi}, changes linearly with the fill height [8], so would in this case increase by 25 %. In the upper central part of the cooling tower the droplet eliminators are damaged, which results in an increased air resistance. The air resistance was estimated to decrease by 10 % when re-

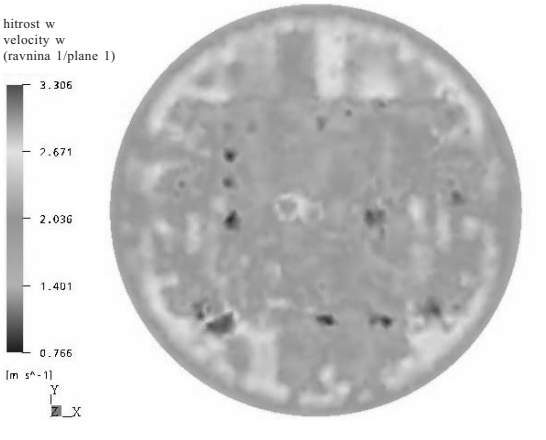

Sl. 7. *Hitrostno polje zraka nad izločevalniki kapljic po spremembah (višina polnil na obodu je povečana, poškodovani izločevalniki so zamenjani, spremenjen je zračni upor in vrednost izvirnega člena energije)*

Fig. 7. *Air-velocity field above the droplet eliminators if the fill height is increased, the eliminators are replaced and the air resistance and energy sources are changed*

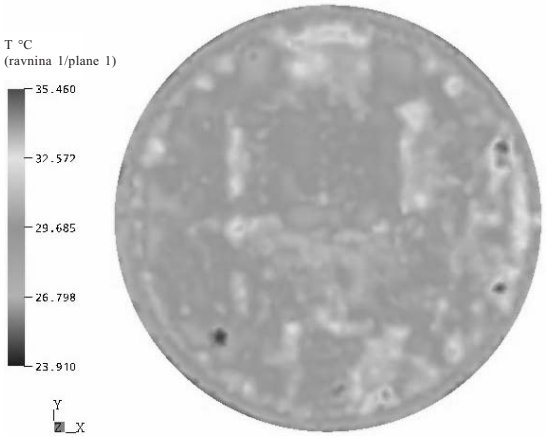

Sl. 8. *Temperaturno polje zraka nad izločevalniki kapljic po spremembah (višina polnil na obodu je povečana, poškodovani izločevalniki so zamenjani, spremenjen je zračni upor in vrednost izvirnega člena energije)*

Fig. 8. *Air-temperature field above the droplet eliminators if the fill height is increased, the eliminators are replaced and the air resistance and energy sources are changed*

bolj homogeno temperaturno polje, ki je posledica učinkovitejšega prenosa toplote in snovi, smo predlagali spremembo porazdelitve vode, kar se v numerični simulaciji kaže s spremembo vrednosti izvirnega člena energije, definiranega s stalnico *WATT*. V zgornjem srednjem delu stolpa smo vrednosti izvirnega člena zmanjšali, sorazmerno s tem pa povečali vrednosti izvirnega člena na obodu stolpa. Napovedani hitrostni in temperaturni polji zraka za popravljeno stanje sta prikazani na slikah 7 in 8.

Sliki 7 in 8 prikazujeta homogenejše temperaturno in hitrostno polje od tistih, prikazanih na slikah 5 in 6. Rezultat je torej učinkovitejše delovanje hladilnega stolpa, kar mora potrditi tudi celostna analiza numeričnega modela.

Z uporabo enačbe 4 za suh zrak lahko določimo povprečno gostoto toplotnega toka skozi celotni prerez hladilnega stolpa. Primerjava gostote toplotnih tokov pred uvedbo in po uvedbi sprememb kaže na povečanje gostote toka za 2,5 odstotka. Pričakujemo lahko, da se bo za enako vrednost povečala tudi učinkovitost hladilnega stolpa.

7 SKLEPI

V prispevku je bila predstavljena eksperimentalna metoda določanja krajevnih anomalij in numerična analiza izboljšav aero- in termodinamičnih lastnosti v hladilnem stolpu na naravni vlek elektrarne Doel-3. Za opis enofaznega trirazsežnega turbulentnega toka zraka skozi hladilni stolp smo uporabili računsko dinamiko tekočin (CFD) numerično simulacijo. V simulacijo so bili, z izvirnimi členi v momentni in energijski enačbi, vključeni rezultati meritev hitrosti in temperature zraka nad izločevalniki kapljic.

Opazili smo krajevne nepravilnosti hitrosti in temperatur zraka nad izločevalniki kapljic. Predlagani so bili nekateri ukrepi, ki bi vodili k bolj homogenemu temperaturnemu polju zraka nad izločevalniki kapljic. Preizkus predlaganih sprememb smo opravili s pomočjo numerične simulacije. Predlagane spremembe so sprememba porazdelitve hladilne vode, dodajanje polnil na obodu stolpa in sprememba značilke upora polnil. Rezultati kažejo na bolj homogeno hitrostno in temperaturno polje zraka nad izločevalniki kapljic,

placing the damaged droplet eliminators. To achieve an even more uniform temperature field, which is the consequence of the more efficient heat and mass transfer, a rearrangement of water distribution was proposed as well. Such a rearrangement influences the value of the energy source term (constant *WATT*) in the numerical simulation. In the upper central part of the tower the local temperatures are higher, so the energy sources were decreased in this area. Accordingly, the energy sources at the circumference of the tower were proportionally increased. The results of the proposed changes are shown in Figs. 7 and 8.

Figs. 7 and 8 show the temperature and velocity fields, which are more homogeneous when compared to those depicted in Figs. 5 and 6. Such a homogeneity results in the increased efficiency of the cooling tower's operation, which should in turn be confirmed by the integral analysis of the numerical model.

Using Eq. 4 for dry air the average heat-flux density through the cooling tower's transverse section can be established. According to the numerical results, the comparison of the heat-flux density before and after the reconstruction shows that after reconstruction the heat-flux density increased by 2.5 %. It is to be expected that the cooling tower's efficiency would increase by the same amount as well.

7 CONCLUSIONS

The experimental method for determining local anomalies and the numerical analysis of the improvement of the aero- and thermodynamic characteristics in a natural-draft cooling tower of the Doel-3 powerplant is presented. A computational fluid dynamics (CFD) numerical simulation was used to model the single-phase 3D turbulent air flow through the cooling tower. The experimental data of the local values of the air velocities and temperatures above the drift eliminators were introduced into the numerical simulation through source terms in the momentum and energy equations.

The local irregularities in the air-velocity and temperature fields above the droplet eliminators were detected. Certain technical measures were suggested in order to achieve a more uniform air-temperature field above the droplet eliminators. The influence of the suggested changes on the homogeneity of the air-temperature field was tested using a numerical simulation. The suggested changes comprised the rearrangement of the water distribution, the addition of fills at the cooling tower's circumference and the changing of the fill resistance's characteristics. The results show more uniform air-velocity and

kar se kaže na večji učinkovitosti hladilnega stolpa.

Predstavljeni eksperimentalni in numerični postopki so splošni in jih lahko uporabimo na poljubnih že znanih stolpih kot mogoče metodo odkritja in napovedovanja popravnih ukrepov s ciljem doseganja večje učinkovitosti stolpov in termoenergetskih postrojenj.

temperature fields above the droplet eliminators, which results in a better cooling-tower efficiency.

The presented experimental and numerical procedures are universally applicable and can be applied to any cooling tower as a possible method of detecting and predicting correction measures in order to increase the efficiency of cooling towers and thermoenergetic systems.

8 SIMBOLI
8 NOMENCLATURE

specifična toplota pri nespremenljivem tlaku	c_p	J/kg K	specific heat at constant pressure
kvadratični koeficient upora	C_{R2}	kg/m^4	quadratic resistance coefficient
stalnica turbulentnega modela k-ε, 1,44	$C_{\varepsilon 1}$		k-ε turbulence model constant, 1.44
stalnica turbulentnega modela k-ε, 1,92	$C_{\varepsilon 2}$		k-ε turbulence model constant, 1.92
stalnica turbulentnega modela k-ε, 0,09	C_μ		k-ε turbulence model constant, 0.09
težnostni pospešek	g	m/s^2	gravitational acceleration
entalpija vlažnega zraka	h_a	J/kg	enthalpy of humid air
turbulentna kinetična energija na enoto mase	k	m/s^2	turbulence kinetic energy per unit mass
količnik izgub sistema polnil	k_{fi}	/	fill-system loss coefficient
empirični količnik izgub	k_{loss}	m^{-1}	empirical loss coefficient
višina polnil	L	m	fill height
masni tok	$\dot{m}$	kg/m^3	mass-flow rate
statični tlak	p	Pa	static pressure
nastanek turbulence	P_k	kg/m s^3	shear production of turbulence
gostota toplotnega toka	$\dot{q}$	W/m^2	heat-flux density
toplotni tok	$\dot{Q}$	W	heat flux
latentna toplota	r	J/kg	latent heat
pretočna površina	S	m^2	flux area
vir energije	S_E	kg/m s^3	energy source
vir momenta	S_M	kg/m^2 s^2	momentum source
čas	t	s	time
temperatura	T	°C	temperature
hitrost	u	m/s	velocity
prostorninski tok	$\dot{V}$	m^3/s	volume flow rate
hitrost	v	m/s	velocity
razmerje vlažnosti	x	kg/kg	humidity ratio
toplotna razteznost	β	K^{-1}	thermal expansivity
raztrosna hitrost turbulence	ε	m/s^3	turbulence dissipation rate
toplotna prevodnost	λ	kg m/s^3 K	thermal conductivity
molekularna viskoznost	μ	kg/m s	molecular viscosity
turbulentna viskoznost	μ_t	kg/m s	turbulent viscosity
dejanska viskoznost	μ_{eff}	kg/m s	effective viscosity
gostota tekočine	ρ	kg/m^3	fluid density
stalnica turbulentnega modela k-ε, 1,0	σ_k		k-ε turbulence model constant, 1.0
stalnica turbulentnega modela k-ε, 1,3	σ_ε		k-ε turbulence model constant, 1.3
Indeksi			**Subscripts**
vlažen zrak	a		humid air
vzgon	$buoy$		buoyancy

suh zrak	*da*	dry air
sistem polnil	*fi*	fill system
koordinatna os	*i*	coordinate axes
primerjalna vrednost	*ref*	reference
vodna para	*v*	water vapour
voda	*w*	water

9 LITERATURA
9 REFERENCES

[1] Cooling Towers; 2000 ASHRAE Systems and equipment handbook (SI); Chapter 36.

[2] M. Novak, B. Širok, B. Blagojevič, M. Hočevar, M. Rotar (2003) CTP method – diagnostic method for control of cooling tower operation, *VGB PowerTech* Vol. 83 (2003) 61-67.

[3] D.R. Baker, H.A. Shryock (1961) A comprehensive approach to the analysis of cooling tower performance, *Journal of Heat Transfer* (1961) 339-350.

[4] M.N.A. Hawlader, B.M. Liu (2002) Numerical study of the thermal-hydraulic performance of evaporative natural draft cooling towers, *Applied Thermal Engineering* 22 (2002) 41-59.

[5] B. Širok, B. Blagojević, M. Novak, M. Hočevar, F. Jere (2001) Energy and mass transfer phenomena in natural draft cooling towers, the fifth world conference on experimental heat transfer, *Fluid Mechanics, and Thermodynamics*, Thessaloniki - Greece (2001) 2243-2248.

[6] K. Tan, S. Deng (2003) A numerical analysis of heat and mass transfer inside a reversibly used water cooling tower, *Building and Environment* 38, 1, 91-97.

[7] J.C. Kloppers, D.G. Kröger (2003) Loss coefficient correlation for wet-cooling tower fills, *Applied Thermal Engineering* 23 (2003) 2201-2211.

[8] B. Širok, T. Rus, M. Novak, G. Vrabič (1998) Thermal performance pre-upgrade exit air mapping and engineering analysis of cooling tower performance, *Proc. 60th Annual American Power Conference*, Chicago, USA 282-286.

[9] B. Širok, M. Hočevar, F. Jere, M. Novak (2003) Nuclear power station Doel-3, *Cooling Tower Measurement Report* No. 2742, Ljubljana.

[10] B. Širok, M. Hočevar, T. Bajcar, B. Blagojević, M. Dvoršek, M. Novak (2006) Thermovision method for diagnostics of local characteristics of natural draft cooling towers, *Instrumentation Science and Technology* 34 (2006) 289-304.

[11] CFX Ltd., *CFX-5 Solver Models*, Harwell, UK (2003).

[12] M. Rotar, B. Drobnič, M. Novak, B. Širok, B. Donevski (2003) Numerical modelling of transfer phenomena in natural draft cooling towers, *Proc. 4th Baltic Heat Transfer Conference*, Kaunas, Lithuania, 713-722.

[13] J.L. Ferziger, M. Perić (2002) Computational methods for fluid dynamics, *Springer-Verlag*, Heidelberg.

[14] Standard DIN 1947: Thermal acceptance test on wet ccoling towers (VDI cooling tower code) (1989)

Avtorjev naslov: prof. dr. Brane Širok
dr. Maja Rotar
dr. Marko Hočevar
dr. Matevž Dular
Jure Smrekar
dr. Tom Bajcar
Univerza v Ljubljani
Fakulteta za strojništvo
Aškerčeva 6
1000 Ljubljana
brane.sirok@fs.uni-lj.si

Authors' Address: Prof. Dr. Brane Širok
Dr. Maja Rotar
Dr. Marko Hočevar
Dr. Matevž Dular
Jure Smrekar
Dr. Tom Bajcar
University of Ljubljana
Faculty of Mechanical Eng.
Aškerčeva 6
1000 Ljubljana, Slovenia
brane.sirok@fs.uni-lj.si

Prejeto: 2.11.2006
Received:

Sprejeto: 25.4.2007
Accepted:

Odprto za diskusijo: 1 leto
Open for discussion: 1 year

Strojniški vestnik - Journal of Mechanical Engineering 53(2007)5, 285-296
UDK - UDC 681.586:007.52
Izvirni znanstveni članek - Original scientific paper (1.01)

Položajno zaznavalo za premični robot

Position Sensor for a Mobile Robot

Rajko Mahkovic
(Fakulteta za računalništvo in informatiko, Ljubljana)

V prispevku predstavljamo izvirno položajno zaznavalo za premični robot. Zaznavalo je namenjeno natančnemu merjenju položaja premičnega robota. Sestavljajo ga merilno kolesce, absolutni kodirnik za merjenje robotove smeri gibanja in relativni kodirnik za merjenje dolžine opravljene poti. Podajamo matematično izpeljavo razmerja med spreminjanjem smeri merilnega kolesca, njegove prevožene razdalje in spremembo robotovega položaja v kartezičnem koordinatnem sistemu. Obravnava je razdeljena na dve stanji: ko je merilno kolesce usklajeno s smerjo premikanja robota in ko ni usklajeno. Predstavljeni so eksperimentalni rezultati na dveh vrstah poti premičnega robota: vožnji v obliki osmice in vožnji po dolgem in ozkem hodniku. Rezultati kažejo, da je predlagano položajno zaznavalo tako natančno, kakor klasična rešitev z dvema merilnima kolescema, nameščenima na vsako stran od pogonskega kolesa. Položajna napaka zaznavala na omenjenih poteh, dolgih 20 m, v obliki osmice, in 120 m v primeru hodnika, znaša manj ko 0,4 odstotka prevožene poti. Položajnemu zaznavalu moramo določiti vrednosti štirih parametrov: obseg merilnega kolesca, ničelni kot zasuka, odmaknjenost merilnega kolesca in oddaljenost mesta namestitve zaznavala od referenčne točke premičnega robota.

(Ključne besede: mobilni robot, položajna zaznavala, merilni sistemi, odometrija)

A new position sensor is presented, designed for accurate measurements of the relative position of a mobile robot. It consists of a measurement wheel, an absolute optical encoder for measurements of the robot's orientation and a relative encoder for measurements of the distance covered by the robot. A mathematical description of the relation between the measurement wheel's orientation alteration, the distance that has been covered and the change of the robots' position in the Cartesian coordinate system is given. The discussion is divided into two situations: the first, in which the measurement wheel is aligned with the current robot's path, and the second, in which it is not. In the experiments the robot was sent to drive along a figure-of-eight-shaped path and along a long and narrow corridor. The results prove that the proposed sensor is as accurate as the classical solution of two additional measurement wheels, mounted on each side of the driving wheels. The error in the position remains below 0.4% of the travelled path for both types of paths. The position sensor needs to be calibrated with the values of four parameters: the circumference of the measurement wheel, the initial offset (the angle of the absolute encoder corresponding to the zero orientation of the robot), the eccentricity of the measurement wheel, and the distance between the sensor and the reference point of the robot.

(Keywords: mobile robots, position sensors, measurement systems, odometry)

0 UVOD

Odometrične merilne metode, merilne metode, ki temeljijo na merjenju prevožene poti, so, kakor kaže, še vedno dovolj natančno in ceneno sredstvo za določanje trenutnega položaja premičnega robota. Vrsta metod [1], ki določajo absolutno lego robota, sicer zagotavlja poznavanje njegove lege, vendar le

0 INTRODUCTION

Odometric measurement methods, i.e., methods based on the covered-path measurement, still seem to be a reasonably accurate and cheap means of supplying a mobile robot with its position. There are many methods [1] for determining a mobile robot's absolute position; however, only at specific

na posebnih mestih delovnega prostora. Navadno moramo za to poseči v delovni prostor robota, z nameščanjem, recimo, nalepk, dejavnih oddajnikov, ali pa se zanesti na razpoznavanje njegovih krajevnih značilnosti (stene, vrata, predmeti itn.) Zelo primerne so, na primer, Voronoijeve točke posplošenega istoimenovanega diagrama delovnega prostora [6]: ne samo, da dajejo rekalibracijo robotove lege, osvežimo lahko tudi njegovo usmeritev. Ob tem, da je gibanje v delovnem prostoru načeloma najbolj varno, saj je Voronoijev diagram krčenje praznega prostora, zato je robot pri premikanju vzdolž Voronoijevega diagrama najbolj oddaljen od ovir, kot je to le mogoče.

Pri delu z notranjimi premičnimi roboti imamo običajno na voljo njihovo absolutno lego le v posameznih točkah prostora, za premik od ene absolutne lege do druge pa se odločimo za neko relativno merilno metodo. Odometrija se v ta namen izkaže kot primerna izbira, njena najbolj natančna izvedba, uporaba dodatnih merilnih kolesc, pa kot poceni in učinkovita relativna merilna metoda ([4] in [5]). Taka merilna kolesca se običajno namesti na levo in desno stran pogonskih koles premičnega robota.

Ker se je pokazalo, da je namestitev takih merilnih kolesc tako konstrukcijsko, kakor gibalno (premični robot se ne more premikati vzvratno) precej omejujoče, smo želeli poiskati tako konstrukcijo merilnega kolesca, ki za robota ne bi bila tako omejujoča, ne bi bila tako odvisna od razlik v izdelavi merilnih kolesc, a bi še vedno ohranila vse prednosti odometrije. Razlika v, na primer, obsegu merilnih kolesc se tako na koncu izraža kot zasuk v usmeritvi robota; ta poleg tega lahko nastane dodatno tudi zaradi daljše prevožene poti enega od kolesc, ker se pač kolesca kotalita po različno ravnih podlagah.

1 POLOŽAJNO ZAZNAVALO

Položajno zaznavalo na sliki 1 sestavljata relativni optični enkoder za merjenje prevožene poti, zapis premika, in absolutni optični kodirnik za merjenje trenutne robotove usmeritve, kodirnik smeri. Zasnova kodirnika poti ni običajna: namesto osvetlitve skozi masko, ki pri kolesu pač ni izvedljiva, smo uporabili odboj od maske, nalepljene na merilno kolesce. Maska, izjedkana iz plošče za izdelavo električnih tiskanih vezij, ima tri sledi: zunanji dve s po 180 zarezami na zasuk sta fazno premaknjeni za 90° (tak fazni premik mask je pri kodirnikih običajen način za podvojitev ločljivosti).

positions of the working space. Nevertheless, some kind of intervention in the working space is necessary for them to be applied, e.g., the placement of labels, active transmitters, or recognition of the local features of the working space (walls, doors, various objects, etc.). For example, Voronoi points of the generalized Voronoi diagram could serve for this purpose [6]: not only the robot's position, but also its orientation could be recalibrated. In addition to this, the motion of the robot is safer, since the Voronoi diagram is a *retraction* of the free space, which guarantees that the robot is as far from obstacles as possible.

An indoor mobile robot is supplied, as already mentioned, with its absolute position only at specific places of the working space; to move among these places it needs to rely on a kind of relative measurement method. Odometry has proved to be a quite effective choice, especially in its most accurate implementation, with the use of *additional* measurement wheels ([4] and [5]). Such measurement wheels are normally placed to the right- and left-hand sides of the robot's driving wheels.

Unfortunately, such wheels turn out to be awkward to mount, and they restrict the movements of the robot. Therefore, it was our intention to find such a construction of an additional measurement wheel that would not depend so strongly on the differences between both wheels (which actually introduce positional errors), yet it would still preserve all the advantages of odometry. The difference, for instance, in wheels' circumferences manifests itself as an additional turn in the orientation of the robot; the same effect could be produced by the difference in the lengths of the paths the measurement wheels travel along, caused by an uneven floor.

1 POSITION SENSOR

The position sensor in Figure 1 consists of a relative optical encoder, designed to measure the traversed path, a *distance encoder*, and an absolute optical encoder, applied to measure the robot's changes in orientation, a *steering encoder*. The design of the distance encoder is not the common one: instead of lighting through the glassy mask, which is not applicable on the wheel, the *reflection* from the mask, glued directly on the wheel, is used. The mask, etched from an electronic circuit board, has three tracks: the outer two, with 180 lines around the circumference, are shifted in phase by 90° (this phase

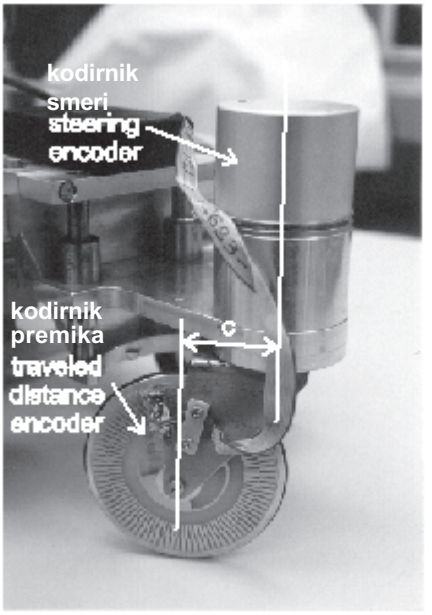

Sl. 1. *Zaznavalo sestavljata kodirnik smeri in kodirnik premika*
Fig. 1. *The sensor consists of a steering encoder and a distance encoder*

Tretja sled ima vsega eno označbo, ki je uporabljena za izhodišče merjenja po krogu, primerjalni sunek.

Merilno kolesce se, kakršen koli že je njegov začetni zasuk, med vožnjo postopno poravna s smerjo vožnje; glede na os kodirnika smeri je namreč nameščeno izsredno. Med vožnjo se torej iz prevožene razdalje in trenutne smeri izračunava premik robota v kartezičnem koordinatnem sistemu.

Matematični opis merilnega sistema podajamo v nadaljevanju. Izkaže se, da moramo obravnavo pravzaprav razdeliti na dva primera: prvič, da je merilno kolesce v smeri vožnje poravnano, in drugič, da merilno kolesce v smeri vožnje robota še ni poravnano.

V nadaljevanju bomo obravnavali najprej zahtevnejši drugi primer, pri katerem torej merilno kolesce ni poravnano s smerjo vožnje; predvidevamo, da nam bo obravnava tega primera ponudila zadosten vpogled tudi za obravnavo primera, pri katerem je merilno kolesce poravnano.

2 NEPORAVNANO MERILNO KOLESCE (NMK)

Predpostavimo, da se robot giblje vzdolž krožnega dela poti. Referenčno točko robota bomo označili s T_{1x}, središčno točko kodirnika smeri z B_x, dotikališče merilnega kolesca s tlemi A_x; pri čemer

shift is commonly applied in optical encoders to double the resolution); the third track has only one line, used to mark the position of each full turn of the wheel, the reference pulse.

The measurement wheel, whatever its initial orientation, aligns gradually with the direction of the path; because it is mounted eccentrically in terms of the axis of the orientation encoder. During the movements, the traversed distance and the current orientation determine the change of the position in the Cartesian coordinate system.

A mathematical description of the measuring system is given below. It turns out that the discussion should be divided into two situations: the first, in which the measurement wheel is *aligned* with the orientation with the robot, and the second, in which it is not.

The following discussion will first focus on the second, more demanding situation, in which the measurement wheel is not aligned with the orientation of the robot; we believe this case will also give us sufficient insight into the former.

2 NON-ALIGNED MEASUREMENT WHEEL (NMW)

Let us suppose the mobile robot moves along a circular arc. We denote the reference point of the robot by T_{1x}, the centre of the steering encoder by B_x, the contact point of the measurement wheel with the

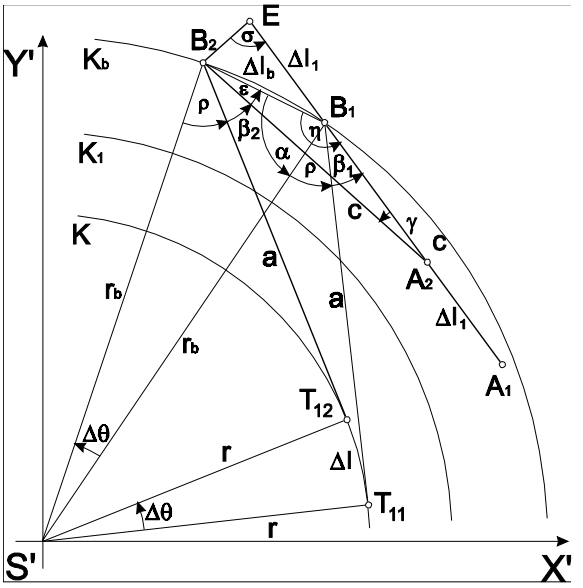

Sl. 2. *Geometrijska oblika premika za NMK*
Fig. 2. *Geometrical illustration of NMW-type movements*

x označuje indeks položaja pred premikom robota (1) in po premiku (2). Dolžini $|A_1B_1|$ in $|A_2B_2|$ pomenita premik *c*, označen na sliki 1, *a* pa razdaljo med referenčno točko robota in osjo kodirnika smeri (dolžini $|T_{11}B_1|$ in $|T_{12}B_2|$).

Ko se, na primer, referenčna točka robota premakne po krožnem loku z ukrivljenostjo *K* iz T_{11} v T_{12}, se središče enkoderja smeri premakne po krožnem loku z ukrivljenostjo K_b iz B_1 v B_2, dotikališče merilnega kolesca pa iz A_1 v A_2. Pri tem referenčna točka robota opravi premik po krožnem loku Δl, smer oziroma usmeritev robota pa se spremeni za $\Delta\Theta$. Če bi bilo nadalje, merilno kolesce že poravnano glede na smer vožnje, bi A_1 in A_2 ležali na krožnem loku s polmerom K_1. Predpostavimo, da je premik dovolj majhen, da lahko vzamemo, da A_2 leži kar na daljici $\overline{A_1B_1}$. Premik Δl_1 je pri tem razdalja, izmerjena z kodirnikom poti. (Vidimo, da sta Δl_b in Δl krožna loka, medtem ko je Δl_1 daljica.) Točko *E* določimo tako, da dobimo enakokraki trikotnik ΔA_2B_2E.

2.1 Izračun spremembe robotove usmeritve

Iz enakih pravokotnih trikotnikov $\Delta S'T_{11}B_1$ in $\Delta S'T_{12}B_2$ lahko izračunamo kot ρ:

floor by A_x, where *x* denotes the index of the position before the movement (1) and after the movement (2). The straight lines $|A_1B_1|$ and $|A_2B_2|$ are the eccentricity *c* from Figure 1, whereas *a* is the distance between the robot's reference point and the centre of the steering encoder (straight lines $|T_{11}B_1|$ and $|T_{12}B_2|$).

As, for example, the robot's reference point moves along a circular arc with the curvature *K* from T_{11} to T_{12}, the centre of the steering encoder moves along the circular arc with the curvature K_b from B_1 to B_2, whereas the contact point of the measurement wheel moves from A_1 to A_2. During this movement, the robot's reference point moves along the arc Δl, while the change in the orientation of the robot amounts to $\Delta\Theta$. Furthermore, if the measurement wheel was aligned with the path of the movement, the points A_1 and A_2 would lie on the circular arc with curvature K_1. Let us presume that the movement is small enough to assume that A_2 lies on the straight line $\overline{A_1B_1}$. The length Δl_1 is the distance measured by the distance encoder. (Note that Δl_b and Δl are circular arcs, whereas Δl_1 is a straight line.) Point *E* is determined in such a way that an isosceles triangle, ΔA_2B_2E, is formed.

2.1 Calculation of the change in the robot's orientation

We calculate the angle ρ from the observation of two rectangular triangles $\Delta S'T_{11}B_1$ and $\Delta S'T_{12}B_2$:

$$\rho = \arccos(a / r_b) \quad (1).$$

Kota α in σ izračunamo iz enakokrakih trikotnikov $\Delta S'B_1B_2$ in ΔA_2B_2E:

Next, angles α and σ are calculated from the isosceles triangles $\Delta S'B_1B_2$ and ΔA_2B_2E:

$$\alpha = (\pi - \Delta\Theta)/2$$
$$\sigma = (\pi - \gamma)/2$$

S tem pa že lahko izračunamo vse tri kote v trikotniku $\Delta A_2B_2B_1$:

And now, all three angles in the triangle $\Delta A_2B_2B_1$ can be determined:

$$\varepsilon = \pi/2 - \Delta\Theta/2 - \rho - \beta_2$$
$$\eta = \pi/2 - \Delta\Theta/2 + \rho + \beta_1$$
$$\gamma = \Delta\Theta + \Delta\beta$$

kjer je $\Delta\beta$ razlika med končnim kotom β_2 in začetnim kotom β_1. Po določitvi še vseh treh stranic trikotnika $\Delta A_2B_2B_1$, lahko na njem uporabimo sinusni izrek:

where $\Delta\beta$ denotes the difference between the angles after, β_2, and before, β_1, the movement. After the sides of the triangle $\Delta A_2B_2B_1$ are established, the sine theorem can be applied to it:

$$\frac{2r_b \sin(\Delta\Theta/2)}{\sin(\Delta\Theta + \Delta\beta)} = \frac{c}{\sin(\pi/2 - \Delta\Theta/2 + \rho + \beta_1)} = \frac{c - \Delta l_1}{\sin(\pi/2 - \Delta\Theta/2 - \rho - \beta_2)} \quad (2).$$

Iz razmerja prvih dveh ulomkov že lahko dobimo diferencialno enačbo, tako da pošljemo spremembi $\Delta\beta$ in $\Delta\Theta$ proti nič. Zavedati pa se moramo, da če hkrati pošljemo $\Delta\beta$ in $\Delta\Theta$ proti nič, bodo vse izpeljane enačbe veljale le v primeru, če je kodirnik smeri neporavnan v smeri vožnje. Dobimo naslednjo diferencialno enačbo:

By limiting the changes $\Delta\beta$ and $\Delta\Theta$ towards zero, the relation of the first two fractions supplies us with the differential equation. However, we have to keep in mind that sending both differences to zero simultaneously implies that all the derived equations will hold only to the NMW situation. The following equation is obtained:

$$\frac{r_b d\Theta}{d\Theta + d\beta} = \frac{c}{\cos(\beta + \rho)} \Leftrightarrow r_b \cos(\beta + \rho) d\Theta = c d\Theta + c d\beta \quad (3),$$

iz katere izrazimo $d\Theta$:

from which $d\Theta$ can be determined:

$$d\Theta = \frac{c}{r_b \cos(\beta + \rho) - c} d\beta \quad (4).$$

Po integraciji leve strani enačbe od 0 do $\Delta\Theta$ in desne strani od β_1 do β_2 ter zapisu ukrivljenosti namesto obratne vrednosti polmera krožnega loka $K_b = 1/r_b$, dobimo enačbo spremembe usmeritve robota

After the integration of the left-hand side from 0 to $\Delta\Theta$ and the right-hand side from β_1 to β_2, and the use of the curvature $K_b = 1/r_b$ is introduced, the equation that gives the change of the robot's orientation can be written as:

$$\Delta\Theta = \frac{cK_b}{\sqrt{1 - cK_b}} \ln \frac{\Phi_+(\beta_2)\Phi_-(\beta_1)}{\Phi_-(\beta_2)\Phi_+(\beta_1)} \quad (5),$$

kjer sta

where

in

$$\Phi_-(\beta_i) = (1 + cK_b) \tan\left(\frac{\beta_i + \rho}{2}\right) - \sqrt{1 - cK_b^2}$$

and

$$\Phi_+(\beta_i) = (1 + cK_b) \tan\left(\frac{\beta_i + \rho}{2}\right) + \sqrt{1 - cK_b^2}$$

2.2 Izračun prevožene poti merilnega kolesca

Prevožena pot merilnega kolesca Δl_1 je sicer podatek, ki ga preberemo iz kodirnika premika, toda

2.2 Calculation of the length measured by the measurement wheel

The length measured by the measurement wheel Δl_1 is data read directly from the distance encoder; how-

potrebujemo njegovo povezavo s preostalimi spremenljivkami v merilnem sistemu. Postopek izračuna je podoben zgornjemu izračunu spremembe robotove usmeritve, le da tokrat uporabimo trikotnik $\Delta B_1 B_2 E$. Najprej izračunamo vse trikotnikove notranje kote:

ever, it should be related to the other system variables. The procedure we will use is somewhat similar to the one above, except that triangle $\Delta B_1 B_2 E$ is observed this time.

All three angles are determined first:

$$\sigma = (\Delta\Theta + \Delta\beta)/2$$

$$\angle B_1 B_2 E = \sigma - \varepsilon = \beta_2 + \rho - \Delta\beta/2$$

$$\angle B_2 B_1 E = \pi - \eta = \pi/2 - \beta_1 - \rho + \Delta\Theta/2$$

nato pa še dolžine njegovih stranic. Tudi v tem trikotniku uporabimo sinusni izrek in dobimo:

and all three sides. After that the sine theorem is applied for this triangle too, obtaining:

$$\frac{2c\sin((\Delta\Theta+\Delta\beta)/2)}{\sin(\pi/2-\beta_1-\rho+\Delta\Theta/2)} = \frac{\Delta l_1}{\sin(\beta_2+\rho-\Delta\beta/2)} = \frac{2r_b\sin(\Delta\Theta/2)}{\sin(\pi/2-(\Delta\Theta+\Delta\beta)/2)}$$

Iz razmerja prvih dveh ulomkov dobimo diferencialno enačbo, če pošljemo spremembi $\Delta\beta$ in $\Delta\Theta$ proti nič. Spet pa se moramo zavedati, da vse nadaljnje enačbe veljajo le v primeru, da merilno kolesce ni poravnano:

From the relation between the first two fractions another differential equation is obtained, limiting the differences $\Delta\beta$ and $\Delta\Theta$ to zero. Again, the equations hold for the NMW case:

$$\frac{c(d\Theta+d\beta)}{\cos(\beta+\rho)} = \frac{dl_1}{\sin(\beta+\rho)} \Leftrightarrow c\frac{\sin(\beta+\rho)}{\cos(\beta+\rho)}(d\Theta+d\beta) = dl_1$$

Na mesto $d\Theta$ vstavimo diferencialno enačbo (4):

The differential equation (4) is applied in the place of $d\Theta$:

$$dl_1 = \frac{\sin(\beta+\rho)}{\cos(\beta+\rho)}\left(\frac{c}{r_b\cos(\beta+\rho)-c}+1\right)d\beta$$

Levo stran diferencialne enačbe integriramo od 0 do Δl_1, desno stran pa od β_1 do β_2 in po integraciji dobimo:

The left-hand side of the equation is integrated from 0 to Δl_1, whereas the right-hand side is integrated from β_1 to β_2, giving:

$$\Delta l_1 = c\ln\left(\frac{\cos(\beta_1+\rho)-cK_b}{\cos(\beta_2+\rho)-cK_b}\right) \quad (6),$$

kjer smo števec in imenovalec v ulomku logaritma pomnožili z $1/r_b$ ter le tega, kakor zgoraj, v izračunu za $\Delta\Theta$, zapisali z ukrivljenostjo K_b.

Kakor smo med samo izpeljavo enačb merilnega sistema že omenili, smemo izraza za $\Delta\Theta$, enačba (5) in K_b, enačba (6), uporabiti le v primeru, da merilno kolesce ni bilo poravnano. Raziskati je torej potrebno še primer, da je merilno že poravnano glede na smer gibanja robota.

where the numerator and the denominator of the logarithm fraction were multiplied by $1/r_b$ and replaced, as above, by the curvature K_b.

As already mentioned, the expressions for $\Delta\Theta$ Eq. (5) and Δl_1, Eq. (6), apply to the NMW case only. What is left is the discussion of the AMW case, which follows below.

3 PORAVNANO MERILNO KOLESCE (PMK)

Geometrijska oblika premika v primeru poravnanega merilnega kolesca je prikazana na sliki 3.

Na sliki smo si pomagali s premaknjenim koordinatnim sistemom, kjer je *S*' središče krožnic, po kateri se giblje robotova referenčna točka (z ukrivljenostjo *K*), oziroma krožnice, po kateri se giblje dotikališče merilnega kolesca (K_1); *E* in *G* sta pomožni točki.

3 ALIGNED MEASUREMENT WHEEL (AMW)

The geometry of the robot's movement is illustrated in Fig.3.

A translated coordinate system, where *S*' denotes the centre of the circular arcs that are the robot's reference point (curvature *K*), or the measurement-wheel contact point (K_1), which they are moving along, can be seen in the figure. *E* and *G* are the auxiliary points.

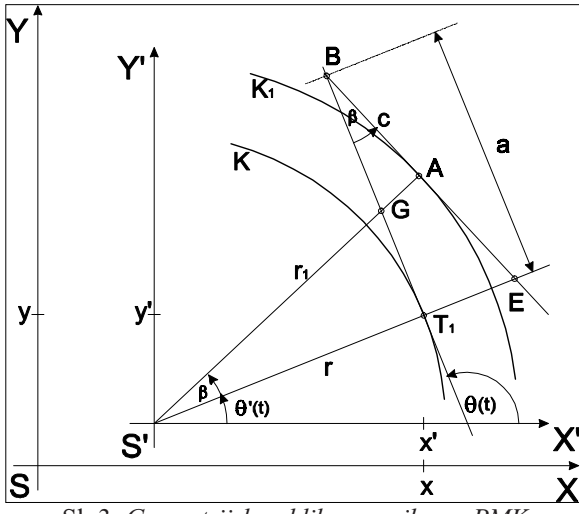

Sl. 3. *Geometrijska oblika premika za PMK*
Fig. 3. *Geometrical illustration of the AMW-type movements*

Pri izpeljavi enačb si pomagamo s podobnimi trikotniki:

The appropriate equations are derived from similar triangles:

$$\Delta S'T_1G \approx \Delta BAG \approx \Delta S'AE \approx \Delta BT_1E$$

Izraza za ukrivljenost krožnic K in K_1 izpeljemo, ker sta kota $\angle S'T_1G$ in $\angle BAG$ prava, iz osnovnih trigonometričnih funkcij:

Since the angles $\angle S'T_1G$ and $\angle BAG$ are rectangles, the expressions for the curvatures K and K_1 can be obtained using trigonometric functions:

$$K = \frac{\sin(\beta)}{a\cos(\beta) - c}$$

$$K_1 = \frac{K\cos(\beta)}{1 + Kc\sin(\beta)}$$

Nadalje torej lahko izračunamo spremembo smeri $\Delta\Theta$ in spremembo premika Δl, saj velja

The expressions for the change of the orientation $\Delta\Theta$and the distance Δl can then be written:

$$\Delta\Theta = \frac{\Delta l}{r} = \frac{\Delta l_1}{r_1} = \Delta l_1 K_1 = \frac{\Delta l_1 K\cos(\beta)}{1 + Kc\sin(\beta)} \quad (7)$$

$$\Delta l = \frac{\Delta\Theta}{K} = \frac{\Delta l_1 K_1}{K} = \frac{\Delta l_1\cos(\beta)}{1 + Kc\sin(\beta)} \quad (8).$$

4 IZVEDBA SKUPNEGA MERILNEGA SISTEMA (NMK IN PMK)

Enačba (6) podaja razmerje med ukrivljenostjo K_b, začetnim kotom β_1, končnim kotom β_2 in razdaljo, ki jo prevozi merilno kolesce Δl_1. Vrednosti β_1, β_2 in Δl_1 so znane, izračunati pa je treba K_b, najbolje kar skupaj z odmaknjenostjo, ker se pač pojavljata skupaj.

Enačbo (6) delimo s c in damo obe strani v eksponent. Upoštevamo še kosinus vsote kotov in vpeljemo novo spremenljivko F:

4 REALIZATION OF THE ENTIRE MEASUREMENT SYSTEM (NMW AND AMW)

Eq. (6) determines the relationship among K_b, the starting angle β_1, the final angle β_2 and the length of the straight line Δl_1, covered by the measurement wheel. The values β_1, β_2 and Δl_1 are known, whereas K_b should be calculated, conveniently together with the eccentricity, since they appear together.

We divide Eq. (6) by c and put both sides in the exponent. After the cosine of the sum of the angles is taken into account, we introduce a new variable, F:

$$\cos(\beta_1 + \arccos(\frac{a}{c}cK_b)) = \frac{a}{c}cK_b\cos(\beta_1) - \sin(\beta_1)\sin(\arccos(\frac{a}{c}cK_b))$$

$$F = \frac{cK_b}{\sin(\arccos(\frac{a}{c}cK_b))} = \frac{cK_b}{\sqrt{1-(\frac{a}{c}cK_b)^2}} \quad (9).$$

Dobimo enačbo:

The following equation is obtained:

$$E = e^{\frac{\Delta l_1}{c}} = \frac{\frac{a}{c}\cos(\beta_1) - \frac{\sin(\beta_1)}{F} - 1}{\frac{a}{c}\cos(\beta_2) - \frac{\sin(\beta_2)}{F} - 1}$$

iz katere izrazimo F:

from which F can be expressed:

$$F = \frac{E\sin(\beta_2) - \sin(\beta_1)}{E(\frac{a}{c}\cos(\beta_2) - 1) - \frac{a}{c}\cos(\beta_1) + 1} \quad (10).$$

Sedaj lahko iz (10) izračunamo cK_b:

cK_b follows from Eq. (10):

$$cK_b = \pm\frac{F}{\sqrt{1+(\frac{a}{c}F)^2}} \quad (11).$$

(Ta enačba ima dve rešitvi, $+cK_b$ in $-cK_b$. Prav tako dobimo dve rešitvi tudi iz enačbe za ρ (1), skupaj imamo torej štiri kombinacije vrednosti ρ and cK_b.)

(Since this equation has two solutions, $+cK_b$ and $-cK_b$, and two more are obtained from the equation for ρ Eq. (1), we are left with four combinations of ρ and cK_b.)

4.1 Postopek merjenja

1. Iz kodirnika smeri preberemo trenutno vrednost kota β_2, iz kodirnika premika pa premik Δl_1.
2. Če je trenutni kot zasuka merilnega kolesca β_2 enak zasuku iz prejšnje meritve β_1, je merilno kolesce poravnano v smeri vožnje, primer PMK, zato izračunamo $\Delta\Theta$ in Δl iz (7) in (8). Sicer nadaljujemo s točko 3.
3. Izračunamo vrednost cK_b ((10) in (11)).
4. Določimo kot $\rho = \arccos(a/c\ cK_b)$.
5. Preverimo kateri par $\{(+\rho,+cK_b),(+\rho,-cK_b),(-\rho,+cK_b),(-\rho,-cK_b)\}$ ustreza (6).
6. Pravi par vstavimo v enačbo (5) in izračunamo spremembo kota $\Delta\Theta$.
7. Iz spremembe kota $\Delta\Theta$ določimo premik Δl:
   - Če je sprememba kota $\Delta\Theta$ enaka nič, premični robot vozi naravnost, merilno kolesce pa se poravnava v smer vožnje: medtem ko se referenčna točka robota premakne za, recimo, l, se odmaknjenost merilnega kolesca zmanjša z β_1 na β_2. Premik l je podan z enačbo:

     $$l = c\left(\frac{\tan(\beta_1/2)}{\tan(\beta_2/2)}\right)$$

     (natančna obravnava poravnavanja kolesca je podana v [3]).
   - Sicer iz spremembe $\Delta\Theta$ in ukrivljenosti K_b izračunamo premik referenčne točke robota Δl (glej trikotnika $\Delta S'T_{11}B_1$ in $\Delta S'T_{12}B_2$ na sliki 2):

4.1 Measurement procedure

1. Read current values: the value of angle β_2 from the steering encoder, and the length Δl_1 from the distance encoder.
2. If the current angle β_2 is equal to the angle β_1, from the previous measurement, the AMW case applies; $\Delta\Theta$ and Δl are calculated from Eq. (7) and Eq. (8). Otherwise we proceed with point 3.
3. Calculate cK_b (Eq. (10) and Eq. (11)).
4. Determine $\rho = \arccos(a/c\ cK_b)$.
5. Check which pair among $\{(+\rho,+cK_b),(+\rho,-cK_b),(-\rho,+cK_b),(-\rho,-cK_b)\}$ correspond to Eq. (6).
6. Put the corresponding pair into Eq. (5) and calculate the change of orientation $\Delta\Theta$.
7. From $\Delta\Theta$ calculate Δl:
   - If the change of the orientation $\Delta\Theta$ is zero, the mobile robot drives along a straight line, while the measurement wheel is still aligning with the direction of the drive: if the reference point moves by, for example, l, the nonalignment of the measurement wheel is decreased from β_1 to β_2. The move l is defined by the equation:

     (the complete explanation is given in [3]).
   - Otherwise, calculate the movement of the robot's reference point Δl, using $\Delta\Theta$ and the curvature K_b (observe the triangles $\Delta S'T_{11}B_1$ and $\Delta S'T_{12}B_2$ in Fig.2):

$$\Delta l = \Delta\Theta \sqrt{\left(\frac{c}{cK_b}\right)^2 - a^2}$$

8. Iz spremembe kota $\Delta\Theta$ in premika Δl izračunamo z uporabo dobro znanih razmerij spremembo položaja premičnega robota v kartezičnem koordinatnem sistemu.

5 DOLOČITEV PARAMETROV POLOŽAJNEGA SISTEMA

Opisano položajno zaznavalo zahteva določitev vrednosti štirih parametrov: odmaknjenost c, ničelni kot β_0 (kot, ki ga kaže kodirnik smeri pri vožnji naravnost), obseg merilnega kolesca o_1, oddaljenost položajnega zaznavala od referenčne točke robota a.

Na začetku moramo te parametre seveda določiti ročno, toda tako dobljene vrednosti so le grobe ocene; natančnejše vrednosti določimo tako, da robot vozi po poteh, pri katerih se vpliv posameznih parametrov čim bolj osami. Pri vožnji naravnost, na primer, parameter a ne vpliva kaj dosti, vsak od preostalih treh pa vpliva drugače. Za določitev vrednosti parametrov smo zato izbrali prav vožnjo naravnost. Ob njej smo spremljali potek robotove lege in graf usmeritve robota Θ. Grafi izmerjenih leg robota in njegove usmeritve so potrdili, da odmaknjenost c vpliva samo na začetku, ko merilno kolesce še ni poravnano, da ničelni kot β_0 določa nagib spreminjanja kota Θ (ki bi pri vožnji naravnost sicer moral ostati stalen) ter da obseg kolesca o_1 ne vpliva bistveno na spreminjanje Θ, občutno pa vpliva na dolžino poti.

Podrobnejše rezultate parametrične analize si lahko ogledamo v [3], kjer je tudi razloženo, zakaj mora biti vrstni red določanja parametrov naslednji: c, β_0 in o_1. Parameter a določimo z vožnjo po krogih.

Ker je položajno zaznavalo zasnovano na relativnem merjenju, se njegova napaka neprestano povečuje, zato je zelo pomembna ocena njegovih parametrov. V našem primeru so končne vrednosti parametrov bile: $\beta_0 = 196{,}708°$, $c = 0{,}04014$ m, $o_1 = 0{,}2985$ m in $a = 0{,}5678$ m. Vse so bile seveda pridobljene programsko, na temelju testnih voženj robota.

8. The change of the robot's position in the Cartesian coordinate system is calculated from $\Delta\Theta$ and Δl using the well-known relations.

5 DETERMINATION OF THE PARAMETERS OF THE SENSOR

The position sensor requires the determination of four parameters: the eccentricity c, the zero angle β_0 (the angle, the steering encoder reports when the robot is moving straight ahead), the circumference of the measurement wheel o_1, and the distance from the position sensor to the reference point of the robot a.

At the beginning these parameters have to be determined manually, yet these are only coarse approximations of the real values; the finer values are obtained by letting the robot move along the kind of paths on which the impact of the individual parameter is isolated as much as possible. If the robot moves along the straight line, for example, parameter a does not have much influence, while each of the remaining affect the movement in their own way. That is why we chose exactly this type of movement to determine the parameters values. The robot's position and the graph of its orientation were observed carefully along the path. The graphs of these positions and orientations proved that the eccentricity c has an impact at the beginning only, when the measurement wheel is still not aligned, that zero angle β_0 determines the inclination of the Θ graph, which should stay constant, when moving straight ahead- constant, and that circumference of the wheel o_1 does not have an observable impact on the graph Θ, but it does have a substantial influence on the length of the paths.

Detailed results of the parametric analysis can be found in [3], where the explanation as to why the order of the parameter determination should be c, β_0 and o_1, is given. The parameter a is determined by the circular paths.

Since the presented sensor is based on relative measurements, its error grows without bounds, so a correct estimation of the parametric values is crucial. The final values in our case were: $\beta_0 = 196.708°$, $c = 0.04014$ m, $o_1 = 0.2985$ m and $a = 0.5678$ m. All of them were, of course, obtained from the dedicated software that analyzed the paths of the robot

6 REZULTATI

Položajno zaznavalo smo preizkusili na lastnem premičnem robotu (sl. 4). Premični robot je bil opremljen z dvema merilnima sistemoma. Ob pogonskih kolesih zadaj je imel pritrjen par pomožnih merilnih kolesc, ki zagotavljajo tudi za več ko red velikosti [4] natančnejšo lego, kot jo dobimo na podlagi kodirnikov, pritrjenih na samih pogonskih kolesih, spredaj pa v prispevku predstavljeni pozicijski merilnik (sl. 4a). Podlaga so bila gladka tla iz linoleja (sl. 4b).

Položajno zaznavalo smo preizkušali na dveh vrstah poti: na prvi (sl. 5a), smo robota programirali, da je vozil "osmico", torej štiri leve in štiri desne zavoje; na drugi (sl. 5b), smo preverili vožnjo naravnost, po dolgem in ozkem hodniku.

6 RESULTS

The position sensor was tested on our own mobile robot, Fig.4. The robot was equipped with two measuring systems. To the left and to the right of the driving wheels there was a pair of additional measurement wheels, which guarantee an order more accurate position than the one calculated from the readings of the encoders mounted directly on the driving wheel shaft; in the front, the presented position sensor can be observed, Fig.4a. The floor was smooth, made of linoleum, Fig.4b.

The position sensor was tested on two types of paths: on the first (Fig.5a), the robot was programmed to make 8 turns, i.e., four left and four right turns; on the second (Fig. 5b), the robot moves along a long and narrow corridor.

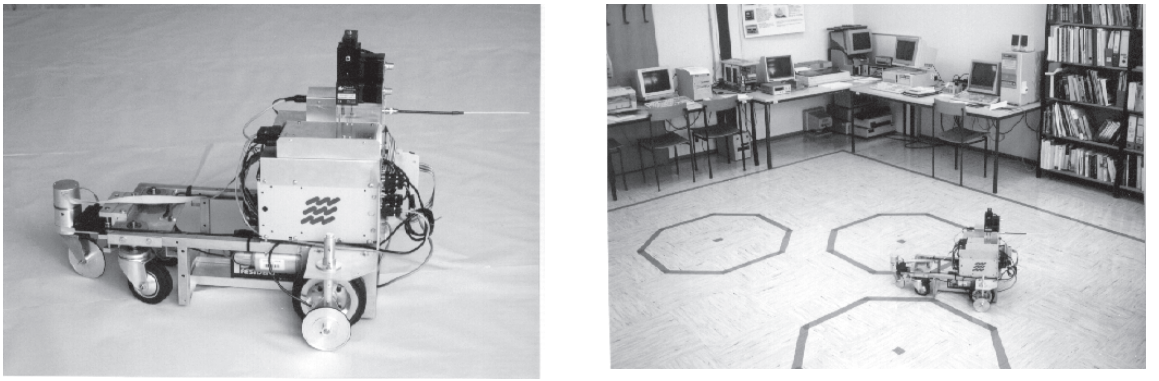

a) b)

Sl. 4. *V preizkusih uporabljeni premični robot: a) zadaj, ob pogonskih kolesih, klasični par dodatnih merilnih kolesc; spredaj, v prispevku predstavljeno zaznavalo; b) vožnja v laboratoriju*

Fig. 4. *The mobile robot from the experiments: a) at the back, on each side of the driving wheels, a pair of classical measurement wheels, at the front, the proposed sensor, b) the drive in the laboratory*

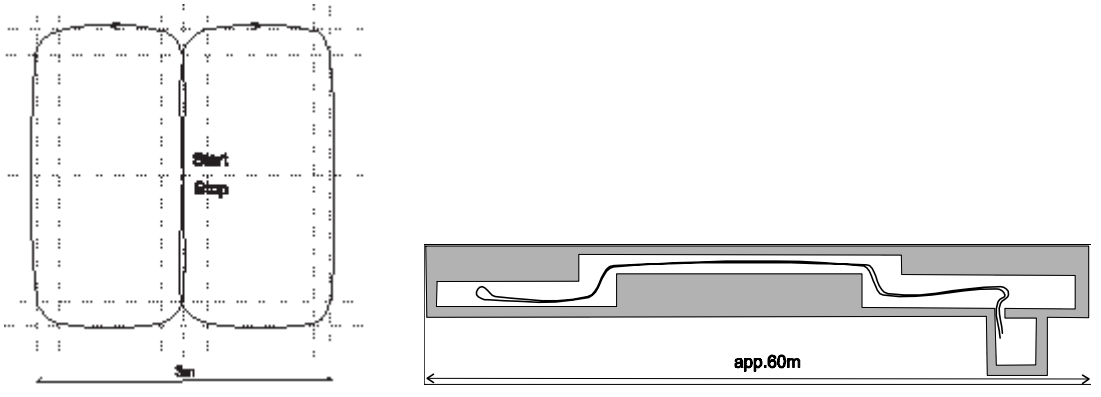

a) b)

Sl. 5. D*ve vrsti poti: a) osmica, b) dolg in ozek hodnik*

Fig. 5. *Two types of paths: a) a figure-of-eight path, b) a long and narrow corridor*

6.1 Prva vrsta poti: osmica

V tem primeru naj bi se robot, potem ko je na približno trimetrskem kvadratu opravil osem zavojev za 90°, vrnil v izhodiščno točko. Namen tega testa je bil preverjanje položajnega merilnika ob zavijanju. Dolžina poti je bila približno 20 m, robotovo napako po desetih preizkusih pa vidimo na sliki 6a. Napaka je nekoliko večja v vzdolžni smeri (Y), kot v prečni smeri (X), vendar še vedno precej majhna (<0,4%), tudi za skupino robotov s pomožnimi merilnimi kolesi [2].

6.2 Druga vrsta poti: hodnik

Glavni problem dolgih in ozkih poti, kakršen je hodnik pred laboratorijem (sl. 5b), je natančnost ničelnega kota β_0 kodirnika smeri, ki na usmeritev robota vpliva najbolj. Nenatančen povzroči vrtenje izračunanih poti, zato se pri tako dolgih poteh robot kaj lahko znajde v bližnjih stenah. Naše ocene za β_0 so se tako z že omenjenih 196,708° znižale na 196,617°, dokler se robotu pri 196,608° končno ni uspelo vrniti skozi vrata laboratorija na izhodiščni položaj; po prevoženih približno 120 m. Relativna napaka je tudi v tem primeru ostala <0,4% (sl. 6b).

6.1 The first type: figure-of-eight path

The robot was supposed to come back to the starting point, after accomplishing eight 90° turns on a square of 3m × 3m. The purpose of the test was to examine the behaviour of the sensor when a lot of turning is involved. The length of the path was approximately 20m; the positional error after ten trials can be seen in Fig.6. The error is somewhat bigger in the longitudinal (Y) than in the lateral (X) direction, but it is still reasonably small (<0.4%), even for the group of robots with additional measurement wheels [2].

6.2 The second type: corridor

The main problem with long and narrow working places, like the corridor in front of the lab, Fig. 5b, is the accuracy of the zero angle β_0 of the steering encoder, which has the strongest impact among all the parameters. An inaccurate β_0 results in the rotation of the paths, and the robot can quickly find itself hitting the walls. Our starting estimations for the β_0 values were reduced from the value already mentioned, 196.708°, to 196.617°, until the robot finally at 196.608° managed to re-enter through the lab door to the approximate starting position; after a 120-m-long journey. The relative error also remained <0.4% in this case (Fig. 6b).

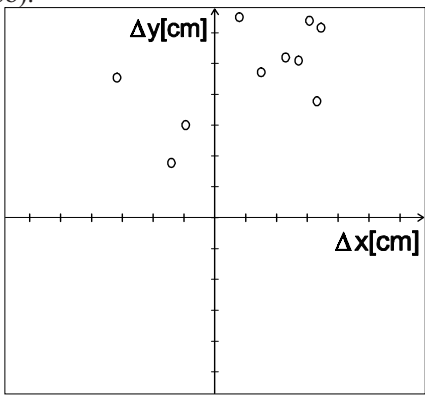

a)

Št. preizkusa Exp. no.	Δx [m]	Δy [m]
1	-0,101	-0,309
2	0,079	0,430
3	0,024	0,261
4	0,068	0,372

b)

Sl. 6. *Napaka po opravljenih testnih poteh: a) napaka robotove lege po prevoženih osmicah; b) napaka robotove lege po vožnjah v hodniku*

Fig. 6. *Position error after the tests: a) position error after the figure-of-eight turns ; b) position error after the journey in the corridor*

7 SKLEPI

Predstavili smo rezultate položajenja premičnega robota z izvirnim odometričnim položajnim zaznavalom, zasnovanim na samo enem dodatnem

7 CONCLUSIONS

The results of the experiments with a new odometrical position sensor, designed with one additional measuring wheel only, are presented. The

merilnem kolescu. Položajno zaznavalo sestavljata absolutni kodirnik za merjenje usmerjenosti merilnega kolesca in relativni kodirnik za merjenje prevožene poti. Preizkusi so pokazali, da je predlagano zaznavalo v natančnosti povsem primerljivo običajni rešitvi z dvema dodatnima merilnima kolescema ob pogonskih kolesih. Njegova prednost pa je v tem, da ga lahko namestimo na poljubnem mestu na robotu, zato je uporabnik z njegovo namestitvijo bistveno manj omejen. Pravzaprav bi lahko robota opremili celo z več takimi zaznavali in njihove rezultate povprečili.

Težavo pri uporabi pa pomeni razmeroma zamudno določanje vrednosti štirih parametrov: β_0, c, o_1 in a.

Na prvi pogled se zdi, da bi bila lahko težava, ali pa vsaj omejitev, morebitna neporavnanost med usmerjenostjo robota in izmaknjeno nameščenim merilnim kolescem zaznavala ob vklopu robota: izkaže se, da matematični opis v primeru NMK povsem zadovoljivo podaja položaj tudi v tem primeru. Kako je merilno kolesce zasukano, torej ni treba skrbeti niti pred prvo vožnjo.

sensor consists of an absolute encoder, which measures the orientation of the measuring wheel, and of a relative optical encoder, which measures the length of the path. Experiments proved the proposed sensor to be completely comparable to the classical solution with two measurement wheels mounted on each side of the driving wheels. However, it has the advantage that it can be mounted at an arbitrary place around the robot, so the user is far less restricted in terms of its use. In fact, one could equip the robot with even more position sensors and average their results.

The main problems associated with its use relate to the determination of its four parameters, β_0, c, o_1 and a.

At first sight it appears that the problem might be a possible misalignment of the orientation of the robot and the eccentrically mounted measuring wheel; however, it turned out that the discussion given in the case of NMW also holds good in this example. The actual orientation of the measuring wheel is not a problem, even before the first run.

8 LITERATURA
8 LITERATURE

[1] J.Borenstein, H.R.Everett, L.Feng (1996) Navigating mobile robots-systems and techniques, *A K Peters, Wellesley*, Massachusetts.

[2] J.Borenstein, L.Feng (1994) UMBmark - a method for measuring, comparing and correcting dead-reckoning errors in mobile robots, Technical Report UM-MEAM-94-22, *University of Michigan*.

[3] M.Blatnik (1996) Navigacija mobilnega robota z enim merilnim kolesom, Diplomsko delo, *Fakulteta za računalništvo in informatiko*, Ljubljana.

[4] Z.Fan, J.Borenstein, D.Wehe, Y.Koren (1995) Experimental evaluation of an encoder trailer for dead-reckoning in tracked mobile robots. *Proc. of the 10th IEEE Int.Syposium on Intelligent Control*.

[5] J.Borenstein (1994) Internal correction of dead-reckoning errors with smart encoder trailer, *Proc. of International Conf. on Intelligent Robots and Systems (IROS'94)*, Munich, Germany, September 12-16, 1994, str. 127-134.

[6] R.Mahkovic, T.Slivnik (2000) Constructing the generalized local Voronoi diagram from laser range scanner data, *IEEE Transactions on Systems, Man, and Cybernetics*, let.30, št.6, str.710 – 719, 2000.

[7] N.S.V.Rao, S.Kareti, S.S. Iyengar (1993) Robot navigation in unknown terrains: Introductory survey of non-heuristic algorithms. Tecnical report, ornl/tm-12410, *Oak Ridge National Laboratory*, Oak Ridge, Tennessee, 37831.

Avtorjev naslov: doc. dr. Rajko Mahkovic
Univerza v Ljubljani
Fakulteta za računalništvo in informatiko
Tržaška 25
1000 Ljubljana
rajko.mahkovic@fri.uni-lj.si

Author's Address: Doc. Dr. Rajko Mahkovic
University of Ljubljana
Faculty of Computer and Information Science
Tržaška 25
1000 Ljubljana, Slovenia
rajko.mahkovic@fri.uni-lj.si

Prejeto: 15.3.2006
Received:

Sprejeto: 25.4.2007
Accepted:

Odprto za diskusijo: 1 leto
Open for discussion: 1 year

Strojniški vestnik - Journal of Mechanical Engineering 53(2007)5, 297-309
UDK - UDC 628.83:531.755
Izvirni znanstveni članek - Original scientific paper (1.01)

Vzroki nezanesljivosti vzorčnih meritev pri določevanju koncentracije delcev v plinastem okolju

Causes of Sampling Measurement Uncertainties when Determining the Particle Concentration in a Gaseous Environment

Nastia Degiuli[1] - Nikola Barbalić[2] - Goran Marijan[2]
([1]University of Zagreb, Croatia; [2]Hrvatska elektroprivreda Zagreb, Croatia)

Merjenje koncentracij delcev je pomembno za veliko področij uporabe. Tako je predvsem od šestdesetih let prejšnjega stoletja, ko je bilo dokazan njihov škodljiv vpliv na zdravje ljudi. Pri merjenju koncentracij delcev pride do precej večjih napak, kakor pri merjenju emisij in/ali imisij drugih onesnaževal na področju ohranjanja kakovosti zraka. Pregledovanje posebnosti delcev v skupini onesnaževal zraka ter priprava splošnih standardnih oznak za emisijske in/ali imisijske količine za primer delcev zahtevata uporabo ene od dveh nasprotujočih si in skrajnih poenostavitev: sistem plin-delci obravnavamo v razmerah kontinuiranega okolja ali kot niz diskretnih trajektorij delcev v plinu. Zaradi omejitev razpoložljivih merilnih postopkov je rezultat v obeh primerih prikaz srednje vrednosti jakosti masnega toka, kot zmnožek srednje hitrosti in srednje vrednosti koncentracij, ki že v naprej vsebuje merilno napako. V tem prispevku smo se osredotočili na vzorčne lastnosti med določevanjem koncentracije delcev, ki so glavni vir merilne nezanesljivosti, ter na omejitve njihove izločitve v praksi.

(Ključne besede: koncentracija delcev, merilne negotovosti, vzorčenje, pogreški)

Measuring particle concentrations is very important in many applications; this has been particularly so since the 1960s, when their harmful influence on human health was proved. Measuring particle concentrations has a much greater measurement error than when measuring the emissions and/or immissions of other pollutants in the field of air-quality protection. Viewing the peculiarities of particles within the group of air pollutants, the elaboration of general standard specifications for emissions and/or immission quantities in the case of particles requires an approach to one of the two contradictory and extreme simplifications: the gas-particle system is either viewed in terms of a continuous environment or as a set of discrete particle trajectories in a gas. Due to the limitations of the available measurement procedures the result in both cases is the presentation of the mean value of the mass flow density as a product of velocity and concentration mean values, implying in advance a measurement error. In this paper attention has been focused on the sampling characteristics during the determination of the particle concentration, which are the main sources of measurement uncertainty, and on the limitations of their elimination in practice.

(Keywords: particles concentration, measurement uncertainties, sampling, measurement errors)

0 INTRODUCTION

An investigation of the state and/or the motion of a discrete, dispersed particle system in a fluid environment is of great importance for scientific and professional developments in many areas of human activities: the power industry, processing techniques, agriculture, meteorology, protection of the environment, health services, etc. For example, fluid flows and their dispersed particles (solid particles, droplets, bubbles) are the working body in various types of equipment with technical applications. In

such cases, the behaviour of the dispersed phase directly determines the equipment's operational characteristics, and for this reason particle trajectories represent an important step in the investigation of their function and are a basis for the development of their designs. Moreover, the problem of air pollution caused by flowing particles has been given increasing importance since it has been proved that their concentration in the air is one of the components that determines the level of their harmful influence on health. Other important components of health risks are the proportions in particular fractions according to particle size, chemical composition, mixtures, corrosiveness, radioactivity, fusibility, roughness, etc. Because of this, measurement procedures for the determination of the properties of different flowing particles are more demanding and are subject to a greater measurement uncertainty than the measurement procedures for the determination of the properties of other air pollutants. For every investigation of particles it is necessary to ensure a representative material sample. Exceptions are particular optical procedures that are preceded by a calibration with a material particle sample. Sampling is almost always a major source of measurement uncertainty when determining the particle state and/or the properties in a particle–fluid discrete, dispersed system. For such a system the sampling is realized by the suction of a limited volume (sample) of the particle–fluid dispersed system through a corresponding suction opening. The basic requirement is the sample's representative quality, i.e., its (sufficiently approximate) identity with the authentic dispersed system, with regard to the quantity that is established (concentration, particle size distribution, chemical composition, etc.). The question of representative quality should be dealt with during every sampling procedure.

Changes in the characteristics of the particle–fluid dispersed system sample, especially its concentration and particle size spectrum, can occur at the spot where the sample was taken, i.e., before being taken into the measurement device, as well as on the path through the suction pipe and through other components of the device, and finally, during further handling actions to the place where the desired analysis is performed. In this way, smaller or greater differences between the measured and the real quantities that are measured occur, resulting in corresponding measurement errors that belong to the group of systematic errors. Attention will be directed to the part of the errors that occur during the sampling of the particle–fluid dispersed system to the point where the sample is taken into the suction opening of the measurement equipment. As opposed to gas mixtures, for which the representative sample is relatively simply achieved, the representative sample of particle–fluid, and especially particle–gas, dispersed system is always questionable and requires additional verification.

1 DEFINITIONS OF EMISSION AND IMMISSION QUANTITIES

According to HRN ISO – Vocabulary [1], emission and emission quantities are expressed as follows:

D.1. Emission: Discharge of substances into the atmosphere. The point or the area from which the discharge takes place is called the source. The term is used to describe the discharge and the rate of discharge. The term can also be applied to noise, heat, etc.

D.2. Emission rate (emission velocity): The mass (or any other physical quality) of pollutant emitted into the air per unit of time.

D.3. Emission rate density (emission flux): Emission flux divided by the area of a corresponding emission source.

Immission and immission quantities have the same meaning as emission and emission quantities, but with the opposite sign. Simply, the receptor substitutes the source, and all the rates/transitions are in the direction from the air to a particular receptor instead of in the direction from a source into the air. Thus, the HRN ISO Vocabulary [1] confirms: "immission…..is the opposite of emission". A mathematical determination of the terms *immission* and *emission* is given in ISO/TR 4227 [2] in terms of immission and emission flow, but unfortunately, with some omissions and errors [3]. Taking into consideration the discussion in paper [3], the immission/emission flow terms, in relation to ISO/TR 4227 [2], could be correctly defined in the following manner:

D.4. Immission rate $I(t)$ to a particular receptor is defined by the enveloping surface integral:

$$I(t) = \int_{F_I} \rho \cdot (\vec{v} \cdot \vec{n}) \cdot \mathrm{d}F_I \qquad (1).$$

D.5. Emission rate $E(t)$ of a source is defined by the enveloping surface integral:

$$E(t) = \int_{F_E} \rho \cdot (\vec{v} \cdot \vec{n}) \cdot \mathrm{d}F_E \qquad (2),$$

where (in two preceding equations):
$F_I||F_E$ – is the smallest enveloping surface around the receptor||source,
ρ – is the density (a property divided by volume) at the enveloping surface $F_I||F_E$,
$\vec{v}$ – is the velocity vector of the property at the enveloping surface $F_I||F_E$,
$\vec{n}$ – is the normal vector of the enveloping surface element $\mathrm{d}F_I||\mathrm{d}F_E$ pointing outwards so that the following is valid:

$$\int_{F_I}\left(\vec{v}\cdot\vec{n}\right)\mathrm{d}F_I \geq 0\,,\ \int_{F_E}\left(\vec{v}\cdot\vec{n}\right)\mathrm{d}F_E \geq 0 \qquad (3),$$

$\rho\cdot\vec{v}$ – is the immission||emission flux/rate density on the enveloping surface $F_I||F_E$.

The definition of Equation (1)||(2) for the immission||emission rate cannot be strictly applied to solid or liquid particles because of their discrete distribution. Here, the quantity ρ – property (for particles it is usually the mass m) divided by volume, might be considered in the following two ways:
(i) The elementary volume ΔV in the vicinity of each observed point $P(\vec{r})$ in space is sufficiently large at a given moment of time and it still contains a large number of particles, which makes it representative for describing the spatial distribution of particles. Thus:

$$\rho = \frac{\Delta m_p}{\Delta V} = c_m\left(\vec{r},t\right) \qquad (4),$$

represents the particle mass concentration field that, from the said condition, is continuous at all points on the surface $F_I||F_E$ so the immission||emission rate according to Equation (1)||(2) is equal to:

$$I(t)\left\|E(t)=\dot{m}_p(t)=\int_{F_I\|F_E} c_m\left(\vec{r},t\right)\cdot\vec{v}_p\left(\vec{r},t\right)\cdot\vec{n}\left(\vec{r}\right)\mathrm{d}F = \right. \qquad (5),$$
$$=\left[\overline{c_m(t)\cdot v_p(t)}\right]\cdot F \neq \overline{c_m(t)}\cdot\overline{v_p(t)}\cdot F$$

where for average values $\overline{c_m(t)}$ and $\overline{v_p(t)}$ over the surface $F_I||F_E$ the following applies:

$$\overline{c_m(t)}=\frac{1}{F}\int_{F_I\|F_E} c\left(\vec{r},t\right)\mathrm{d}F$$
$$\overline{v_p(t)}=\frac{1}{F}\int_{F_I\|F_E}\left[\vec{v}_p\left(\vec{r},t\right)\cdot\vec{n}\left(\vec{r}\right)\right]\mathrm{d}F \qquad (6),$$

where $F = F_I||F_E$.
(ii) The elementary volume ΔV in the vicinity of each observed point $P(\vec{r})$ at a given moment in time is sufficiently small (to the continuity limit of the dispersed medium – fluid phase). Then:

$$\rho = \lim_{\Delta V\to 0}\frac{\Delta m}{\Delta V} = \begin{cases}\rho_p & \text{for} \quad P\left(\vec{r}\right)\in V_p\\ \rho_f & \text{for} \quad P\left(\vec{r}\right)\in V_f\end{cases} \qquad (7),$$

where it has been taken into account that the observed volume V consists of the particle volume, V_p, and the fluid volume, V_f, i.e.,

$$V = V_p + V_f \Leftrightarrow F = F_p + F_f\,,\left(V = k\cdot F\right) \qquad (8).$$

For the particle volume concentration $\overline{c_v}$ and porosity $\overline{\varepsilon}$, the following is valid:

$$\overline{c_v} = \frac{V_p}{V} = \frac{F_p}{F} = 1-\frac{F_f}{F} = 1-\frac{V_f}{V} = 1-\overline{\varepsilon} \qquad (9),$$

i.e.,

$$F_p = \overline{c_v}\cdot F,\quad F_f = \left(1-\overline{c_v}\right)\cdot F \qquad (10).$$

From the definition of Equation (1)||(2), the immission||emission rate is as follows:

$$I(t)\left\|E(t)=\dot{m}_p(t)=\int_{F_I\|F_E}\rho\left(\vec{r},t\right)\cdot\vec{v}_p\left(\vec{r},t\right)\cdot\vec{n}\left(\vec{r}\right)\mathrm{d}F = \right.$$
$$=\int_{F_p}\rho_p\cdot\vec{v}_p\left(\vec{r},t\right)\cdot\vec{n}\left(\vec{r}\right)\mathrm{d}F=\rho_p\sum_i\left[\vec{v}_p\left(\vec{r},t\right)\cdot\vec{n}\left(\vec{r}\right)\right]_i\cdot\left(\Delta F_p\right)_i =$$
$$=\rho_p\cdot\left(\overline{v_p\cdot c_v}\right)\cdot F\neq\rho_p\cdot\overline{v_p(t)}\cdot\overline{c_v(t)}\cdot F=\overline{c_m(t)}\cdot\overline{v_p(t)}\cdot F \qquad (11),$$

where,
$\left[\vec{v}_p\left(\vec{r},t\right)\cdot\vec{n}\left(\vec{r}\right)\right]_i$ – is the projection of i-th particle velocity in the direction $\vec{n}$,
$(\Delta F_p)_i$ – is the projection surface of the i-th particle normal to $\vec{n}$,
taking into account that,

$$\vec{v}_p\equiv 0 \quad \text{for} \quad P\left(\vec{r}\right)\notin F_p \qquad (12).$$

In Equations (5) and (11), in which the particle immission||emission rate is reduced to the mean values over the surface $F_I||F_E$, attention should be drawn to the inequality sign, which emphasises that the immission||emission particle flow is not equal to the product of the product of concentration and velocity mean values over the surface $F_I||F_E$. This product is the basis of the measurement procedures for determining the immision||emission particle flow. Thus, the initial measurement uncertainty is built-in in advance into the measurement procedures for the determination of the immision||emission particle rate. The value of the measurement uncertainty for a particular measurement procedure is proportional to the quantity ratio on the left- and right-hand sides of the inequality in Equations (5) and (11).

Generally, the particle mass concentration is determined by Equation (4). However, according to the regulations [4], a definition for the mass concentration of the pollutants is:
D.6. The mass concentration of pollutants in exhaust gases is the pollutant mass per volume unit of dis-

charged gas at a temperature of 273.15 K and a pressure of 101.325 kPa. It is obvious that this defines the mass of the discharged pollutant in the discharged gas. Thus, it is the mass flow concentration c_M:

$$c_M(t)=\frac{\dot{m}_z(t)}{\dot{V}_n(t)}=\rho_n\cdot\frac{\dot{m}_z(t)}{\dot{m}_f(t)} \quad (13),$$

where the indices denote z for the pollutant and n for the standard gas parameters (e.g., 273.15 K, 101.325 kPa). The denominator in Equation (13) is determined from the following equation:

$$\dot{V}_n(t)=\frac{1}{\rho_n}\dot{m}_f(t)=\frac{T_n}{p_n}\cdot\int_F\frac{p(\vec{r},t)}{T(\vec{r},t)}\cdot\vec{v}_f(\vec{r},t)\cdot\vec{n}(\vec{r})\,\mathrm{d}F= \\ =\frac{T_n}{p_n}\cdot\left[\overline{\frac{p(t)}{T(t)}\cdot v_f(t)}\right]\cdot F \quad (14).$$

From Equations (5), (13) and (14), the mass flow concentration for the particulate matter (index: $z=p$) is:

$$c_M(t)=\frac{p_n}{T_n}\cdot\frac{\left[\overline{c_m(t)\cdot v_p(t)}\right]}{\left[\overline{\frac{p(t)}{T(t)}\cdot v_f(t)}\right]} \quad (15).$$

Furthermore, the volume flow concentration, c_V, for particulate matter is:

$$c_V(t)=\frac{\dot{V}_p(t)}{\dot{V}_n(t)}=\frac{\rho_n}{\rho_p}\cdot\frac{\dot{m}_p(t)}{\dot{m}_f(t)}=\frac{1}{\rho_p}\cdot c_M(t) \quad (16).$$

A concentration measurement is essential for any measurement method for determining the immission and emission quantities. In an immission measurement, that is usually the final objective: the concentration field of some area, space and the like, on the basis of which the immission rate, the rate density, and the immission dose are evaluated in relation to particular receptors. The concentration for emission monitoring and evaluating has the meaning of a subsidiary quantity in order to determine/monitor the source emission flow, i.e., its significance in terms of the environmental contamination.

2 SAMPLING OF PARTICLES IN THE DETERMINATION OF THEIR CONCENTRATIONS IN A GASEOUS ENVIRONMENT

There are two essentially different cases of sampling of particles that can be found in applications [5]: (i) the sampling of flowing particle-gas systems, (ii) the sampling of stationary particle-gas systems. A direct quotation from the English original [5] describes the division as: (i) *sampling of flowing aerosols*, (ii) *sampling of stationary aerosols*. The correct interpretation of the term aerosol can be considered as questionable. This headword in the Croatian version of the three-language dictionary [1] is cited with following meaning:

D.7. Aerosol: a two-phase system in which the continuous phase is gaseous and the dispersed phase is liquid and/or solid; dispersed system particles have a negligible deposition velocity in the gravitational field.

In this definition, the limit of neglecting the deposition velocity is not determined and with no reason aerosols are attributed to a relatively narrow subclass of particle-fluid dispersed systems. Since during every sampling of the particle-gas system care must be taken about the influence of gravitational forces (i.e., how to avoid their influence on the measurement error), it is more correct to accept the following definition [6]:

D.8. Aerosol: a two-phase system in which solid and/or liquid particles are dispersed in a gas.

Yet, for that, as well as for any other particle system dispersed in a fluid, it should be kept in mind that its existence depends on the mutual ratio of the gravitational and carrying forces. According to such a rule, aerosols would be a subclass of a particle-fluid dispersed system, for which, approximately, the size of the dispersed solid/liquid particles is in the range (aerodynamic diameter) of 2 nm to 100 μm [6]. Essentially, such a particle size range covers aerodispersed systems, which are a subject of interest for environmental protection (air-quality protection). In accordance with the introduced classification, the sampling of the flowing gas-particle system includes aerosols that flow through pipe ducts and the like, as well as atmospheric aerosols in the presence of wind, while the sampling of the stationary gas-particle system includes aerosols in quiet conditions, including both the outside air and the air of working or indoor living spaces. In the sampling of flowing aerosols, measurement errors are mainly a consequence of particle inertia forces that condition the deviation of the particle trajectory from the streamline (Fig. 1) [7]. If the sample opening is not placed isoaxially (Fig. 1.a)), or if the sample suction velocity is higher (Fig. 1.b)) or lower (Fig. 1.c)) than the fluid velocity in the undisturbed flow, the sample particle concentration will be smaller (Fig. 1.a) and b)) or greater (Fig. 1.c)) than the real particle concentration.

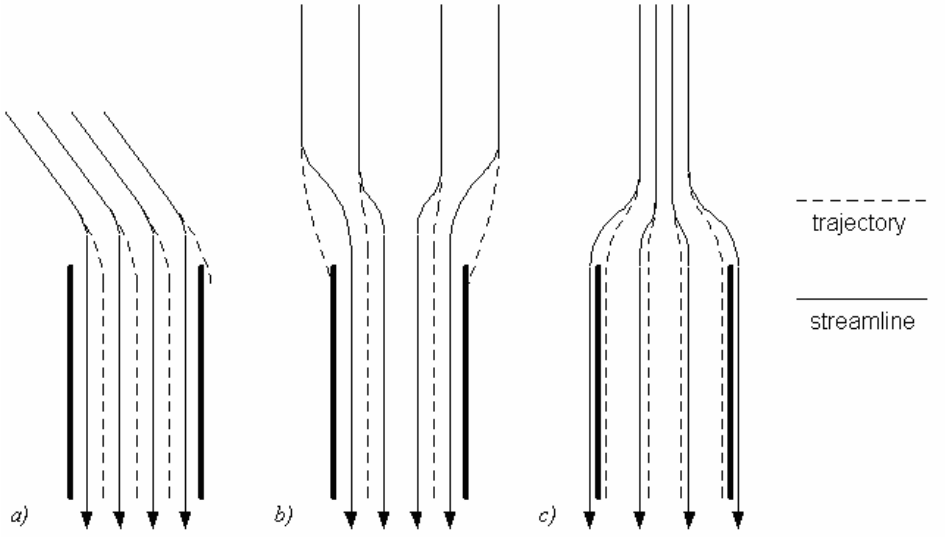

Fig. 1. *Errors in the flowing aerosol sampling: a) non-isoaxial, b) non-isokinetic, c) sub-isokinetic*

Therefore, sampling should be isoaxial, isokinetic and the wall of the suction pipe (probe) should be sufficiently thin.

The sampling of stationary aerosols has no analogy with the sampling of flowing aerosols because the flow field in the neighbourhood of the sampler opening in the case of the flowing fluid environment (Fig. 1) is completely different from the flow field created around the sampler opening in the case of the stationary fluid environment (Fig. 2). In addition, this type of sampling has been less frequently investigated than the sampling of flowing aerosols. Regardless of the difference in the fluid flow field created in the two mentioned opposite cases in the neighbourhood of the sampler input opening, the increase in the measurement error of aerosol sampling, compared to other (gaseous) pollutants, is a consequence of the particle trajectory in the fluid environment.

3 PARTICLE TRAJECTORY PROPERTIES

The measure of the particle size is its equivalent diameter [1]:

D.9. The equivalent diameter is the diameter of a round particle that has the same geometrical, optical, electrical or aerodynamic behaviour as the tested particle.

The hydrodynamic/aerodynamic particle behaviour is of major importance for the sampling of aerosols. As such, the measure of the particle size is its diameter, the Stokes diameter or the aerodynamic diameter. If u_s denotes the stationary deposition velocity of some observed particle in an infinitely spread fluid environment at rest under the action of gravitational force, the equivalent diameter of that particle in relation to the deposition velocity comes to:

$$x_s = x = \frac{3}{4} \cdot C_w\left(Re\right) \cdot \frac{\rho_f}{\left(\rho_p - \rho_f\right) \cdot g} \cdot u_s^{\,2} \qquad (17),$$

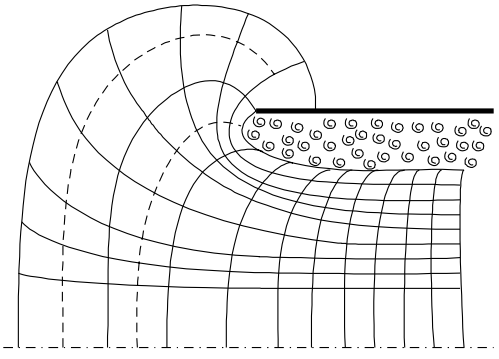

Fig. 2. *Flow field during suction from a stationary fluid environment*

where $C_w(Re)$ is the resistance coefficient of a sphere of diameter x and

$$Re = \frac{u_s \cdot x \cdot \rho_s}{\mu} \tag{18}$$

is the Reynolds number.

For $Re \le 0.25$ (the range in which the Stokes law is valid), according to [8] the following is valid:

$$C_w = \frac{24}{Re}, \quad Re \le 0.25 \tag{19},$$

and the diameter determined by Equation (17), according to (19), is the Stokes equivalent particle diameter :

$$x_{st} = \sqrt{\frac{18 \cdot \mu \cdot u_s}{g \cdot (\rho_p - \rho_f)}} \tag{20}.$$

Regarding the range in which the Stokes law is valid (Equation (19)), Equation (20), in usual fluid conditions, can be applied up to $x_{st} < 50$ μm for air, and up to $x_{st} < 80$ μm for water. When aerosols are concerned, one can also use the aerodynamic equivalent diameter x_{ae} for which the particle deposition velocity is reduced to the Stokes sphere deposition velocity at $\rho_p - \rho_f = 1$ g/cm^3, i.e.,

$$x_{ae} = x_{st} \cdot \sqrt{\rho_p - \rho_f} \tag{21}.$$

Also, in the application of Equations (17), (20) and (21) for aerosols, because $\rho_f / \rho_p \approx 10^{-3}$, ρ_f is neglected in most cases.

A starting model for the aerosol sampling analysis in order to determine the corresponding immission and emission quantities is based on the following assumptions:

- particles are considered individually, without taking into account their mutual influence,
- the particle motion equation is set on the basis of the equilibrium of inertia, resistance, gravitational and pressure forces, i.e.,

$$\frac{\mathrm{d}\vec{u}}{\mathrm{d}t} = C_w(Re) \cdot F_p \cdot \frac{\rho_f}{2 \cdot m} \cdot |\vec{v} - \vec{u}| \cdot (\vec{v} - \vec{u}) + \left(1 - \frac{\rho_f}{\rho_p}\right) \cdot \vec{g} + \frac{\rho_f}{\rho_p} \cdot \frac{\mathrm{d}\vec{v}}{\mathrm{d}t} \tag{22},$$

where now,

$$Re = \frac{|\vec{v} - \vec{u}| \cdot \rho_f \cdot x}{\mu} \tag{23},$$

where x is the equivalent diameter in relation to the deposition velocity, and

$$m = \rho_p \cdot \frac{\pi \cdot x^3}{6}, \quad F_p = \frac{\pi \cdot x^2}{4} \tag{24}.$$

In the application for aerosols, it is justified in the second and the third terms on the right-hand side of Equation (22) to take the value $\pi_1 = \rho_f / \rho_p \approx 0$, thus obtaining the motion equation,

$$\frac{\mathrm{d}\vec{u}}{\mathrm{d}t} = \frac{3}{4} \cdot \frac{\rho_f}{\rho_p} \cdot |\vec{v} - \vec{u}| \cdot \frac{1}{x} \cdot C_w(Re) \cdot (\vec{v} - \vec{u}) + \vec{g} \tag{25},$$

and to accept the fact that the investigation of aerosols in the range of smaller particles ($Re < 0.25$), for which Equation (22) has a much simpler form, is particularly important, i.e., according to (19), (22), (23) and (24):

$$\frac{\mathrm{d}\vec{u}}{\mathrm{d}t} = \frac{18 \cdot \mu}{\rho_p \cdot x^2} \cdot (\vec{v} - \vec{u}) + \vec{g} \tag{26}.$$

However, for very small particles (for example $x_{st} < 1$ μm), the assumption of a fluid environment continuity gradually retreats as their magnitudes approach the magnitude of the free trajectory of fluid molecules, λ (for air in standard conditions $\lambda \approx 65$ nm). Then the particle resistance coefficient, C_w, depends on the Knudsen number

$$Kn = \frac{\lambda}{x} \tag{27},$$

so, the following is valid (for: $0.1 < Kn < 1000$; $Re < 0.25$):

$$C_w = \frac{24}{Re} \cdot \left\{1 + \frac{\lambda}{x} \cdot \left[2.514 + 0,800 \cdot \exp\left(-0.55 \cdot \frac{\lambda}{x}\right)\right]\right\}^{-1} = \frac{24}{Re} \cdot Cu^{-1} \tag{28},$$

where Cu denotes the Cunningham correction factor. When applying Equations (27) and (28) one should know how the equivalent particle diameter, x, has been determined because, due to the importance of the resistance coefficient, C_w, for the deposition velocity, the following is valid:

$$x = x_{st} \cdot \sqrt{\frac{1}{Cu}} \tag{29}.$$

The possibility of reducing Equation (22) to its forms (25) and (26), and the possible necessity of using corrections (28) and (29), is validated by means of the values of the similitude numbers:

$$\pi_1 = \frac{\rho_f}{\rho_p}, \ \pi_2 = Re = \frac{|\vec{v} - \vec{u}| \cdot \rho_f \cdot x}{\mu}, \ \pi_3 = Kn = \frac{\lambda}{x} \tag{30}.$$

In order to reach a complete understanding of the terms in Equation (26) it is necessary to recognize the remaining important similitude numbers. By applying the integral analogy procedure [9], from

Equation (26) it follows that:

$$\tau \cdot \frac{u}{t} \propto v \propto u \propto \tau \cdot g \tag{31}$$

where

$$\tau = \frac{\rho_p \cdot x^2}{18 \cdot \mu} = \frac{u_s}{g} \tag{32}$$

is the so-called particle relaxation time. Taking into account that for the characteristic length ratio the relation $L = v \cdot t$ is valid, the following similitude numbers are derived:

$$\pi_4 = \frac{u}{v} \tag{33}$$

$$\pi_5 = \frac{\tau \cdot \frac{u}{t}}{u} = \frac{\tau}{t} = \frac{\tau \cdot v}{L} = St \tag{34}$$

$$\pi_6 = \frac{\tau \cdot g}{v} = \frac{u_s}{v} = \frac{\tau \cdot v}{L} \cdot \frac{g \cdot L}{v^2} = St \cdot Fr^{-2} \tag{35}$$

where

$$St = \frac{\tau \cdot v}{L} = \frac{\rho_p \cdot x^2 \cdot v}{18 \cdot \mu \cdot L} \tag{36}$$

is the Stokes number, and

$$Fr = \frac{v}{\sqrt{g \cdot L}} \tag{37}$$

is the Froude number.

In a general case, Equations (25) or (26) cannot be analytically solved. To solve them it would be necessary to know the fluid velocity field $\vec{v} = \vec{v}(\vec{r})$, and then the solution could be obtained numerically (for example, the Runge-Kutta method). However, possible analytical solutions, for the simplest cases, give very important data concerning the behaviour of aerosol particles in sampling procedures.

a) Uniform particle motion. If the fluid velocity $\vec{v}$ is constant, particle motion can be divided into two periods. The first one (usually very short), in which a particle is decelerated or accelerated, and the second one, in which a particle is moving at constant speed, i.e., when $\mathrm{d}\vec{u}/\mathrm{d}t = 0$. According to (25), for the second period the motion equation reads,

$$\frac{3}{4} \cdot \frac{\rho_f}{\rho_p} \cdot |\vec{v} - \vec{u}| \cdot \frac{1}{x} \cdot C_w(Re) \cdot (\vec{v} - \vec{u}) + \vec{g} = 0 \tag{38}$$

Obviously, in this case, the relative fluid velocity (here, it is a gas) and the particle velocity have the direction of the vector $\vec{g}$, so Equation (38) can be written in scalar form, from which the vector $(\vec{v} - \vec{u}) \parallel \vec{g}$ is obtained. For a fluid at rest $|\vec{v}| = 0$, the particle deposition velocity $(u_s = |\vec{u}|)$ will be obtained.

b) Vertical motion. If all the vectors in Equation (25) or (26) have the direction of the vector $\vec{g}$, it is possible to find a complete solution for Equation (26) (which includes the period of acceleration/deceleration and the period of uniform motion), while in a general case ($Re > 0.25$) the solution of Equation (25) should be limited to the period of the particle uniform motion (i.e., the case described in a)).

c) Accelerated particle motion. If the first term on the right-hand side of Equation (25) is distinctly predominant in relation to the other term, that other term (gravitational acceleration) can be neglected. This is valid for very small particles. If the particle motion in the field with constant velocity ($\vec{v} = \text{const.}$) is concerned, the particle motion equation becomes,

$$\frac{\mathrm{d}(\vec{v} - \vec{u})}{\mathrm{d}t} = -\frac{3}{4} \cdot \frac{\rho_f}{\rho_p} \cdot |\vec{v} - \vec{u}| \cdot \frac{1}{x} \cdot C_w(Re) \cdot (\vec{v} - \vec{u}) \tag{39}$$

from which it follows that a change in the relative fluid and particle velocities can happen only in the direction of that relative velocity, i.e., only the intensity of the relative velocity can change, not its direction. The case for the range $Re \le 0.25$ (i.e., the range for very small particles) is of particular importance. Then, the differential Equation (39) assumes the form

$$\frac{\mathrm{d}(\vec{v} - \vec{u})}{\mathrm{d}t} = -\frac{18 \cdot \mu}{\rho_p \cdot x^2} \cdot (\vec{v} - \vec{u}) = -\frac{1}{\tau} \cdot (\vec{v} - \vec{u}) \tag{40}$$

and the equation for the intensity of the relative velocity $(\vec{v} - \vec{u})$ follows,

$$\frac{\mathrm{d}|\vec{v} - \vec{u}|}{|\vec{v} - \vec{u}|} = -\frac{1}{\tau}\mathrm{d}t \tag{41}$$

the solution of which is,

$$|\vec{v} - \vec{u}| = |\vec{v} - \vec{u}|_0 \cdot \exp\left(-\frac{t}{\tau}\right) \tag{42}$$

where $|\vec{v} - \vec{u}|_0$ is the initial intensity of the relative velocity. Obviously,

– for $t = \tau$ $\quad |\vec{v} - \vec{u}| = (1/e) \cdot |\vec{v} - \vec{u}|_0$ is valid (43),

– for $t \to \infty$ $\quad |\vec{v} - \vec{u}| = 0$ is valid (44),

i.e., the particle assumes the fluid velocity.

In a fluid at rest ($\vec{v} = 0$), according to (42),

$$\frac{\mathrm{d}s}{\mathrm{d}t} = u = u_0 \cdot \exp\left(-\frac{t}{\tau}\right), \quad \left(u = |\vec{u}|,\ u_0 = |\vec{u}|_0\right) \tag{45}$$

i.e.,

$$s = u_0 \cdot \tau \cdot \left[1 - \exp\left(-\frac{t}{\tau}\right)\right] \tag{46}$$

from where, for $t \to \infty$, the so-called stopping particle path (the penetration of the particle into the fluid at the starting velocity u_0) is obtained:

$$s_\infty = u_0 \cdot \tau \tag{47}$$

Thus, during the sampling of aerosols the ratio s_∞/D is very important because,

$$St = \frac{s_\infty}{D} = \frac{u_0 \cdot \rho_p \cdot x^2}{18 \cdot \mu \cdot D} \tag{48}$$

where D is the diameter of the suction probe opening.

However, as a rule, the upper limit of the applicability of equations derived from the condition $Re > 0.25$ (which is, for the air, approximately equivalent to the condition $x_{st} < 50$ μm) is not taken into account in applications. For the range $Re > 0.25$, the relaxation time $\tau = \tau^*$ should be defined directly from Equation (25), so then,

$$\tau^* = \frac{4}{3} \cdot \frac{\rho_p \cdot x}{\rho_f \cdot |\vec{v} - \vec{u}| \cdot C_w(Re)} \tag{49}$$

and the stopping trajectory,

$$s_\infty = u_0 \cdot \tau^* = u_0 \cdot \tau \cdot \varphi(Re_0) \tag{50}$$

where $\varphi(Re_0)$ is the correction function depending on the Reynolds number,

$$Re_0 = \frac{u_0 \cdot x \cdot \rho_f}{\mu} \tag{51}$$

the values of which are given in Table 1.

Table 1. *Correction function values*

Re_0	10^{-1}	10^0	10^1	10^2	10^3
$\varphi(Re_0)$	1.00	0.97	0.72	0.38	0.17

According to the correction function values, it follows that for $Re > 0.25$ the calculation of the stopping path from Equation (47) would give overestimated values.

4 SAMPLING WHEN DETERMINING THE EMISSION AND IMMISSION QUANTITIES

4.1 Emission measurements

Since it is either almost impossible or very difficult to correctly measure the pollutant emission at corresponding points of the minimum enveloping surface around the source (definition D.5), in the case of point sources, the emission measurements are best conducted on the discharge lines (e.g., smoke ducts, stacks, various exhaust pipes and the like). Generally, such measurements are particularly important in fossil-fuel fired power generation facilities, district heating and the chemical industry. If there are no reverse air flows or particle depositions or similar phenomena, i.e., generally, if there is no source and sink in the discharge conduit, then the below applies for steady-state conditions (Fig. 3):

$$\dot{m}_p = \text{const}(F_E), \qquad \dot{m}_g = \text{const}(F_E) \tag{52}$$

i.e., as from Equations (11) and (14):

$$c_M = \text{const}(F_E), \qquad c_V = \text{const}(F_E) \tag{53}$$

it would generally be irrelevant where (in which cross-section of the discharge duct) the emissions are measured. Even a possible reverse flow of air in the discharge line and/or gas discharge downstream of the measurement point and/or the deposition of particles upstream of the measurement point, and the like, do not affect emission quantities, which are, according to the regulations, reduced to dry gases, their standard condition and specified oxygen percentages. The selection of an appropriate measurement cross-section is actually determined by the limitations imposed by the measurement procedures and equipment. Specified rules (or guidelines) pertaining to the specified monitoring of emission usually regulate the selection of an appropriate measurement cross-section. Particularly important is the distance from the upstream and/or downstream sources of the fluid flow disturbance (expressed through a hydraulic diameter multiple) ([10] to [12]) and, for particles, the properties related to their inertial characteristics: possible deposition (the advantage of vertical in relation to horizontal ducts); a possibly more pronounced non-uniform particle concentration across the section of discharge ducts, for example, after flow disturbances; the dependence of inertial effects on the particle granulometric composition and the particle density [12].

In applications, when monitoring pollutant emissions into the air, the selected conditions are usually those that enable a rational use of the available measurement techniques and also enable simplifications, while having an acceptable effect on

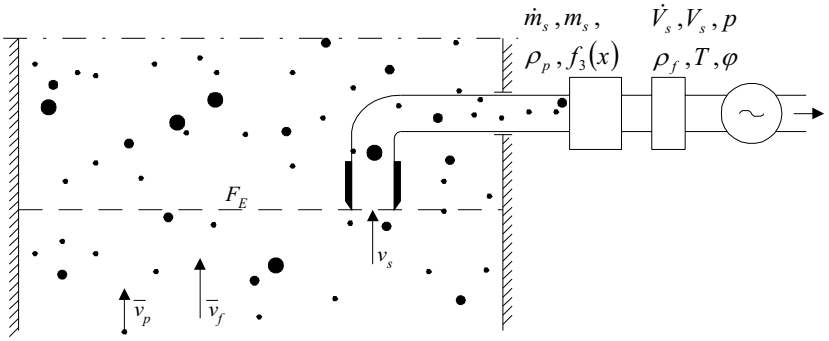

Fig. 3. *Arrangement of the gravimetric and photometric measurement of particulate emission quantities*

the reliability of the final results. These are as follows:

(i) Selection of the measurement surface, F_E, in a plane of the discharge section where the following applies:

$$\vec{v}_p \parallel \vec{v}_f \parallel \vec{n} \tag{54}$$

and at points at which there are no (local) particle concentrations and/or gas velocity gradients in the direction of the unit vector $\vec{n}$.

(ii) The pressure $p(t)$ and the temperature $T(t)$ are measured at a single representative point on the surface, F_E (with a possible exception for scientific purposes), i.e., they are accepted as invariable in the average plane points.

(iii) The following is accepted (see Equations (5) and (11)):

$$\begin{aligned} \overline{c_m(t)\cdot v_p(t)} &= \overline{c_m(t)}\cdot\overline{v_p(t)} \\ \overline{v_p(t)\cdot c_v(t)} &= \overline{v_p(t)}\cdot\overline{c_v(t)} \end{aligned} \tag{55}$$

Obviously, compared to gaseous pollutants, it is more difficult to satisfy conditions (i) and (iii) when measuring particulate emission because the particles are exposed to the inertia forces.

Considering conditions (i)–(iii), Equations (5), (11), (14) and (15) may be simplified for the discharge ducts and, consequently, a simpler measurement procedure can be applied. For the said conditions, the following applies to the discharge ducts:

$$\dot{m}_p(t) = \overline{c_m(t)}\cdot\overline{v_p(t)}\cdot F_E \tag{56}$$

$$c_M(t) = \frac{p_n}{p(t)}\cdot\frac{T(t)}{T_n}\cdot\frac{v_p(t)}{v_f(t)}\cdot\overline{c_m(t)} \tag{57}$$

An important characteristic of gravimetry is the acceptance of the iso-kinetic suction of particulate matter samples. At the *i*-th point of the measurement plane, F_E (Fig. 3), the following is chosen:

$$v_{si} = v_{fi} \tag{58}$$

With the standardized measurement procedure, and the already introduced simplifications (described, for example, in [11]), the gravimetric mass concentration, c_{GR}, will be:

$$c_{GR} = \rho_n\cdot\frac{m_p}{m_f} = \frac{p_n}{p}\cdot\frac{T}{T_n}\cdot\frac{\sum_i\left(v_p\cdot c_m\right)_i\cdot\Delta F_{Ei}\cdot\Delta t_i}{\sum_i v_{fi}\cdot\Delta F_{Ei}\cdot\Delta t_i} \tag{59}$$

and with the specified condition,

$$\Delta F_{Ei} = \mathrm{inv}(i), \qquad \Delta t_i = \mathrm{inv}(i) \tag{60}$$

this gives:

$$c_{GR} = \frac{p_n}{p}\cdot\frac{T}{T_n}\cdot\frac{\overline{\left(v_p\cdot c_m\right)}}{\overline{v_f}} \tag{61}$$

where p and T are either the average time values during the period $\sum_i \Delta t_i$ or the measurement has been conducted under (nearly) steady-state conditions. However, only if,

$$v_{pi} \approx v_{fi} \tag{62}$$

is assumed, it will give,

$$c_{GR} = \frac{p_n}{p}\cdot\frac{T}{T_n}\cdot\frac{\overline{\left(v_f\cdot c_m\right)}}{\overline{v_f}} = \overline{c_m} \tag{63}$$

i.e., from Equation (61), and taking into account Equations (5), (11) and (15), the emission gravimetry corrects the procedure of averaging over the points in the plane F_E. For emission flow (averaged for the period $\sum_i \Delta t_i$), the following applies:

$$\dot{m}_p = c_{GR}\cdot\frac{\dot{m}_f}{\rho_n} = \overline{\left(v_p\cdot c_m\right)}\cdot F_E \approx \overline{\left(v_f\cdot c_m\right)}\cdot F_E \neq \overline{v_f}\cdot\overline{c_m}\cdot F_E \tag{64}$$

4.2 Immission measurements

The sampling of aerosols is a particularly complex procedure if it is carried out in outdoor conditions, because the intensity, line and direction of

the wind and, also, the concentration and size of the flowing particles are very changeable quantities [13]. For example, an increase in the wind velocity causes, in most cases, an increase in the size of the dispersed particles, so, in this way, the Stokes number value (Equation (48)) is significantly increased. It is almost impossible to ensure the conditions of isokinetic suction of an aerosol sample for all possible values of wind velocity; therefore, the measurement error increases with the increase in Stokes number. Theoretical approaches to the problem of aerosol sampling are reduced to the range of laminar fluid flow, although, in the real atmosphere, the flow of the air is more or less turbulent. The necessity of simulating the flows of monodispersed particles with a constant concentration accounts for the limitations and relatively large errors of the experimental approach. In applications, for routine emission measurements, suction is usually carried out through an opening with a section mounted in the horizontal plane, in the top-to-bottom direction. In order to make the direct deposition of (especially big) particles in the suction opening impossible, and to prevent the penetration of atmospheric precipitation, the suction opening is covered with plates of different shapes, placed at a small distance from the opening. In this way, a relatively efficacious suction of particles of approximately 100 μm is realized, and there is only a slight probability of the suction of significantly larger particles. The aerosol sampled in this way can be conducted through impaction degrees if it is necessary to determine the particle size distribution or the concentration of particle PM_{10} or $PM_{2.5}$ in the aerosol (the concentration of the fine particle fraction with the limiting particle size of 10 μm or 2.5 μm). In theoretical procedures, because of the difficulties in solving particle trajectory equations (Section 4), the cases where either inertia or gravitational forces can be neglected are usually considered separately. Evidently, while sampling, no inertial particles with a probe/pipe placed in the vertical line, at the suction velocity v_s, the particle concentration $(1 \pm u_s / v_s)$ times changed ("+": top-to-bottom; "–": bottom-to-top) is obtained in the sample.

The theoretical solution of the case of aerosol suction through a point sink placed in a vertical plane (wall) ([5] and [7]) is of particular importance. The starting point of the consideration is a two-dimensional case (Fig. 4): the aerosol is sucked in through an infinitely narrow clearance of infinite length (point 0) from the half-space (right half-plane in Fig. 4) limited by the wall plane. The differential equation of the motion of small particles ($Re \leq 0.25$), according to (26) and (32), is,

$$\frac{\mathrm{d}\vec{u}}{\mathrm{d}t} = \frac{1}{\tau} \cdot \left(\vec{v} - \vec{u}\right) + \vec{g}, \quad \left(\tau = \frac{u_s}{g}\right) \tag{65}.$$

Neglecting the inertia forces, the following is valid:

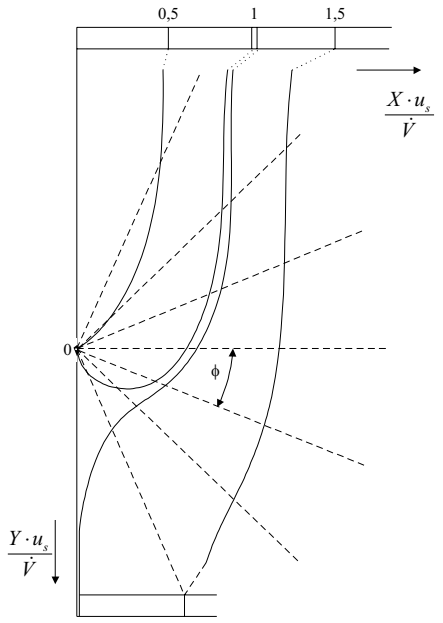

Fig. 4. *Sampling of aerosols through an infinitely narrow clearance*

$$\vec{u} = \vec{v} + \tau \cdot \vec{g} \quad (66),$$

i.e.,

$$\frac{\mathrm{d}\xi_i}{\mathrm{d}t} = v_i + u_s \cdot \delta_{i2} \quad (67),$$

where ξ_i are coordinates of particle position vector,

$$\xi_i = \{X, Y\} \quad (68).$$

If $\dot{V}$ is the volume flow of the air that is sucked per unit length of clearance, the components of the air velocity vector are (Fig. 4):

$$v_i = \left\{ -\frac{\dot{V} \cdot X}{R^2 \cdot \pi}, \; -\frac{\dot{V} \cdot Y}{R^2 \cdot \pi} \right\}, \qquad \left(R^2 = X^2 + Y^2\right) \quad (69).$$

System (67) reduces to the following differential equation,

$$\frac{\mathrm{d}Y}{\mathrm{d}X} = \frac{Y}{X} - \frac{\pi \cdot u_s}{\dot{V}} \cdot \frac{X^2 + Y^2}{X} \quad (70),$$

i.e.,

$$\mathrm{d}\left(\frac{Y}{X}\right) = -\frac{\pi \cdot u_s}{\dot{V}} \cdot \left[1 + \left(\frac{Y}{X}\right)^2\right] \cdot \mathrm{d}X \quad (71),$$

with the solution,

$$\Phi = \frac{\pi \cdot u_s}{\dot{V}} \cdot \left[X_0 - X\right], \quad \Phi = \operatorname{arctg}\left(\frac{Y}{X}\right) \quad (72),$$

where X_0 is the particle initial position for $Y = -\infty$.

In terms of the obtained trajectories, the particle trajectory for which $X_0 \cdot u_s / \dot{V} = 1$ separates the particles that will be sucked from those that will miss the clearance. Consequently, all the particles, which for $Y = -\infty$ started from the length $L = \dot{V} / (1 \cdot u_s)$, pass through the unit of clearance length. Then, for $Y = -\infty$, particles move only at the velocity u_s, so if c is their concentration, the mass flow through the surface $L \cdot 1$ amounts to $\dot{m} = c \cdot u_s \cdot 1 \cdot L = c \cdot u_s \cdot 1 \cdot \dot{V} / (1 \cdot u_s) = c \cdot \dot{V}$. The concentration of particles sucked through the clearance is exactly $\dot{m} / \dot{V}$, i.e., it is equal to the initial concentration. Obviously, it is clear (Fig. 4) that inertial particles depart from these trajectories and that they either run into the wall under the clearance or keep on moving in the positive direction of the Y axis. Consequently, the final result is a decrease in the sample concentration. The magnitude of the deviation is exactly proportional to the stopping path $s_\infty = u_s \cdot \tau$. Because of this, the suction velocity should usually be several times higher than the deposition velocity, but then the question of the representative quality of the deposition velocity still needs to be dealt with because aerosol particles are regularly polydispersed in the range of several orders of magnitude. Regarding a possible exceptional influence of the wind on sampling errors, it is important to mention the conclusions of the experimental results of Maya and Druetta [5]: if the suction velocity, v_s, is constant, and the inlet velocity, v, of the particle-fluid dispersed system changes from 0 to v_s, the ratio of the sample particle concentration to the inlet aerosol A will change in a way that for $v = 0$, $A = 1$, so with the increase in v, A decreases, passes through a minimum and again, for $v = v_s$, assumes the value of $A = 1$. It should be pointed out that the departure of the value A from unity significantly decreases with the decrease of the particle size and is practically negligible for a particle size of approximately 1 μm.

5 CONCLUSION

In the group of measurement procedures intended for the determination of immission and emission quantities of substances considered as air pollutants, the measurement procedures for the determination of quantity, the condition and properties of the particle-fluid dispersed systems have particular significance because these procedures are subject to a significantly greater measurement uncertainty than the same measurement procedures intended for the determination of the immission and emission quantities of other air pollutants. Because of the discrete particle distribution in space, the definition of particle concentration in a gaseous environment demands a two-pronged approach: either by taking into account the discrete characteristics of particles, or by accepting the assumption of their continuous distribution – according to the conditions of the continuous environment. Using both the above mentioned approaches, the definition equations for the immission and emission flow are reduced to analogue expressions that are the basis for the corresponding measurement procedures. In these expressions it is necessary to accept approaches in relation to the averaging of the measurement quantities per surface of particle transition (emission/emission surface). In this way, the measurement uncertainty is built-in in advance.

The greatest cause of measurement uncertainty is the non-representative quality of the particle sample, as a consequence of the inertial properties of the particles, i.e., the impossibility of real-

izing the condition of the isoaxial and/or isokinetic sample suction, and the difference between the particle and the gas velocity vectors inside the sucked control volume of the particle-gas system. Regarding the fluid flow field that is formed in the neighbourhood of the suction opening, the difference between the sampling of the stationary and the flowing particle-gas system is of crucial importance because in the former and the latter cases the particle trajectories have a qualitatively different shape and hence a different demonstration of inertial action.

The immission monitoring of air pollution with particles is particularly subject to sampling errors. In this case, the measurement uncertainty decreases with the particle size decrease, so the regulatory evaluation of the air quality with respect to pollution with particles by using the fraction PM_{10} (the concentration of the fine particle fraction with a limiting particle size of 10 μm), as recently introduced in the European Union, is more convenient from the point of view of measurement uncertainty in relation to the former evaluations carried out by means of the concentration of the total amount of flowing particles.

6 NOMENCLATURE

$\bar{a}$	average of variable a
$\dot{a}$	time derivation of variable a
c	concentration
const(a)	constant concerning the choice of a
$E(t)$	emission rate
$I(t)$	immission rate
F	surface
inv(a)	invariance concerning a
k	constant
L	length
m	mass
p	pressure
$\vec{r}$	position vector
t	time
T	temperature
u	particle velocity
v	velocity
V	volume
x	equivalent particle diameter
δ	Kronecker symbol: $\delta_{ij} = \begin{cases} 1 & (i = j) \\ 0 & (i \neq j) \end{cases}$
ε	porosity
$\in$	is an element of
μ	dynamic viscosity
ρ	density
τ	particle relaxation time

Indices

E	emission
I	immission
f	fluid/gas
g	gas
GR	gravimetry
m, M	mass
n	standard parameters
N	number
p	particle
s	sample; deposition
v, V	volume

7 LITERATURE

[1] HRN ISO 4225: 1997, Air quality – General views – Dictionary (ISO 4225: 1994), Threelingual edition, Zagreb, 1997 – in Croatian.

[2] ISO/TR 4227, Planning of ambient air quality monitoring (1989) *ISO*, Genève.

[3] Barbalić N., Marijan G., Bilić Ž. (2001) Conditions and phenomena which a priori limit the confidence of continuous measurement of particulate emission in the air, *12th IUAPPA world clean air and environment congress*. Proceedings: ref. TS1-72c, Seoul.

[4] Regulation of limiting values for pollutant emission from stationary sources, *Narodne novine* No. 140, pp. 4406 – 4425, 1997; *Narodne novine*, No. 105, pp. 4008 – 4096, 2002.

[5] Fuchs N.A. (1975) Sampling of aerosols, *Atmospheric Environment* 9, pp. 697-707, 1975.

[6] Šega K. (2004) Flowing particles, *Gospodarstvo i okoliš* 12, No. 66, pp. 11-16, 2004.

[7] Fuchs N.A. (1955) Mehanika aerozoli, *Izd. AN SSSR*, Moskva.

[8] Löffler F. (1988) Staubabscheiden, *Georg Thieme Verlag*, Stuttgart – New York.

[9] Smolik J. (1977) Odlučovaní tuhých částic, *Fakulta strojní, ČVUT*, Praha.

[10] BS 893: Measurement of the concentration of particulate matter in ducts carrying gases, 1978; BS 3405: Measurement of particulate emission including grit and dust (simplified method), 1983; HRN ISO 9096: 1997, Stationary source emissions – Determination of concentration and mass flow rate of particulate material in gas-carrying ducts – Manual gravimetric method (ISO 9096: 1992), *State Office for Standardization and Metrology*, Zagreb, 1997.
[11] Bilić Ž., Barbalić N. (1985) Gravimetric procedure for concentration and mass flow measurements of solid particles in flowing gases in flow ducts, *Recommendation SDČVJ 301*, SDČVJ, Sarajevo – in Croatian.
[12] Hawksley P. G. W., Badzioch S., Blackett J. H. (1961) Measurements of solids in the flue gases, *The British Coal Utilization Research Association*, Leatherhead.
[13] Belyaev S.P., Levin L.M. (1974) Techniques for collection of representative aerosol samples, *Aerosol Science* 5, pp. 325-328, 1974.

Author' Addresses:
Doc. Dr. Nastia Degiuli
University of Zagreb
Faculty of Mechanical Engineering and
Naval Architecture
Ivana Lučića 5
10000 Zagreb, Croatia
nastia.degiuli@fsb.hr

Prof. Dr. Nikola Barbalić
Goran Marijan
Hrvatska elektroprivreda
Sektor za termoelektrane
Ulica grada Vukovara 37
10000 Zagreb, Croatia
goran.marijan@hep.hr

Prejeto: 6.6.2006
Received:
Sprejeto: 25.4.2007
Accepted:
Odprto za diskusijo: 1 leto
Open for discussion: 1 year

Strojniški vestnik - Journal of Mechanical Engineering 53(2007)5, 310-318
UDK - UDC 620.17:669.715
Pregledni znanstveni članek - Review scientific paper (1.02)

Overitev trajnosti aluminijastih sestavnih delov

Structural Durability Validation of Aluminium Components

Vatroslav V. Grubišić
(Reinheim, Germany)

Zaradi povečane uporabe aluminijevih zlitin za sestavne dele vozil je treba povzeti najsodobnejša spoznanja o presoji trajnosti sestave v delovnih pogojih. V prispevku smo predstavili postopke za preizkusno in numerično vrednotenje delovne trdnosti vlitka, kovanih in varjenih sestavnih delov iz aluminijevih zlitin. Predstavili smo tudi rezultate raziskav vpliva korozije, prav tako pa tudi metode pospešenega odobravanja preizkusov. Ti so nato potrjeni in priporočeni za uporabo v praksi.

(Ključne besede: delovni pogoji, trdnost materialov, trajnost, vplivi korozije, utrujenost materialov)

The increasing trend to use aluminium alloys for vehicle components makes it necessary to summarize the state of the art related to the approval of their structural durability under operational conditions. In this paper the procedures for the experimental and the numerical service-strength evaluations of cast, forged and welded aluminium-alloy components are presented. We also present the results of investigations of the influence of corrosion as well as the methods for accelerated test approval; these are then validated and a practical approach recommended.

(Keywords: service evaluation, strength of materials, structural durability, corrosion-fatigue-influence)

0 INTRODUCTION

The demands of the automotive industry for lightweight design and weight saving can only be fulfilled by going to the limits of the materials' properties, the manufacturing process, the behaviour of the structural part and the behaviour of the system. An increase in the reliability is required, but at the same time there is a desire to reduce test costs, coupled with efforts to improve the methods of numerical design.

Structural durability validation covers, on the one hand, special event loading and loading during misuse, and, on the other hand, service fatigue loading, characterized by the criteria of the structural yield point, the fracture behaviour and the fatigue strength ([1] and [2]), Fig. 1. Whereas an experimental proof of the strength safeguards the product safety, the numerical service strength evaluation serves as a pre-design procedure.

An intensive cooperation between the Fraunhofer Institute for Structural Durability and System Reliability (LBF), Darmstadt, and the Technical Faculty, Ljubljana, was started about 40 years ago by **Jože Hlebanja** and **Ernst Gassner**, and was continuously supported by co-workers and younger scientists. One of them, who contributed not only to this cooperation but also to the development of structural durability validation, was **Matija Fajdiga**. This cooperative research, especially the investigations related to the **structural durability of aluminium components**, which were supported by the EU ([3], [4] and [6]), are of great value.

This paper is a review of the results of all the available investigations about the structural durability of aluminium components, the study of which was initiated and supported by experts from AUDI AG, BMW AG, Daimler Chrysler AG, Porsche AG and Volkswagen AG, and carried out by authors of Ref. [1]. In it the procedures for the experimental and the

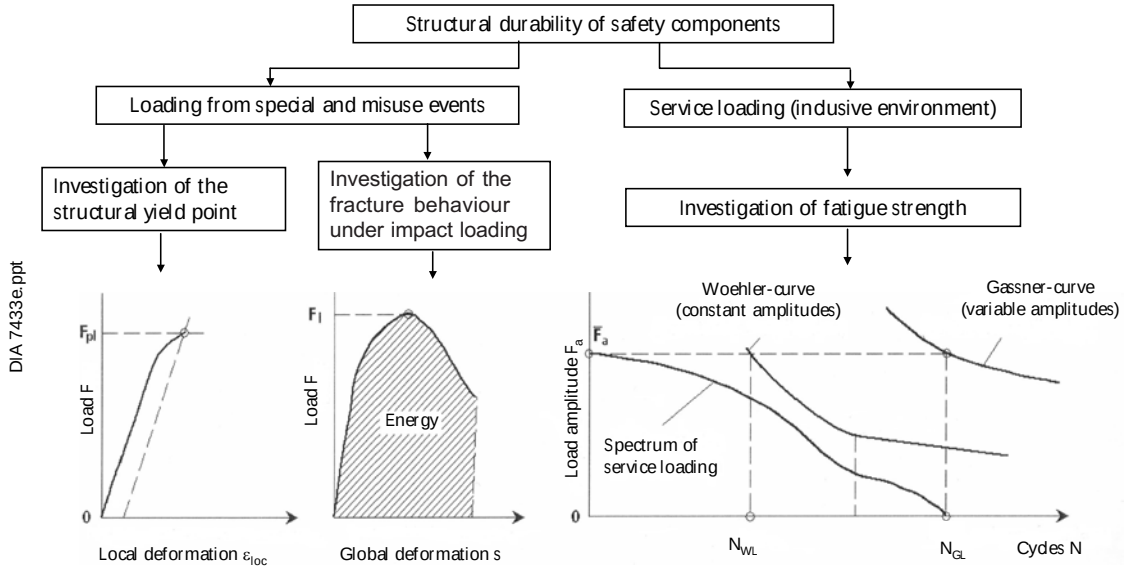

Fig. 1. *Partition of the structural durability*

numerical service-strength evaluation of cast, forged and welded aluminium-alloy components are presented. Furthermore, the results of the investigations of the influences of corrosion as well as the methods for accelerated test approval are presented, validated, and a practical approach is recommended.

1 THE EVALUATION OF SERVICE STRENGTH

1.1 Fracture strength

The relevant design criterion for a special event, for example, pressing a wheel against the curbstone edge when parking or when hitting a pothole with front wheel at braking, is usually the component's yield point. However, depending on the material and the component, a misuse criterion may become more relevant. The component's yield point is defined as the local equivalent strain or the corresponding equivalent stress, causing a plastic deformation of an allowable size, Fig. 2. A prerequisite is that neither an unacceptable global deformation of the component remains nor the required fatigue strength of the component decreases.

Experimental investigations to determine the component's yield point are carried out with vehicle- and component-relevant quasi-static loading, simulating the relevant special event. A recording of the load-local strain behaviour is recommended, making it possible to evaluate the material's fatigue behaviour and make a comparison with calculation results.

Fig. 3 shows the investigations on cast wheels (material G-AlSi7Mg T6), which were preloaded on the inner-rim side before the experimental structural durability validation was carried out. During preloading a special, seldom-occurring event is simulated, when the user drives over a "speed bump" or curbstone. Under such a loading a plastic, simply non-detectable, deformation can occur on the wheel, which could decrease the structural durability because of premature fatigue cracks on the rim, as shown in Fig.3.

Within the pre-design process the component yield point may be estimated by elastic/plastic finite-element analysis based on the monotonic stress-strain curve for the local stress state. If any indications exist that plastic deformations may cause damage, fatigue testing with a load spectrum derived from the component's service-load history is recommended.

The relevant design criterion for misuse events, for example, high-speed curbstone impact, is the fracture behaviour during impact loading, with which fractures without deformation, e.g., brittle fractures, must be excluded.

1.2 Fatigue strength

The fatigue strength of aluminium alloys decreases continuously for a large number of stress cycles. Based on experience, the knee point of the Woehler curve is assumed to be between $1 \cdot 10^6$ and $2 \cdot 10^6$ cycles. However, it may diverge from this, de-

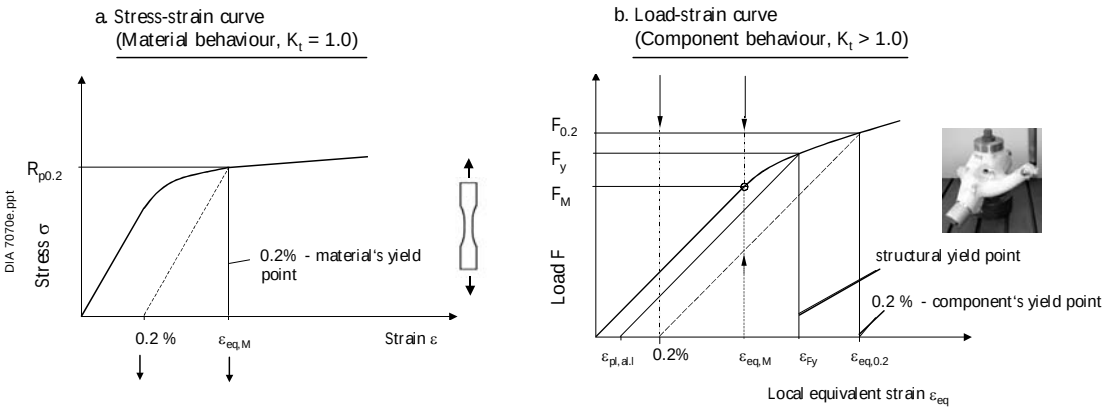

Fig. 2. *Structural yield point and plastic deformation*

Design	Weight [kg]	Plastic Deformation ΔD [mm]	Durability Test Life [km]
A	10.9	- 0.85	cracks at 4 979 ≈0.5
B	11	-0.55	cracks at 10 141 ≈1.0
C	11.35	-0.35	without cracks 14 920 >1.5

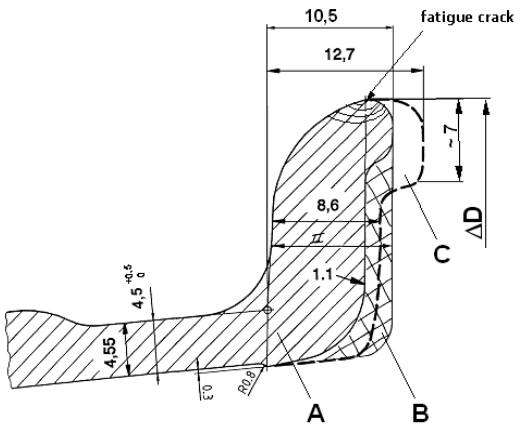

Fig. 3. *Influence of the rim design on plastic deformation and durability*

pending on the component, the material and the loading mode. As separately manufactured specimens do not inherit the shape, the surface condition and the residual stresses of the component, a direct transmission of the specimen's test results to the components is not possible.

Fig. 4 shows the empirically derived shape of the Woehler curve recommended for the pre-designing of the components from wrought or cast aluminium alloys according to the local stress concept when the specific component data are missing. The available, published quantitative material data are summarized in [1].

In Fig. 5 a generalized Woehler-curve for welded aluminium joints is presented. Compared to the aluminium base material the fatigue strength of the welded joint is less by a factor of between 1.3 and 3.0, assuming an equal stress distribution along the highly stressed section. The tensile strength, R_m, and the yield strength, $R_{p,0.2}$, of the base material have only a minor influence on the fatigue strength.

Residual tensile stresses caused by the change of microstructure as well as the solidification may degrade the fatigue strength. Such a degradation prevails in the range of large numbers of cycles ($N>1\cdot10^6$). When the magnitude of the residual stresses is known they may be assessed like mean stresses. Otherwise, it is recommended to cover the effect of residual stresses by choosing the allowable stresses resulting from the fatigue loading with R=0.

In the case of a fatigue-life estimation under variable-amplitude loading the recommended slopes of the Woehler curve are k=5 in the cycle region of $N<1\cdot10^7$ and k' = 2k–2 in the region of $N>1\cdot10^7$, as shown in Figs. 4 and 5.

For the design of welded joints the automotive industry normally applies the structural stress concept ([5] and [6]). The structural stress incorporates the influence of the weld geometry and the loading mode, but should not be mistaken for the maximum notch stress or the hot-spot stress [5], Fig. 6.

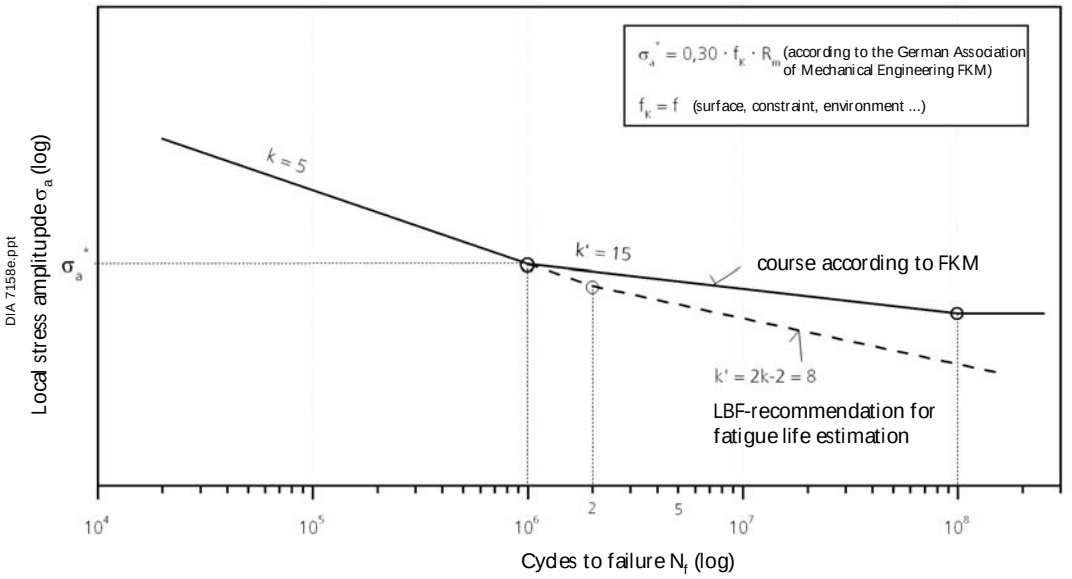

Fig. 4. *Schematical presentation of the Woehler-curve for components of wrought and cast aluminium alloys*

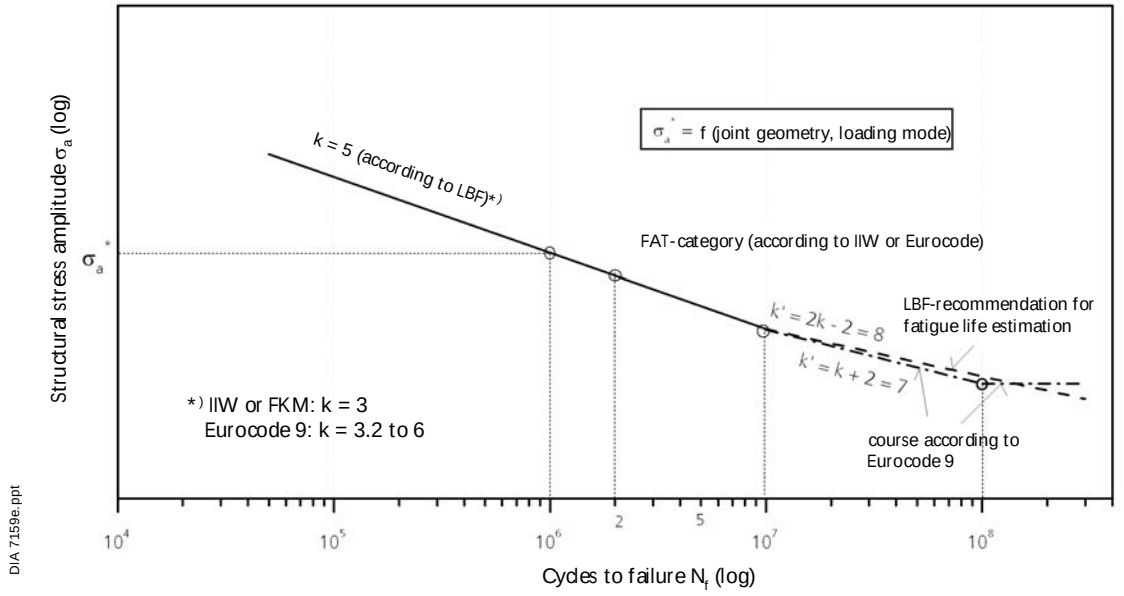

Fig. 5. *Schematical presentation of Woehler-curves for aluminium welded joints*

The local geometry substantially influences the endurable structural stresses of welded joints [6], Fig. 7. If no specific data are available a structural stress of σ_a*(R=-1, N=1·10^6, P_s=90%) = ±40 MPa may be used for the pre-design.

2 THE INFLUENCE OF CORROSION

If components are exposed to a corrosive environment during service the experimental as well as the analytical proof must take into account the influence of the corrosion [7].

For instance, for a cast steering rod and a welded rear-axle carrier the Woehler and Gassner curves resulting from constant and variable amplitude loading in air and in a corrosive medium (5% NaCl) are displayed in Figs. 8 and 9. The applied stress variation and the spectra are presented in Figs. 10 and 11.

Concerning the effect of corrosion on the fatigue strength special attention should be paid to

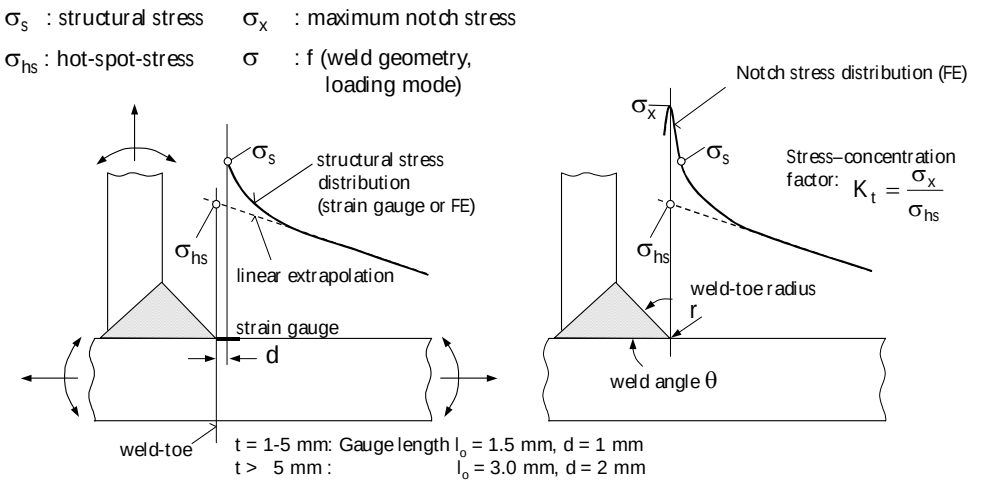

Fig. 6. *Definition of stresses in a weld*

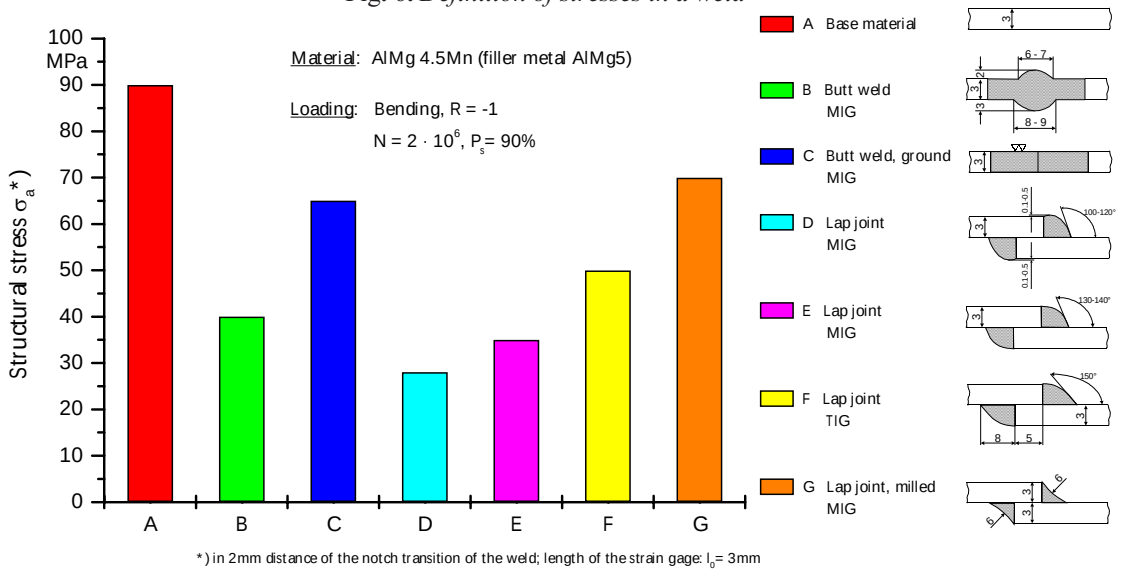

Fig. 7. *Influence of geometry on supportable stresses of aluminium welded joints*

the following:

- To reveal the damaging influence of corrosion fatigue load levels we should allow at least $5 \cdot 10^6$ cycles.
- During corrosion the slopes of the Woehler curves do not change. A constant slope of k = 4 is recommended.
- Available results show a significant drop in the fatigue strength due to the corrosion being less during random loading. If the surface is not treated (coated, shot-penned) the fatigue strength after $5 \cdot 10^6$ load cycles reduces to 50% under constant-amplitude loading and to 20–25% under variable-amplitude loading. This applies to the intensified corrosive conditions imposed in the laboratory on aluminium alloys belonging to the 5000 and 6000 groups of the international alloy register.
- Regarding components made of standard alloys, service experience has confirmed the following approach: the damaging influence of corrosion for a real component can be covered by proof testing in air with a 15% increase in the fatigue loads, provided the component's yield point is not exceeded. Otherwise, a design life increased by a factor of 2 must be proven [1].
- Although cast skin and shot-penning diminish the strength drop due to corrosion this effect should be neglected in the numerical design process. In the case of corrosion protection (surface coats) the design process may be conducted as if no

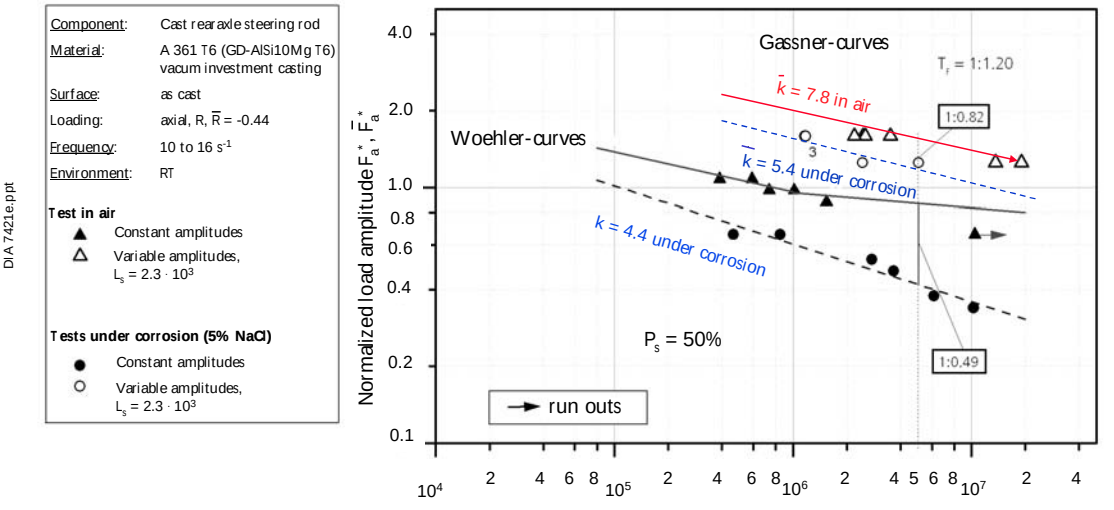

Fig. 8. *Fatigue strength of cast aluminium rear axle steering rods in air and under corrosion*

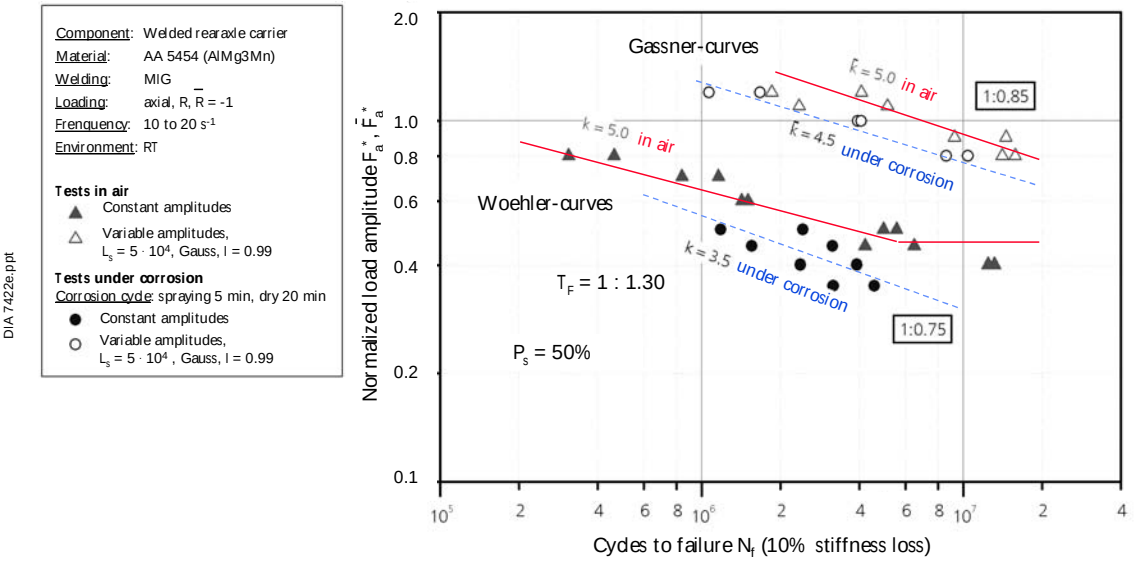

Fig. 9. *Fatigue strength of welded rear axle carriers in air and under corrosion*

corrosive environment were active.

- So far, generally valid knowledge about the influence of distinct corrosion cycles on fatigue behaviour and knowledge about an appropriate selection of service-like environmental conditions are still missing. Thus, for future testing concepts, first of all a unification of simulated environmental conditions is to be recommended, for example, a 5-min period of salt spraying with 5% NaCl solution followed by a drying period of 20 to 25 min.

Investigations on preconditioning with subsequent fatigue loading in air do not have a real influence on the fatigue strength. Therefore, corrosive preconditioning should not be recommended to assess fatigue corrosion.

3 STRUCTURAL DURABILITY VALIDATION

3.1 Experimental validation

The experimental validation of structural durability must be based, on the one hand, on representative operational stress spectra including the loading sequence, and on the other, be carried out in a time- and cost-saving way [8]. Therefore, it is necessary to accelerate the durability testing for which the different possibilities exist:

- The increase of the maximum and of all other spectrum loads with a simultaneous decrease of the spectrum size. This modification is suitable only when the structural yield point of the component

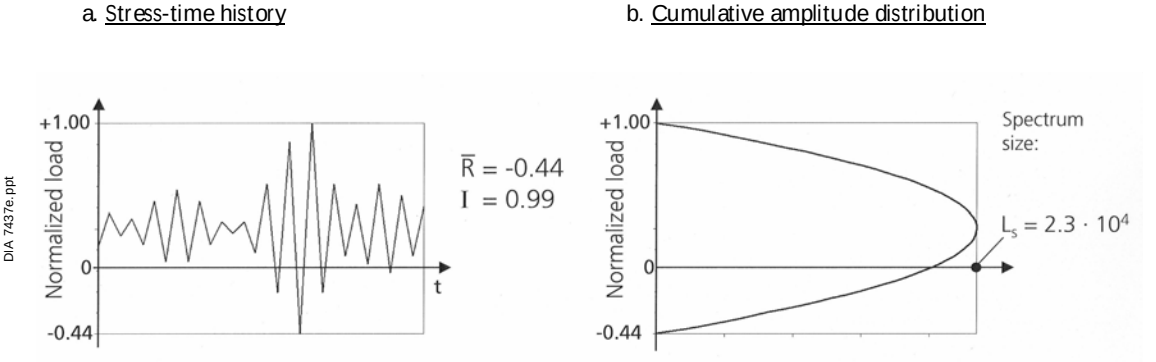

Fig. 10. *Test spectrum of cast aluminium rear axle steering rods*

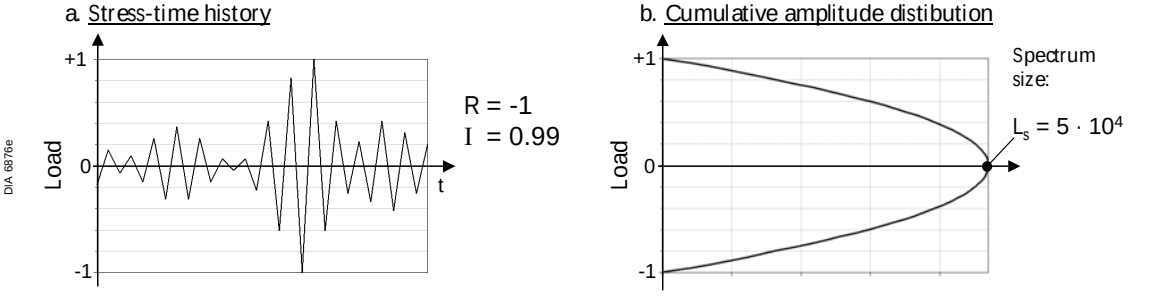

Fig. 11. *Test spectrum of welded aluminium rear axle carriers*

is not exceeded by this measure.

- Omission (cutting off the low loads); "real-time load-sequence testing" applies omission very often. Omitting the small loads with their large number of occurrences may change the component's behaviour, depending on the omission level, the material, the loading mode, the manufacturing and the environment, occasionally leading to a wrong evaluation.
- A change of spectrum shape, keeping the maximum spectrum load, but with an increased load on the lower levels. Here, the omitted small spectrum loads and the corresponding decreased total frequency are compensated by the increased loads, maintaining the damage content of the design spectrum.

The modified load spectra should obey the following rules:

- The load spectrum must contain a sufficient number of cycles, $2 \cdot 10^6$ up to $5 \cdot 10^6$, to cover the eventually occurring effects of fretting and environmental corrosion as well as the degradation of the fatigue strength in the region of a large numbers of cycles.
- The equivalence of the damage caused by the test and the design spectrum, which should be verified by calculation with a modified Palmgren-Miner rule using Woehler curves for wrought or cast aluminium-alloy components, Fig. 4, or for welded joints of aluminium alloys, Fig. 5.
- The sequence length of the test spectrum must be fixed in such a way that a sufficient mix of loads with the appropriate repetition is achieved, as applied during testing, Figs.10 and 11.

3.2 A theoretical estimation of the fatigue life

To estimate the fatigue life two different concepts, namely the concept of local strain or stress for cast and forged components, and the concept of structural stress for welded joints, are used. Correspondingly, the local stress concept utilizes a local stress Woehler curve, as shown in Fig. 4, and the structural stress concept a structural stress Woehler curve, as shown in Fig. 5. A comparison of the experimentally generated strength data with the data derived from a German design guideline (FKM) [9] or from the Uniform Material Law shows large differences caused by the influences of component manufacturing. It is therefore advisable to use data obtained with specimens removed from components or with components.

The local stress concept covers the mean-stress effects with the material-related mean-stress sensitivity parameter $M = [\sigma_a(R=-1) / \sigma_a(R=0)]-1$. It

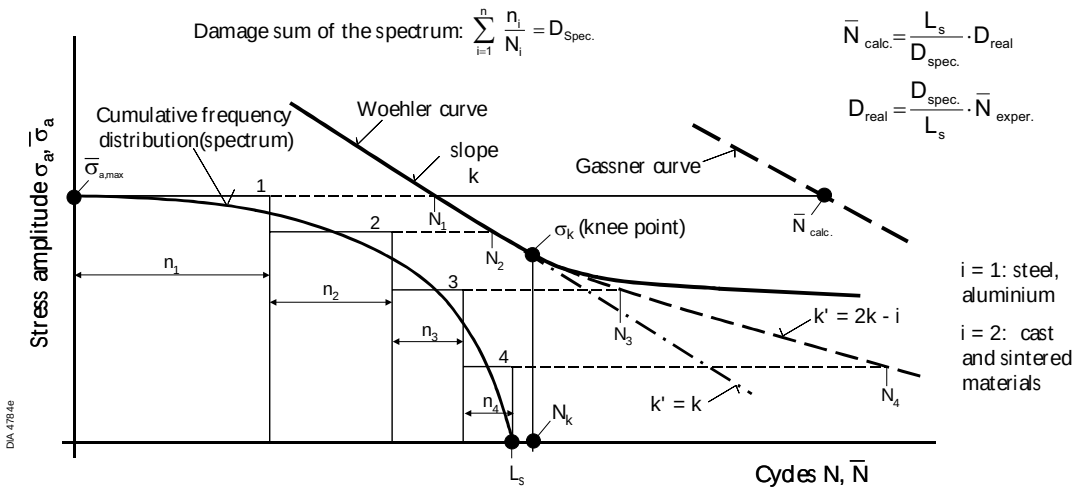

Fig. 12. *Modification of the Woehler-curve and calculation of fatigue life (schematically)*

has values between 0.2 and 0.3 for wrought aluminium alloys ($M_{wrought}$=0.25) and between 0.4 and 0.5 for cast aluminium (M_{cast}=0.45), depending on the tensile strength. For welded joints, mean-stress sensitivity parameters between 0.2 and 0.7 are determined, depending on the residual stress state; M_{weld}=0.45 is recommended.

Furthermore, it is recommended to use Palmgren-Miners-Rule modified by Haibach ([1], [2] and [8]) within the local and structural stress concept to estimate the fatigue life, Fig. 11. The damage accumulation is based on the Woehler curves, Figs. 4 and 5, recommended above. If components are prone to corrosion effects, damage accumulation is recommended by the elementary Palmgren-Miner-Rule using a Woehler curve with a constant slope of $k_{corr}=k_{air}-1$. Various investigations revealed damage sums between 0.05 and 2.0, depending on the stress-time history, the stress distribution and the failure criterion (the cracking or fracture of a test specimen). A real damage sum of D_{real} = 0.5 is recommended for use with the fatigue-life estimation [10]. In the case of a large mean-stress variation, smaller damage values should be used.

Assuming proportional loading and a constant direction for the principal stresses, multi-axial fatigue loading of wrought aluminium-alloy components can be assessed by equivalent stresses based on the distortion energy (Mises) or the shear-stress criterion (Tresca); in the case of cast alloys the normal (principal) stress criterion (Galilei) should be used. In the case of changing the principal stress directions the use of the distortion energy or the shear-stress criterion is not appropriate. They may lead to significantly overestimated fatigue lives of components with ductile material (e>10%) behaviour; thus a ductility-dependent modification is needed. For less ductile cast alloys (e<2%) the normal stress criterion delivers correct equivalent stresses [11]. In welded joints a multi-axial stress state with the constant direction of the principal stresses due to proportional loading can also be represented by equivalent stresses based on the conventional fracture criteria of Mises, Tresca or Galilei. In the case of non-proportional loading and a varying direction of the principal stresses, the fatigue-life estimation applying these criteria results in an unrealistic increase in the life compared to the case of proportional loading. The local equivalent stress, based on a modified Mises criterion, is calculated for the combination of normal and shear stresses in different interference planes of a surface element; the maximum value of the combination determines the critical plane and the equivalent stress [11]. The pre-designing of components, subjected to multi-axial loading with variable amplitudes, still contains large uncertainties requiring experimental verification.

4 CONCLUSIONS

The state-of-the-art knowledge and the already-existing experience make the reliable design of aluminium components feasible. However, in future experimental investigations of components' structural durability the local stresses or strains, with their dependencies on manufacture, geometry, and loading, should be determined, because the resulting data are more appropriate than the data derived from specimen testing or taken from guidelines. Such data may form a basis for verifying calculations and for the transfer of data to other components and for different loading modes.

To profit by eventually extending the available lightweight design potentials, supplementary investigations to extend the database are desirable. This mainly concerns:

- A determination of the maximum allowable plastic deformation with regard to the structural yield point of various components and the effects of special events on the fatigue life under subsequent random loading.
- The influence of temperature combined with the presence of a corrosive environment and random loading.
- The improvement of the accuracy of fatigue-life assessment methods for welded aluminium components, also when they are multi-axially loaded.

5 REFERENCES

[1] Sonsino C. M., Berg A., Grubisic V. (2004) Stand der Technik zum Betriebsfestigkeitsnachweis von Aluminium-Sicherheitsbauteilen (State of the art for the structural durability proof of aluminium alloy safety components). *Fraunhofer-Institute for Structural Durability and System Reliability (LBF)*, Darmstadt, LBF-Report No. TB 225.

[2] Grubisic V. (1998) Bedingungen und Forderungen für einen zuverlässigen Betriebsfestigkeitsnachweis (Conditions and requirements for a reliable structural durability proof). *DVM-Report* No. 125 (1998), pp. 9-22.

[3] Fajdiga M., GrubisicV. et al. (1998) Improvement of strength properties of Aluminium alloy components by manufacturing process. -Partners summary report in Grubisic,V and Wessling,U.- Final report of Copernicus project No. CIPA-CT 94-0219. *Fraunhofer-Institute for Structural Durability and System Reliability (LBF)*,Darmstadt.

[4] Pukl B. (2000) Obratovalna trdnost mehanskih zvez delov iz jekla in aluminijevih zlitin (Fatigue life of mechanical connections made up from steel and aluminium alloys.). Ph.D.-Thesis on Technical Faculty of University of Ljubljana.

[5] Radaj D., Sonsino C. M. (1998) Fatigue assessment of welded joints by local approaches. *Abington Publishing*, Cambridge.

[6] Fischer G., Grubisic V (1999) Data for the design of welded aluminium sheet suspension components. *SAE Paper 1999-01-0662*, Detroit/USA.

[7] Morgenstern C., Streicher M., Oppermann H. (2004) Leichtbau mit Aluminiumschweißverbindungen des Fahrzeugbaus unter korrosiven Umgebungsbedingungen und variablen Belastungsamplituden (Lightweight design of vehicle structures with welded aluminium joints under corrosive environment and variable amplitude loading). *DVM- Report* No. 131 (2004), pp. 75-88.

[8] Grubisic V. (1994) Determination of load spectra for design and testing. *International Journal of Vehicle Design* 15 (1994) No. 1/2, pp. 8-26.

[9] FKM-Richtlinie (German design recommendation): Rechnerischer Festigkeitsnachweis für Bauteile aus Aluminiumwerkstoffen (Numerical strength proof of aluminium alloy components). FKM-Forschungsheft No. 241 (1999), *VDMA-Verlag*, Frankfurt am Main

[10] Grubisic V., Lowak H. (1986) Fatigue life prediction and test. Results of aluminium alloy components. „Fatigue Prevention and Design“, Ed. by J.T. Barnby, *EMAS*, Warley, pp. 171-187.

[11] Küppers M., Sonsino C. M. (2003) Critical plane approach for the assessment of the fatigue behaviour, of welded aluminium under multiaxial loading. *Fatigue & Fract. of Eng. Mat. & Structures* 26 (2003) No.6, pp.507-514.

[12] Eurocode No. 9: Design of Aluminium Structures, Part 2: Structures susceptible to fatigue. *European Committee for Standardization (CEN)*, Brussels, Ref. No. ENV 1999-2: 1998 E.

Author' Address: Prof. Dr. Vatroslav V. Grubišić
Independent Consultant
Zum Stetteritz 1
Reinheim, Germany
vgrubisic@hotmail.com

Prejeto: 10.7.2006 Sprejeto: 25.4.2007 Odprto za diskusijo: 1 leto
Received: Accepted: Open for discussion: 1 year

Strojniški vestnik - Journal of Mechanical Engineering 53(2007)5, 319-328
UDK - UDC 629.7.035:533.6.07
Strokovni članek - Speciality paper (1.04)

Izpopolnjena metoda uravnoteženja modela propelerja v vetrnem kanalu

An Advanced Balancing Methodology for the Propeller of a Wind-Tunnel Model

Aleksandar Veg
(Faculty of Mechanical Engineering Belgrade, Serbia)

Prispevek obravnava učinkovit postopek uravnoteženja, ki je bil razvit zato, da z njim popravimo asimetričnost nastavljivega kota kraka propelerja v razponu od -5 do +35 . Ker s standardnim postopkom uravnoteženja (ISO 1940-1) ni bilo moč doseči zahtevane kakovosti, smo razvili novo tehniko uravnoteženja. Študija propelerjeve neuravnoteženosti je razkrila številne pomembne podrobnosti, ki jih moramo posamično proučiti za potrebe zapletene naloge uravnoteženja. V znanih dokumentih ISO so te podrobnosti omenjene, ne pa tudi natančno opisane. Novi osnutek uravnoteženja pa določa naslednje: sprejemljive tolerance (glede oblike, izsrednosti in hrapavosti), zaporedje poteka uravnoteženja in prednostne naloge, spodnjo mejo neuravnoteženega preostanka, potrebno opremo in postopke, korekcijo neuravnoteženosti in preverjanje rezultatov.

(Ključne besede: veterni kanali, uravnoteženje propelerjev, stopnje kakovosti, dinamično obnašanje)

The focus of this paper is a versatile balancing procedure, developed to compensate for the asymmetries of a propeller blade's settable angle, in the range -5 to +35 . The standard balancing procedure (ISO 1940-1) was found to be inconsistent with the required quality grade, so a new balancing technique was created. A case study of propeller unbalance revealed a set of important details that must be uniquely assessed for such a complex balancing task. For the existing ISO notes, most of these details are descriptive rather than comprehensive. The new balancing concept defines the following: acceptable tolerances (shape, run-out and roughness), balancing order and priorities, a lower margin of residual unbalance, balancing accessories and regimes, unbalance correction and the verification of the results.

(Keywords: wind-tunnels, airplane propellers, balancing control, quality control, dynamic behaviour)

0 UVOD

V postopku razvijanja novega turbopropelerskega letala običajno proučujemo delovanje modela z motorjem v vetrnem kanalu. Hitrost propelerja tovrstnega modela običajno preseže 10.000 min^{-1}. Pri tolikšni hitrosti pa na dinamično obnašanje modela vplivajo različni dejavniki, na primer resonanca motorja, frekvenca vrtenja krakov, neuravnoteženost propelerja, naravna stanja upognjenosti in torzičnosti propelerja, plapolanje in drugo. Med temi dejavniki ima poseben pomen kakovost propelerjeve uravnoteženosti, ki pomeni glavni vir sil vzbujanja.

Z iskanjem nove metode uravnoteženja smo pričeli, ko so testne meritve pokazale, kako lahko

0 INTRODUCTION

The development of a new turbo-prop aircraft usually involves wind-tunnel research with a powered model. The propeller speed with such a model typically exceeds 10,000 rpm. At such a speed, the dynamic behavior of the model is influenced by various factors, for example, power-group resonance, blade-pass frequency, propeller unbalance, flexural and torsional blade natural modes, flutter and so on. From among all these factors, the quality of the propeller balance is of particular importance, as the main generator of excitation forces.

The research process for a new balancing methodology began when the first test measurement

skoraj popolno uravnotežen propeler ob novi nastavitvi kota krakov dramatično pade iz tolerance. Kljub natančno uporabljenemu postopku uravnoteženja ISO (1940-1) nismo mogli izboljšati nastalega stanja, to pa zaradi vplivov geometrijske oblike priležnih elementov in porazdeljenosti mase, ki sta preprečili nastanek potrebne kakovosti. (Več podatkov o tem problemu je v razdelku 1).

Ker je bilo treba ustvariti dobro uravnotežen propeler, ki bi ustrezal različnim kotnim nastavitvam, sta se kot mogoči rešitvi pokazali dve možnosti:

- posamično uravnoteženje za vsako kotno nastavitev posebej (zapletena in dolgotrajna, vendar včasih edina mogoča rešitev);
- neka nova metoda uravnoteženja, ki bi zagotavljala sprejemljivo stopnjo kakovosti za vse kotne nastavitve.

Prva možnost je preprosta ponavljajoča se uporaba standardnega postopka; druga možnost bi bila bolj dobrodošla, a je težko izvedljiva.

Motivacija za premostitev tehničnih in znanstvenih izzivov je bila dovolj velika in prvi korak v raziskavi je bila poglobljena študija spremenljive strukture propelerjeve zgradbe ter študija dejavnikov, ki vplivajo na kakovost uravnoteženosti.

1 DEJAVNIKI, KI ZMANJŠUJEJO KAKOVOST URAVNOTEŽENOSTI

Shema propelerjeve zgradbe (sl. 1) je večplastna; sestoji iz zadnje (01) in prednje (02) puše, ki vpenjata štiri vgrajene krake propelerja (03). Štirje vijaki z valjasto glavo (04) trdno povezujejo prednjo in zadnjo pušo. V zadnjo pušo je izvrtana osrednja odprtina z dvema simetričnima utoroma, ki se prilegata glavni gredi motorja. Ti štirje deli (01 do 04) sestavljajo jedro sestave propelerjeve zgradbe. Preostali deli – matica (05), blokirni obroč (06), vrtavka (07) in pritrdilni vijaki (08) – so drugotnega pomena, četudi njihova uravnoteženost močno vpliva na celotno zgradbo propelerja.

Kraki propelerja so oblikovani v zmanjšanem merilu izvirnih krakov. Izdelani so iz titana 6Al-4V; poprave mase ali oblike niso dovoljene. Vsak krak je z vrhnjim delom vstavljen med zadnjo (01) in prednjo (02) pušo. Vpadni kot določimo z natančnim zavojem ob osi kraka; vsi štirje kraki so nameščeni pod enakim kotom.

Kakor je omenjeno že v uvodu, so vzroki za asimetričnost propelerjevih nastavljivih delov, ki povzroča neuravnoteženost, naslednji:

showed how an almost perfectly balanced propeller dramatically dropped out of tolerance when a new blade-angle setting was applied. However, a strictly applied ISO-proposed balancing procedure (1940-1) provided a poor result, because of the influences of the adjacent parts' geometry and mass distribution, which prevented the required quality grade being achieved. (For more details, see Section 1).

Since it was necessary to obtain a well-balanced propeller for the whole range of angle settings, two options arose as possible solutions:

- Individual balancing for each angle setting (although complicated and time consuming, sometimes the only possible solution),
- Some new balancing methodology that will guarantee an acceptable quality grade across the whole range of angle settings.

The former alternative is a simple, repeated application of a standard procedure, and the latter one, although much preferable, is difficult to realize.

The motivation to overcome the technical and scientific challenge was strong enough, and the first step was to make an in-depth study of the propeller assembly's reconfigurable structure and the factors that affect the balance quality.

1 FACTORS THAT REDUCE THE BALANCE QUALITY

The design of a propeller assembly (Fig. 1) is a complex one, consisting of a rear (01) and a front (02) hub that clamp together four embedded blades (03). Four cylinder-head bolts (04) fix the rear and the front hub tightly together. A central hole is bored in the rear hub, with two symmetrical keyways to fit the engine's main shaft. These four items (01–04) form the core structure of the propeller assembly. The remaining assembly parts: the nut (05), the locking plate (06), the spinner (07) and the fixing bolts (08) are of secondary importance, although their balance seriously affects the complete assembly.

The propeller blades are shaped as a scaled-down version of the original blades. They are made of titanium 6Al-4V, and no mass or shape correction to the body is permitted. Each blade is head-nested between the rear (01) and the front (02) hub and the attack angle is adjusted by a precise twist about body axis, the same amount for all blades.

As mentioned in the introduction, the asymmetry of the propeller's adjustable parts, resulting in the unbalance, originates from:

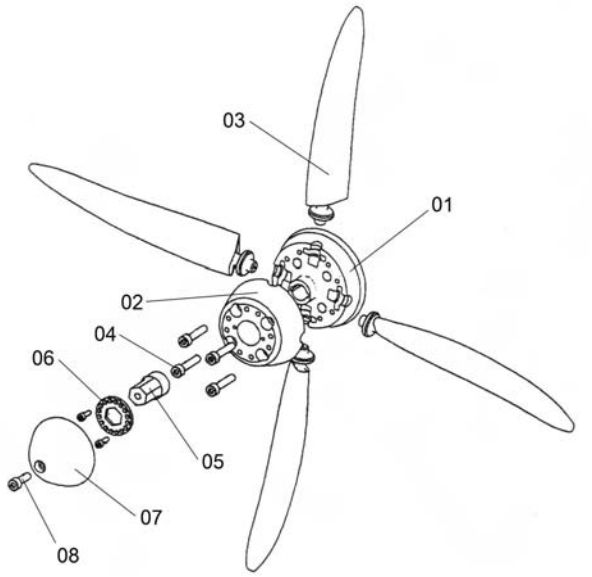

Sl.1. *Sestava propelerja*
Fig. 1. *Propeller assembly*

- geometrična asimetričnost pritrditvenih točk (teža vsakega kraka znaša približno 1/6 celotne teže propelerja). Odstopanje lege težišča posameznega kraka je preveliko, kadar je večje od šestkratne tolerance propelerja;
- ohlapen stik med prileţnimi deli (Netočne tolerance reže bodo povzročile enak učinek, kakor je opisan v prejšnji točki);
- razlika v teži (Vsak krak je enkraten element z določeno porazdelitvijo mase, zaradi katere ima krak tudi svojo lastno maso in statični moment; vsakršna razlika v tovrstnih značilnostih posamičnih krakov povzroči določeno začetno neuravnoteženost);
- nenatančna nastavitev kota (Razlike v nastavitvi začetnih kotov krakov prav tako povzročijo znatno neuravnoteženost).

Glede na te ugotovitve, bi morala nova metoda uravnoteženja določiti naslednje:

- preglednico sprejemljivih toleranc (glede oblike, izsrednosti in hrapavosti);
- zaporedje poteka uravnoteženja in prednostne naloge za vse posamezne dele;
- spodnjo mejo neuravnoteženega preostanka (bolj strogo kakor v priporočilih ISO),
- potrebno opremo in postopke;
- navodila za popravo neuravnoteženosti;
- natančnost nastavitve kota kraka;
- preverjanje rezultatov.

Tako bi nastal izpopolnjen postopek, ki bi omogočal zadovoljivo uravnoteženje.

- geometrical asymmetry of the clamping points (the weight of each blade is approximately 1/6 of the assembly weight). When the variation of the blade's centre-of-gravity position becomes greater than six times the assembly's tolerance it becomes excessive.
- a loose contact between adjacent parts. (Inaccurate tolerances of the gap will cause the same effect as the previous point);
- weight difference. (Each blade is a unique part with a particular mass distribution resulting in its own mass quantity and static moment; any difference in these attributes for opposed blades imposes a certain initial unbalance);
- an inaccurate angle setting. (The dispersion of the blades' preset angle is also a source of significant unbalance).

According to these explanations, the main task for the new balancing methodology would be to propose:

- a table of acceptable tolerances (shape, run-out and roughness),
- a balancing order and priorities for all items,
- a lower margin for residual unbalance (more rigorous than the ISO recommendations),
- balancing accessories and regimes,
- instructions for unbalance correction,
- an accuracy for the blade-angle setting,
- a verification of the results,

so that an advanced procedure would provide satisfactory balancing results.

2 PODLAGA ZA RAZVOJ IZPOPOLNJENE METODE URAVNOTEŽENJA

Preden lahko uporabimo izpopolnjeno metodo uravnoteženja propelerja, moramo sprva opraviti pomembno uvodno nalogo. Glede na njihove mase in statične momente, moramo krake postaviti v ustrezne dvojice; s tem znatno zmanjšamo potrebo po popravi mas v nadaljnjem postopku. Gre za rutinski postopek, ki ga izvedemo vzajemno s primerjanjem in kombiniranjem različnih tež.

Delovanje konstrukcije propelerja obsega širok razpon vrtenja, od 2.000 min^{-1} do 10.000 min^{-1}, in tako največja hitrost (10.000 min^{-1}) določa stopnjo neuravnoteženega preostanka.

Ker je osrednja odprtina konstrukcije izvrtana v zadnjo pušo, moramo ta del obravnavati kot glavni element. Velikost radialne reže Δ med osrednjo odprtino in glavno gredjo, mora biti takšna, da ustvarja manj kot polovično vrednost dovoljenega specifičnega neuravnoteženega preostanka (1). Zadnja puša iz aluminijske zlitine se mora precej tesno prilegati jeklenemu vretenu, ki ustvarja uravnoteženost (sl. 2).

2 THE BASIS OF THE ADVANCED BALANCING METHODOLOGY

An important introductory activity precedes the advanced process of balancing the propeller. The blades must be matched in appropriate pairs, in terms of their mass and static moment, which then significantly reduces the need for any mass correction in subsequent steps. It is a routine operation that is conducted interactively by using weigh-compare matching.

The propeller assembly operates over a wide spinning range, from 2,000 rpm to 10,000 rpm. Consequently, the maximum speed (10,000 rpm) dictates the amount of residual unbalance.

Since the assembly's central hole is machined in the rear hub, this part should be considered as a core element. The radial gap, Δ, between the central hole and the main shaft, must be less than half the value of that allowed for specific residual unbalance (1). There is quite a tight tolerance in the fit of the aluminum-alloy rear hub on the steel-made balancing-tool mandrel (Fig. 2).

$$\mathbf{\Delta} = \tfrac{1}{2}\boldsymbol{\varepsilon}^{\text{G 6.3}}_{\text{10.000 RPM}} \approx 3\ \mu\text{m} \qquad (1).$$

Poleg strogo določenih zahtev glede oblike vretena in njegovega imenskega premera (sl. 3), moramo uvesti še nekaj dodatnih kriterijev:

- hrapavost površine mora biti pod mejo 0,2 μm (kar omogoča gladko drsenje),
- celotna izsrednost mora biti pod mejo 3 μm (kar se ujema z normativi ISO [1]),
- specifični neuravnoteženi preostanek mora biti pod mejo 3 μm.

Glede na meritvene in poprave postopke lahko kasneje sestavne dele in posamezne sklope celotnega propelerja razdelimo v tri stopenjske skupine:

Besides the strictly defined requirement for the mandrel shape and the nominal diameter (Fig. 3), a few additional criteria must be introduced:

- a surface roughness below 0.2 μm (which guarantees smooth sliding),
- an overall run out below 3 μm (which complies with ISO norms [1]),
- a specific residual unbalance below 3 μm.

Later on, the items and subassemblies of the propeller assembly can be classified into three order groups, according to the measuring and correcting procedure:

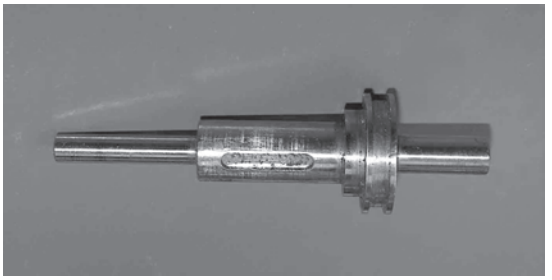

Sl. 2. *Vreteno*
Fig. 2. *Mandrel*

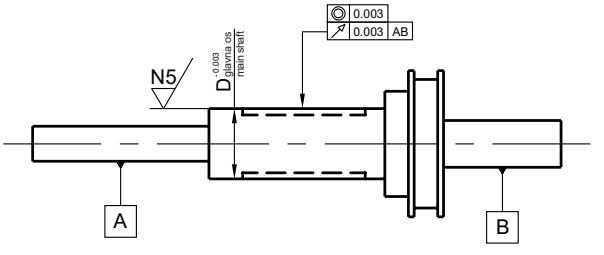

Sl. 3. *Tolerance vretena*
Fig. 3. *Mandrel tolerances*

Preglednica 1. *Vrstni red uravnoteženja*
Tabel 1. *Balancing order*

SESTAVNI DEL ITEM	MERITEV NEURAVNOTEŽENOSTI UNBALANCE MEASUREMENT	POPRAVA NEURAVNOTEŽENOSTI UNBALANCE CORRECTION	STOPNJA ORDER
ZADNJA PUŠA REAR HUB	NEPOSREDNA DIRECT	NEPOSREDNA DIRECT	**I**
PREDNJA PUŠA FRONT HUB	POSREDNA INDIRECT	NEPOSREDNA DIRECT	**II**
VRTAVKA SPINNER	POSREDNA INDIRECT	NEPOSREDNA DIRECT	**II**
KRAKI BLADES	POSREDNA INDIRECT	POSREDNA INDIRECT	**III**

NEPOSREDNA meritev – meritev neuravnoteženosti določenega sestavnega dela z ustreznim orodjem
POSREDNA meritev – meritev neuravnoteženosti z uporabo kakega drugega dela ali sklopa propelerja
NEPOSREDNA poprava – poprava ugotovljene neuravnoteženosti na določenem neuravnoteženem delu propelerja
POSREDNA poprava – neuravnoteženost določenega dela je popravljena na drugem delu propelerja

Osrednje novosti izpopolnjene metode uravnoteženja so:

- uravnoteženje posameznih delov propelerja (namesto enkratnega uravnoteženja celotnega propelerja),
- strogo določene geometrijske tolerance (popolna usklajenost s potrebami kakovosti uravnoteženja),
- seznam prednostnih nalog (vsak del je uravnotežen v skladu z izhodišči *predhodne določitve* uravnoteženosti),
- vnaprej določene ravnine za popravo mase (dosežena kakovost se ne sme zmanjšati ob ponovni namestitvi krakov propelerja)
- dosledna zasnova neuravnoteženega preostanka (določen tako natančno, da omogoča neobčutljivost za spremembe kotov propelerjevih krakov)

Glede na prednostne naloge uravnoteženja lahko oblikujemo vrstni red postopkov uravnoteženja, ki je predstavljen v preglednici 2, pri čemer smo predlagani neuravnoteženi preostanek izračunali z enačbama (2) in (3).

PREDLAGANI SPECIFIČNI NEURAVNOTEŽENI PREOSTANEK

$$\boldsymbol{\varepsilon} = \boldsymbol{\varepsilon}^{\text{G 6.3}}_{10.000\ \text{RPM}} = 6\ \frac{\text{g}}{\text{kg}} \tag{2}$$

PREDLAGANI NEURAVNOTEŽENI PREOSTANEK

$$\mathbf{U} = m\boldsymbol{\varepsilon} = \text{m}[\text{kg}]6\left[\frac{\text{g}}{\text{kg}}\right] \tag{3}.$$

DIRECT measurement – a single-part unbalance measurement using the appropriate balancing tool
INDIRECT measurement – an unbalance measurement, using some other part or subassembly as a tool
DIRECT correction – a correction of the detected unbalance on that particular part
INDIRECT correction – an unbalance of one part is corrected on some other part

The core innovations of the advanced balancing methodology are:

- a decomposed propeller balancing (instead of an overall balancing),
- strictly defined geometrical tolerances (total compliance with the required balance quality),
- a queue of balancing priorities (each part is balanced as *originally allocated* on the pre-balanced platform),
- predefined plains of mass correction (the achieved quality should not be spoiled by the blades' resettlement)
- a firm frame of residual unbalance (as sharp as needed in order to be insensitive to different blade angles)

Regarding the balancing priorities, the balancing-procedure schedule can be formed as presented in Table 2, where the proposed residual unbalance is calculated from the following formulas (2) and (3).

PROPOSED SPECIFIC RESIDUAL UNBALANCE

PROPOSED RESIDUAL UNBALANCE

Preglednica 2. *Postopek uravnoteženja*
Tabel 2. *Balancing procedure*

STOPNJA ORDER	SESTAVNI DEL ITEM	PRIPOMOČEK TOOL	SLIKA DRAWING	PREDLAGANI NEURAVNOTEŽENI PREOSTANEK PROPOSED RESIDUAL UNBALANCE (G 6,3 - ISO 1940) g
0	VRETENO MANDREL	-	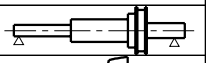	0,78
I	ZADNJA PUŠA REAR HUB	VRETENO MANDREL	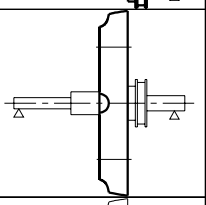	1,32
II	PREDNJA PUŠA FRONT HUB	VRETENO + ZADNJA PUŠA MANDREL + REAR HUB	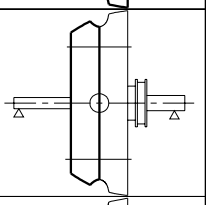	0,90
II	VRTAVKA SPINNER	VRETENO + ZADNJA PUŠA + PREDNJA PUŠA MANDREL + REAR HUB + FRONT HUB	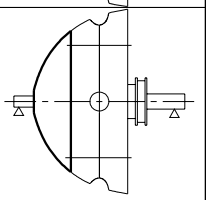	0,30
III	KRAKI BLADES	VRETENO + ZADNJA PUŠA + PREDNJA PUŠA MANDREL + REAR HUB + FRONT HUB	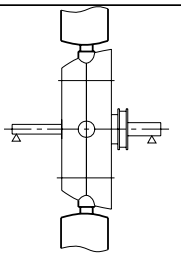	DOLOČEN NA PODLAGI PREJŠNJIH REZULTATOV TO BE DEFINED ACCORDING TO PRELIMINARY RESULTS

3 REZULTATI IZPOPOLNJENE METODE URAVNOTEŽENJA

Postopek uravnoteženja, določen v preglednici 2, smo izvedli do vključno celotne II.stopnje. Tu pa se začne najbolj negotova faza nove metode; negotovost je povezana z uravnoteženjem nastavljivih krakov. Začetno meritev izvedemo za najbolj običajno kotno nastavitev [15°] (sl. 4). Ugotovljeno neuravnoteženost potem popravimo na najbolj zunanjih ravninah ZADNJE in PREDNJE PUŠE (sl. 5). Neuravnoteženi preostanek približamo predlaganemu preostanku (pregl. 3, osenčena vrsta). Vpadni kot nato povečamo do skrajnih vrednosti,

3 THE RESULTS OF THE ADVANCED BALANCING METHODOLOGY

The balancing procedure, specified in Table 2, is realized up to the last issue of order II. At this stage the most uncertain phase of the new method definition starts; this is connected with the balancing of the re-settable blades. An initial measurement is conducted for the most common angle setting [15°] (Fig. 4). The detected unbalance is then compensated in the outer-most planes of the REAR and FRONT HUB (Fig. 5). The residual unbalance is tuned close to the proposed one (Table 3, shaded row). Afterwards, the attack angle is changed to the extreme values [-5°]

Preglednica 3. *Spreminjanje neuravnoteženega preostanka glede na vpadni kot (začetni rezultati)*
Tabel 3. *Fluctuation of residual unbalance vs. attack angle (initial results)*

Vpadni kot Attack angle	Vrsta dejavnosti Sort of activity	Predlagani rezultat Proposed		Dobljeni rezultat Attained		Ocena Evaluation
		Stopnja kakovosti Qual. grade	Neuravnoteženi preostanek Resid. Unbal.	Stopnja kakovosti Qual. grade	Neuravnoteženi preostanek Resid. Unbal.	
°	opis description	preostanek residual	g	dovoljeno permitted	g	-
+ 15	uravnoteženje balancing	G 6,3	6,0	G 4,3	4,5	sprejemljivo acceptable
- 5	preveritev inspection	G 6,3	6,0	G 8,6	9,0	**nesprejemljivo unacceptable**
+ 35	preveritev inspection	G 6,3	6,0	G 7,7	7,2	**nesprejemljivo unacceptable**

[-5°] in [+35°], zdaj preverjanje neuravnoteženosti pokaže znatno povečanje neuravnoteženega preostanka, kar pa ni sprejemljivo (pregl. 3).

Standardna stopnja kakovosti G 6,3 (ISO 1940-1), ki jo pri zgradbi propelerja upoštevamo v prvi fazi (začetni rezultati, pregl. 3), ne ponuja primernega

and [+35°] and the unbalance check-up showed a significantly deteriorated residual unbalance, which is considered to be unacceptable (Table 3).

The standard quality grade, G6.3 (ISO 1940-1), applied to the propeller assembly in the first stage (initial results, Table 3), could not provide adequate

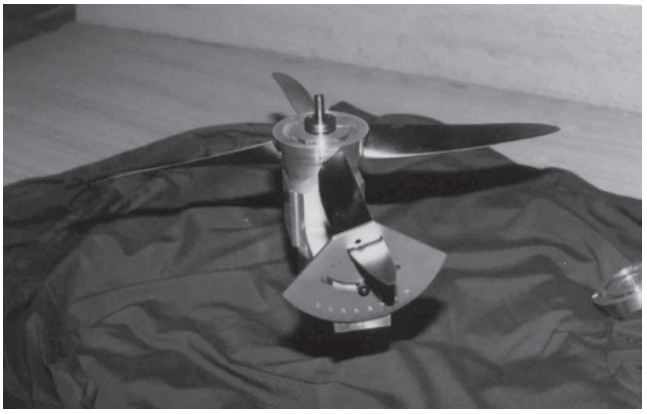

Sl. 4. *Prilagoditev vpadnega kota*
Fig. 4. *Attack-angle readjustment*

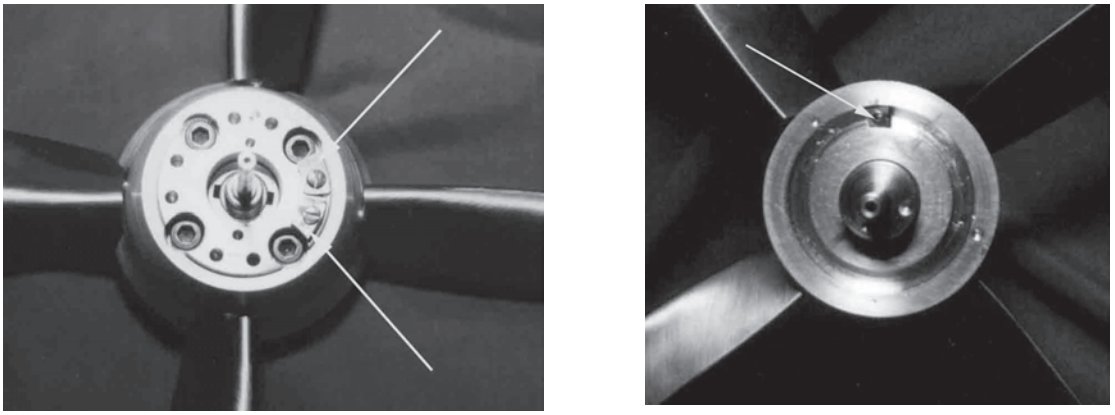

Sl. 5. *Popravne uteži za uravnoteženje krakov propelerja*
Fig. 5 *Correction weights for the blades' unbalance*

uravnoteženja za celoten razpon mogočih vpadnih kotov (-5° do +35°). **Zato določimo bolj zahtevno stopnjo kakovosti: približno G 1,5.** Zdaj ponovno uravnotežimo zgradbo propelerja (sl. 6) v skladu z novim kriterijem, nato pa preverimo nastalo stanje za celoten razpon vpadnih kotov (pregl. 4).

Zdaj so rezultati uravnoteženja, ki smo jih dosegli z upoštevanjem spremenjene stopnje kakovosti neuravnoteženega preostanka G 1,5, v okvirih predlaganih toleranc.

balance quality over the whole range of attack angles (-5° to +35°). **For this reason a more rigorous quality grade is established: approximately G1.5**. The propeller assembly is now rebalanced (Fig. 6) according to the newest criterion, and then verified for the whole range of attack angles (Table 4).

Now the balancing results achieved by the implementation of the new residual quality grade G1.5 are within the proposed tolerances.

4 PREIZKUS DELOVANJA

Preveritev dinamičnega delovanja modela smo izvedli v vetrnem kanalu (sl. 7), z vrtečimi se

4 OPERATIONAL VERIFICATION

The inspection of the model's dynamic behavior was conducted in a wind tunnel (Fig. 7)

Preglednica 4. *Zmanjšano spreminjanje neuravnoteženega preostanka glede na vpadni kot (končni rezultati)*
Tabel 4. *Refined fluctuation of residual unbalance vs. blade angle (final results)*

Vpadni kot Attack angle	Vrsta dejavnosti Sort of activity	Predlagani rezultat Proposed		Dobljeni rezultat Attained		Ocena Evaluation
		Stopnja kakovosti Qual. grade	Neuravnoteženi preostanek Resid. Unbal.	Stopnja kakovosti Qual. grade	Neuravnoteženi preostanek Resid. Unbal.	
°	opis description	preostanek residual	g	dovoljeno permitted	g	-
+ 15	uravnoteženje balancing	G 1,5	1,6	G 1,2	1,3	sprejemljivo acceptable
- 5	preveritev inspection	G 6,3	6,6	G 5,0	5,2	sprejemljivo acceptable
+ 35	preveritev inspection	G 6,3	6,6	G 4,4	4,6	sprejemljivo acceptable

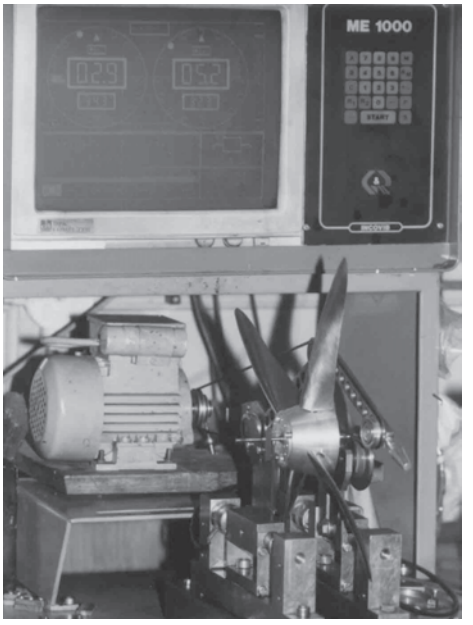

Sl. 6. *Propelerska zgradba na stroju za uravnoteženje*
Fig. 6. *Propeller assembly on the balancing machine*

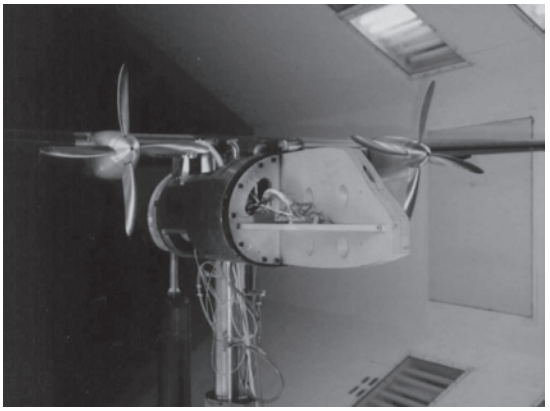

Sl. 7. *Model propelerja v vetrnem kanalu*
Fig. 7. *Propeller model in the wind tunnel*

Preglednica 5. *Celoten razpon vibriranja (10.000 min^{-1})*
Tabel 5. *Vibrations in the whole range (10,000 rpm)*

Merilno mesto **Measuring point**	**Moč vibriranja** **Vibration severity** **(V_{RMS} mm/s)**	**Ocena** **Evaluation**
leva gondola motorja left engine gondola	2,0	sprejemljivo acceptable
desna gondola motorja right engine gondola	1,8	sprejemljivo acceptable
trup fuselage	1,5	dobro good

propelerji, za celoten razpon hitrosti in vpadnih kotov. Vibriranje telesa modela je, ne glede na način delovanja in število vključenih energijskih enot, ostalo znotraj predlaganih mej ISO 10816-1, kar je bil tudi glavni cilj vseh dejavnosti uravnoteženja (pregl. 5).

5 SKLEPI

Na temelju rezultatov pridobljenih s standardno in izpopolnjeno metodo uravnoteženja, lahko sklenemo naslednje:

- Zaradi nezadovoljivega osnovnega postopka uravnoteženja in ne dovolj natančne določitve neuravnoteženega preostanka, z uporabo standardnega postopka uravnoteženja ne moremo dobiti sprejemljivih toleranc.
- Sprejemljive tolerance smo dobili z izpopolnjeno metodo, ki obsega resnično preverjanje vseh pomembnih toleranc, usklajevanje krakov propelerja, postopno izvedbo osnovnega uravnoteženja glede na prednostne naloge, natančno popravo mase in natančno določitev spodnje meje neuravnoteženega preostanka.

with spinning propellers for the whole range of speeds and attack angles. The vibrations of the model body, regardless of the regime and the number of engaged power units, were kept within the ISO 10816-1 proposed limits, which was the main goal of all the balancing activities (Table 5).

5 CONCLUSIONS

Based on the results obtained by standard and advanced balancing procedures one can conclude the following:

- Acceptable tolerances could not be obtained with the standard balancing procedure, because of the inconsistent elementary balancing and the insufficiently sharp residual margin.
- Acceptable tolerances were obtained with the advanced balancing procedure, consisting of a true inspection of all the relevant tolerances, blade matching, step-by-step elementary balancing with priorities, a precise mass correction and a sharp definition of the residual unbalance lower margin

- Izpopolnjen postopek uravnoteženja resnično pripomore k razumevanju pomembnih dejavnikov in lahko prepreči, da bi le-ti vplivali na kakovost uravnoteženosti nastavljivih sestavov.

6 POJASNILO IN ZAHVALA

Opisano metodo uravnoteženja smo razvili in uporabili v postopku proučevanja indonezijskega turbo-propelerskega transportnega letala za srednje proge, z uporabo modela vetrnega kanala, ki smo ga izvedli na Letalskem institutu, VTI Žarkovo, ob pomoči Instituta za strojno dinamiko pri Fakulteti za strojništvo v Beogradu.

Opremo za uravnoteženje in druge pripomočke je priskrbela gospodarska družba Rotech Beograd, proizvajalec strojev za uravnoteženje in vibrodiagnostičnih naprav.

Navedeni partnerji so močno pripomogli k uspehu projekta, zato se jim avtor iskreno zahvaljuje.

- The advanced balancing procedure has real power in the stratification of all the influential factors, and can prevent them affecting the balance quality of reconfigurable structures

6 ACKNOWLEDGMENT

The balancing methodology described in the paper was developed and applied as part of the research on an Indonesian middle-range turbo-prop transport aircraft with a powered wind-tunnel model, which was realized at the VTI Aeronautical Institute Ž arkovo with the assistance of the Machine Dynamics Institute, Faculty of Mechanical Engineering, Belgrade.

The balancing equipment and other accessories were provided by the RoTech Company, Belgrade, a producer of balancing machines and vibrodiagnostic instruments.

All of the above contributed a great deal to the success of the project and are deserving of the sincere gratitude of the author.

7 VIRI
7 REFERENCES

[1] ISO 1940-1 (1986) Mechanical vibration – Balance quality requirements of rigid rotors – Part 1; Determination of permissible residual unbalance.
[2] ISO 10816-1 (1995) Mechanical vibration – Evaluation of machine vibration by measurement on non-rotating part.
[3] Veg A. (1993) Nonlinearity of an isotropic measuring frame, Ph.D. Thesis, *University of Belgrade*.
[4] Victor W. (1995) Machinery vibration – Balancing, *Mc Graw Hill*.

Avtorjev naslov: prof. dr. Aleksandar Veg
Fakulteta za strojništvo
Institut za strojno dinamiko
Kraljice Marije 16
11 000 Beograd, Srbija
aveg@mas.bg.ac.yu

Author's Address: Prof. Dr. Aleksandar Veg
Faculty of Mechanical Eng.
Machine Dynamics Institute
Kraljice Marije 16
11 000 Belgrade, Serbia
aveg@mas.bg.ac.yu

Prejeto: 15.3.2006
Received:
Sprejeto: 25.4.2007
Accepted:
Odprto za diskusijo: 1 leto
Open for discussion: 1 year

Strojniški vestnik - Journal of Mechanical Engineering 53(2007)5, 329-347
UDK - UDC 658.58:620.179/.19-7
Strokovni članek - Speciality paper (1.04)

Vzdrževanje glede na stanje - uporaba endoskopske metode

Condition Maintenance - Applying an Endoscopic Method

Miodrag Bulatović - Jovan Šušić
(University of Montenegro, Podgorica)

Vzdrževanje glede na stanja, ki temelji na merjenju in nadzoru parametrov stanja predmetov z uporabo tehničnega razpoznavanja, je osnova vseh sodobnih zasnov vzdrževanja, predvsem dejavnega vzdrževanja. V prispevku sta na splošno prikazana vloga in pomen tehničnega razpoznavanja ter vrste metod in tehnik razpoznavanja. Posebej sta poudarjena pomen in uporaba endoskopa pri razpoznavanju notranjih površin delov motorjev, na primeru ladijskih motorjev. Podani so delni rezultati obsežnega raziskovalnega projekta. Prikazane so uporabljene metode razpoznavanja, značilke inštrumentov in kratek opis njihove uporabe. Posebej so prikazani rezultati merjenj, ki so ponazorjeni s fotografijami opaženih pojavov. Podani sta preglednična in besedna analiza rezultatov. Namen prispevka je opozoriti na veliko potrebo in učinkovitost uporabe prikazanih metod razpoznavanja v postopkih vzdrževanja, ne samo velikih (ladijskih) motorjev temveč tudi drugih strojev, pri katerih razpoznavanje notranjosti predstavlja osnovni podatek za načrtovanje ustreznih dejavnosti vzdrževanja.

(Ključne besede: vzdrževanje, tehnična diagnostika, endoskopija, parametri stanja)

Maintenance according to a condition based on measuring and controlling the parameters of the object's condition using technical diagnostics represents the basis of all modern concepts of maintenance, and primarily of proactive maintenance. This paper shows the role and significance of technical diagnostics as well as of the various types of diagnostic methods and techniques. The importance and the application of endoscopes, in particular, have been shown in the domain of the diagnostics of the internal surfaces of engine elements in ships' engines. This paper presents research that was performed in the context of a larger research project. It shows applied methods of diagnostics and instrument characteristics and gives a brief description of their use. Furthermore, the results of measurements, illustrated with photographs of the observed phenomena, are shown, followed by an analysis of these results. The aim of this paper is to emphasise the effectiveness of using the described methods of diagnostics in the maintenance processes not only of large ship engines, but also of other engines for which the diagnostics of internal surfaces offers essential information for planning the appropriate maintenance activities.

(Keywords: condition-based maintenance, technical diagnostics, endoscopes, condition parameters)

0 UVOD

Stanje določenega predmeta, stroja opišemo z določeno množico parametrov (pretok tekočine, debelina stene, hrup, temperatura in druge značilnosti), ki naj bi zadovoljili načrtovano funkcijo cilja v določenih razmerah in v določenem časovnem obdobju [1]. Spremembe parametrov vodijo k spremembi funkcije predmeta, najpogosteje se ta poslabša.

Kakovostna analiza razpoznavnega signala temelji na sedanjem znanju o določenih značilnostih

0 INTRODUCTION

The condition of an object or a machine is described by a specific group of parameters, for example, the thickness of a wall, the noise, the temperature, and other characteristics [1]. All of these parameters should achieve the designed function of a goal under particular conditions in a fixed amount of time. However, changing the parameters leads to a change in the object's function, which then usually weakens the object's function.

The qualitative analysis of a diagnostic signal is based on already generated knowledge about

in pojavih različnih primerov in stanj. Vzdrževanje glede na stanje temelji na razpoznavanju stanja z uporabo ([2] in [3]):

- časovne slike stanja oz. analize dejavnikov učinkovitosti sistema v odvisnosti od časa,
- nadzora parametrov stanja z uporabo tehničnega razpoznavanja.

Vzdrževanje glede na stanje z nadzorom parametrov pomeni množico pravil za določanje režima diagnostike sestavnih delov sistema v dejanskem postopku uporabe kakor tudi za odločanje o nujnosti zamenjave ali nujnih dejavnosti vzdrževanja na podlagi informacij o dejanskem tehničnem stanju sistema ter njegovih sestavnih delov.

Merjenje parametrov stanja se izvaja z razstavljanjem ali brez njega, oziroma z zaustavitvijo sistema ali brez nje, z uporabo opreme in sredstev za tehnično diagnostiko. Diagnostika stanja naj bi bila zveznega značaja, brez zaustavitve ali razstavljanja sistema.

Napetosti in deformacije, ki se pojavljajo v mehanskih delih sistema, običajno povzročajo neposredne spremembe kinematike, obstojnosti, vibracij, hrupa, temperature in drugih odločilnih pojavov. Poleg tega posredno povzročajo spremembe mazalnih značilnosti, npr. pojav obrabnih delcev kot znamenje povečanega trenja.

Da bi parameter izhodnega postopka lahko postal parameter razpoznavanja, mora zadovoljiti pogoje homogenosti, široko področje uporabe in dostopnost merjenja. Za zahteven sistem se ne da teoretično podati vseh možnih stanj, zato preizkušamo in ugotavljamo verjetnost pojavljanja posameznih stanj, s čimer se omogoča izbira parametrov razpoznavanja v odvisnosti od stanja celotnega sistema ali dela sistema.

Parametri stanja so definirani z ustreznimi signali. Razvrstitev razpoznavnih signalov sloni na: predmetu razpoznavanja, stanju signala, vlogi razpoznavnih signalov in fizikalnih lastnostih. Postopki in pojavi, ki povzročajo odpovedi, so naključne narave, kar ima za posledico: en simptom – eno razpoznavanje, dva simptoma ali več – eno razpoznavanje, en simptom – dve razpoznavanji ali več.

Merjenje parametrov stanja je mogoče z razstavljanjem ali brez njega oz. z zaustavitvijo celotnega sistema ali brez nje, z uporabo posebnih inštrumentov in opreme za tehnično diagnostiko ([4] do [7]).

the specific characteristics and phenomena of various cases and conditions. The condition maintenance is based on the diagnostics of this condition, using the following elements ([2] and [3]):

- Time pictures, either of a condition or analyses of the effectiveness of a system as a function of time,
- Control of condition parameters, using technical diagnostic methods.

Maintenance according to a condition, by controlling the parameters, represents a group of rules for determining a diagnostic regime in a real exploitation process. In addition, it serves the purpose of making decisions about the necessity for a replacement or maintenance activity, based on information about the real technical condition of the system and its parts.

It is important that the measuring of condition parameters happens with or without disassembling the system, which means with or without detaining the system by using the equipment and the facilities for technical diagnostics. Therefore, a tendency exists for the condition diagnostics to always be continuous, without halting or disassembling the system.

Tensions and deformities appearing in the mechanical segments of the system usually cause a direct change in cinematic forms, resistance, vibrations, noise, temperature and in other crucial phenomena. Furthermore, they indirectly cause changes in lubricant characteristics, such as the appearance of particles as a sign of friction.

In order for the parameter of an output process to become a diagnostic parameter, it must fulfil the conditions of homogeneousness, broad use and measurement attainability. It is not possible to number all the conditions of a complex system; it is therefore useful to examine, investigate and determine the probability of some of them appearing. This makes the selection of diagnostic parameters possible in the function of the whole or a part of the system condition.

The condition parameters are defined by appropriate signals. The categorisation of diagnostic signals is conducted according to the following: the subject of the diagnosis, the signal status, the role of diagnostic signals and the physical characteristics. The processes and occurrences that cause failures have a stochastic character. This means, therefore: one symptom – one diagnosis, two or more symptoms – one diagnosis, one symptom – two or more diagnoses.

The measuring of condition parameters could be done with or without stopping the whole system, using special instruments and equipment for technical diagnostics ([4] to [7]).

Osrednja naloga razpoznavanja je odkriti številne povezave med strukturnimi elementi U_1, U_2, ... U_n in ustreznimi razpoznavnimi parametri S_1, S_2, ... S_n, z uporabo diagnostične matrike [3]:

The main task of a given diagnosis is to discover many relations between the entities U_1, U_2, ... U_n and the diagnostic parameters S_1, S_2, ... S_n, using a diagnostics matrix [3]:

	U_1	U_2	U_3	U_4	U_5
S_1	0	0	1	0	0
S_2	1	1	0	1	1
S_3	0	0	0	0	0
S_4	0	1	1	0	1
S_5	0	1	0	0	0

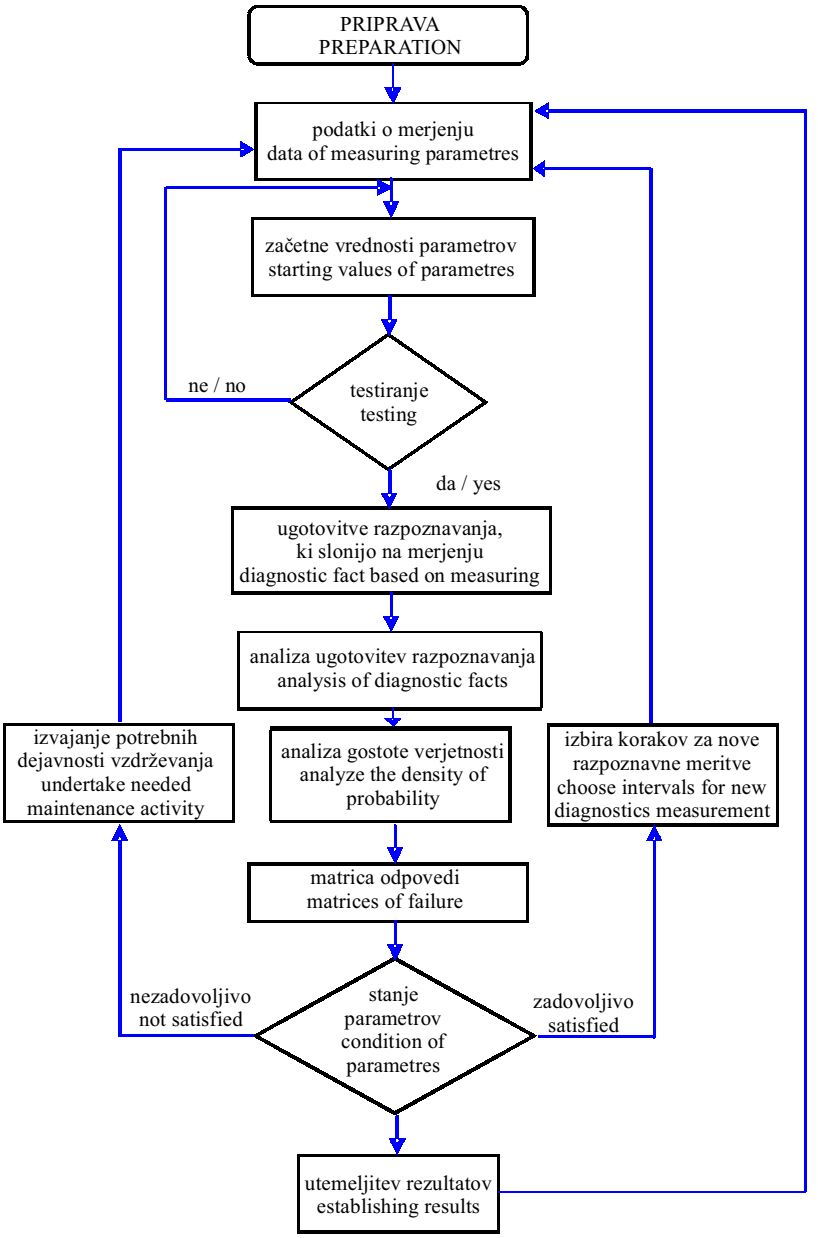

Sl.1. *Algoritem za razpoznavanje parametrov stanja*
Fig.1. *Algorithm of diagnostic parameters' condition*

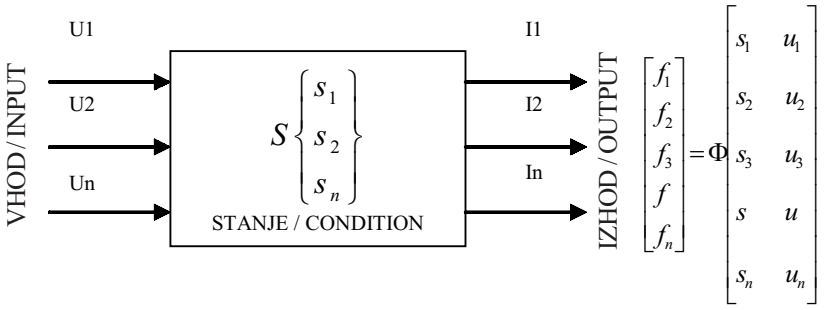

Sl. 2. *Razpoznavna povezovalna shema*
Fig. 2. *Diagnostic block scheme*

Presečišče vrstice in stolpca označuje možnost pojava odpovedi.

Odvisnost med strukturnimi in razpoznavnimi parametri se določa z algoritmom na sliki 1 [3].

V splošnem se postopek razpoznavanja lahko prikaže tudi v obliki povezovalnega diagrama (sl. 2), pri čemer so: $\vec{U}$ - vektor pogojev diagnostike, $\vec{S}$ - vektor stanja predmeta, $\vec{I}$ - vektor diagnostičnih signalov.

0.1 Meje diagnostičnih parametrov stanja

Določiti je treba meje parametrov za razpoznavanje, da bi s tem dosegli boljše rezultate pri oceni stanja. Podana sta dva načina za oceno stanja:

- ocena zmožnosti sistema za načrtovano funkcijo – izmenjujoča ocena ter
- predvidevanje obnašanja sistema pri nadaljnji uporabi. V tem primeru so parametri stanja opazovani v določenem časovnem obdobju uporabe pred pričakovano odpovedjo sistema.

The cross point of the horizontal and vertical column means the possibility of failure exists.

The dependence between the structural and the diagnostic parameters is based on an algorithm (Fig. 1) [3].

The process of diagnostics can be shown using scheme (Fig. 2). Where are: $\vec{U}$ - vector of diagnostic condition, $\vec{S}$ - vector of object condition, $\vec{I}$ - vector of diagnostic signals.

0.1 Limits of diagnostic parameters' conditions

It is necessary to define the limits of the parameters for diagnostics for better results and an evaluation of the condition. There are two principles in the condition evaluation:

- The evaluation of the system's capability for the goals' function – alternative evaluation,
- The prediction of system behaviour during further use. In this case the condition parameters are observed in a specific period of usage until the expected problem or failure.

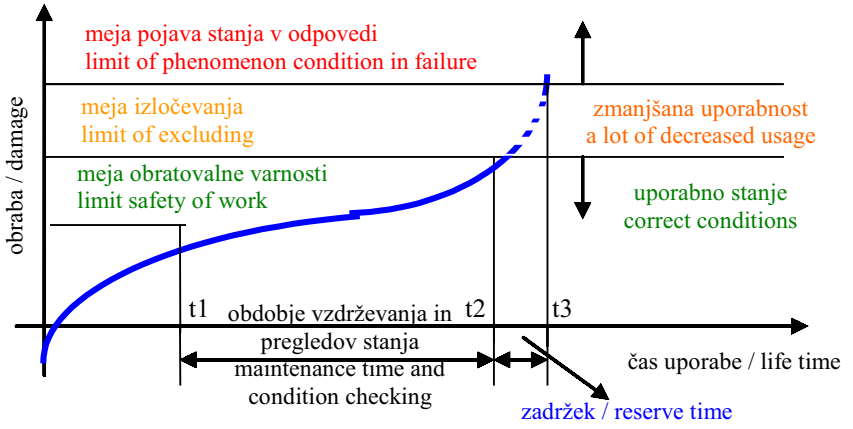

Sl. 3. *Krivulja obrabe*
Fig. 3. *Worn-out curve*

V obeh primerih je treba določiti mejne vrednosti parametrov stanja. V razpoznavanju v strojništvu so posebej zanimive mejne vrednosti, ki so povezane z obrabo, utrujanjem materiala, jamičenjem, spremembami temperature, hrupom, vibracijami itn. V vsakem primeru se pojavi določena obraba, zato se tudi krivulja, ki kaže stanje sistema imenuje krivulja obrabe (sl. 3) [3].

Merila za določanje mej so:

- tehnični in tehnološki,
- ekonomski (stroški ukrepov, finančno tveganje ipd.),
- varnostni (možne posledice napak),
- ergonomski (vpliv hrupa in vibracij ipd.).

Po navadi upoštevamo več meril za oceno mej, ki se določijo na temelju izkustvenih ali eksperimentalnih raziskav.

0.2 Napoved preostalega časa uporabe

Na podlagi poznavanja povprečne obratovalne dobe strojev in naprav, kakor tudi doseženih vrednosti parametrov stanja, je mogoče z uporabo napovedati obnašanje parametrov pri nadaljnji uporabi. Ena od metod za napovedovanje sloni na povprečni statistični vrednosti poškodb. Ta metoda se uporablja, ko ni znano, ali je premalo poznan posamezni potek poškodbe izbranega elementa ali sistema. Napoved temelji na trenutni izmerjeni vrednosti stanja (sl. 4).

Točko tk določimo po obrazcu:

In any case it is very important to define the limits of the condition parameters. The limits connected to wearing out, pitting and changes of temperature, vibration etc., are very interesting for mechanical diagnostics. It is a question of wearing out, so the curve that shows the system condition is called the wearing-out curve (Fig. 3) [3].

The criteria for defining the limits are:

- Technical and technological
- Economic (costs of interventions, financial risk, etc.)
- Safety (possible consequences of failure)
- Ergonomic (influence of loudness and vibration, etc.)

Usually, it is necessary to take more criteria for the evaluation, which are determined on the basis of experience and an experimental investigation.

0.2 Prognoses for the period of usage

Knowing the average lifetimes of machines and equipment usage, as well as the values of condition parameters, it is possible to predict the behaviour of the parameters' usage. One of the prediction methods is based on the middle statistics values of damages. This method is in use when it is not known, or not sufficiently well known, whether there is a single development of damage on a concrete element or on the system. The prediction is based on the measured condition value at that moment (Fig. 4).

The point is defined by the formula:

$$t_k = \frac{S_i - S_j}{S_i - S_o} \cdot \mu_i \qquad (1),$$

So – začetna vrednost opazovanega parametra,
Si – mejna vrednost opazovanega parametra,
Sj – izmerjena vrednost opazovanega parametra stanja,

So – the starting value of the observed parameter,
Si – the limited value of the observed parameter,
Sj - the measured value of the observed parameter condition,

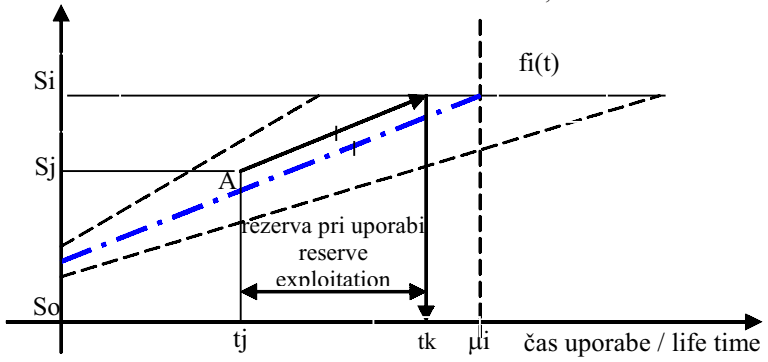

Sl. 4. *Napoved z metodo povprečne statistične vrednosti*
Fig. 4. *Prediction using the method of the middle statistical value*

μ – mejna vrednost obstojnosti elementa,
(*tk-tj*) možen prihranek pri uporabi opazovanega elementa.

1 RAZLIČNE VRSTE IN TEHNIKE TEHNIČNEGA RAZPOZNAVANJA

Tehnično razpoznavanje lahko opazujemo z različnih vidikov, odvisno od namena, rezultatov, načina izvedbe, značilnosti, uporabe in obsega (sl. 5).

- **Preverjanje funkcije** predstavlja razpoznavanje z namenom ugotavljanja funkcionalnosti opreme. Izvaja se z merjenjem delovnih parametrov (npr. tlaka, napetosti, števila vrtljajev) med delovnim postopkom.
- **Določanje odpovedi** predstavlja razpoznavanje, katerega osnovni namen je oceniti stanje pri odpovedi oziroma vzroke tega stanja (merjenje obrabljenosti, korozije, poškodb materiala ipd.) ([3] in [5] do [7]).
- **Zahtevno razpoznavanje** uporabljamo za ugotavljanje splošnega stanja naprave. Obsega spremljanje parametrov stanja, to so kakovost delovanja motorja, moč motorja, pa tudi tlak kompresorja.
- **Poglobljeno razpoznavanje** je, v nasprotju z zahtevno, namenjena za določanje stanja celotnega motorja ali njegovih delov, izvaja pa se z podrobnim raziskovanjem določenih parametrov.
- **Neposredno razpoznavanje** se izvaja z neposrednim merjenjem in analizo določenega parametra stanja. Posredno razpoznavanje pomeni merjenje posrednih veličin za določanje stanja naprave (npr. merjenje hrupa ali vibracij za oceno stanja prenosnikov, ležajev).
- **Pristransko razpoznavanje** se izvaja skozi oceno na podlagi opazovanj stanja. Opazovanja temeljijo na človeških čutilih: vidu, sluhu, vonju ali dotiku. Pri tem se lahko dodatno uporablja specifična oprema (tehnični stetoskop ali endoskop).
- **Nepristransko razpoznavanje** se izvaja z uporabo opreme in merilnih instrumentov, ki kažejo vrednost parametrov. S tem se izključuje pristranskost operaterja (npr. število vrtljajev, tlak, vibracije, hrup ali temperature).
- **Periodično in stalno razpoznavanje** se uporabljata odvisno od potrebe po določitvi

μ – the value limit of the life time,
(*tk-tj*) the possible reserve of the observed element usage

1 DIFFERENT TYPES AND TECHNIQUES OF TECHNICAL DIAGNOSTICS

Technical diagnostics can be seen from several aspects, depending on the goal, the results, the manner of realisation, the performance, the use and the dimensions (Fig. 5).

- An **examination of the function** represents a diagnosis for the purpose of determining the functionality of the equipment. The examination can be done by measuring the functional parameters, for example, the pressure, the tension and the number of turns during the working process.
- A **determination of failure** represents a diagnosis with the goal to examine the condition during failure or the cause of such a condition (measuring the wear, the corrosion, the damages to a material, etc.) ([3] and [5] to [7]).
- **Complex diagnostics** is used to establish the general condition of the equipment. It includes observing the condition parameters, such as the quality of an engine's work, the power of the engine as well as the pressure of the compressor.
- **Deeper diagnostics**, as opposed to complex diagnostics, serves to determine the condition of the whole machine or a part of the machine. This can be done with a detailed investigation of certain parameters.
- A **direct diagnosis** is performed by direct measurements and an analysis of a certain parameter of a condition. Indirect diagnostics means determining the indirect measures for establishing the equipment's condition (for example, measuring the noise or vibration to determine the condition of the transmission).
- **Subjective diagnostics** could be completed by an evaluation on the basis of the observations of a condition. The observations are performed with the human senses: eyesight, hearing, smell or touch. In addition, certain specific equipment can also be used (a technical stethoscope or an endoscope).
- **Objective diagnostics** is performed by using equipment as well as measuring instruments, which show the conditions of the parameters. In this way the subjectivity of the personnel that use the instruments is excluded (for example, the number of turns, the pressure, the vibrations, the noise or the temperature).
- **Periodic and permanent diagnostics** can be completed, depending on the need for determining

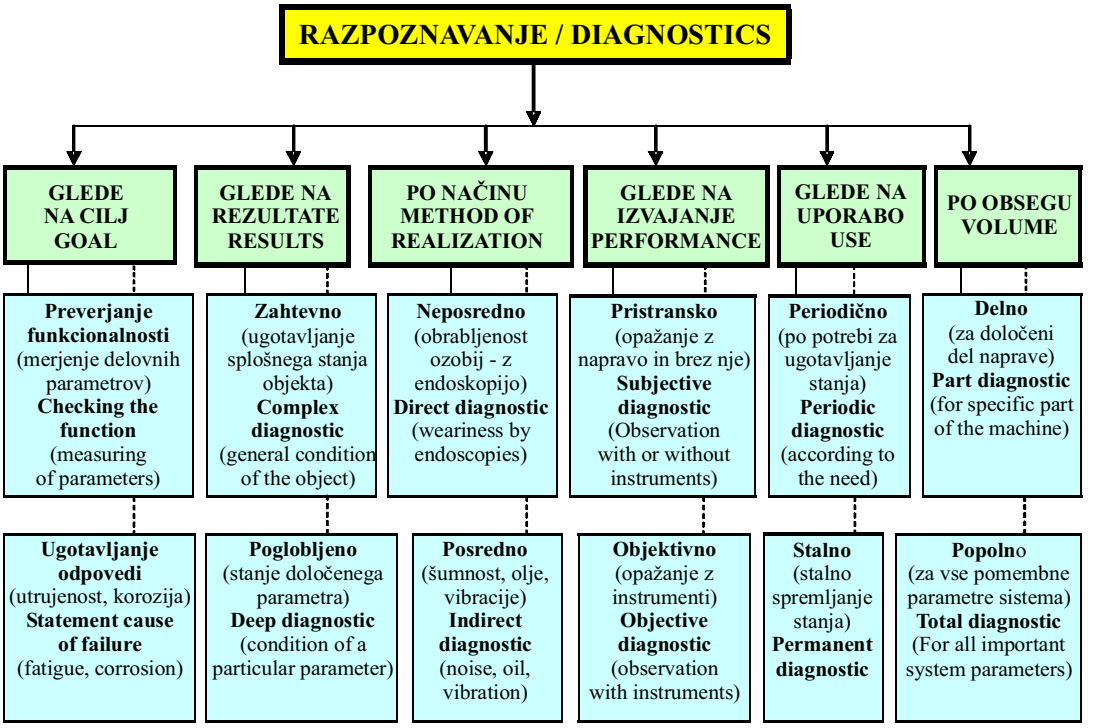

Sl. 5. *Delitev tehničnega razpoznavanja*
Fig. 5. *Division of the technical diagnostic*

stanja naprave (potrebna raven zanesljivosti opreme v funkciji njene uporabe). Delna diagnoza se nanaša na določitev stanja posameznega dela ali enega parametra.

- **Popolno razpoznavanje** se uporablja za celovito oceno vseh pomembnih parametrov stanja naprave. Nepristranski postopki v tehničnem razpoznavanju se izvajajo z inštrumenti za merjenje in prebiranje vrednosti parametrov in s tem izključimo pristranskost sklepov operaterja. Nepristranski tehnični postopki obsegajo tri skupine parametrov:
  - delovni parametri,
  - parametri poškodb elementov naprave,
  - parametri stanja stranskih produktov.

1.1 Endoskopska metoda tehničnega razpoznavanja naprav

V tehniki se vse bolj in bolj uporabljajo optična vlakna za opazovanje težko dostopnih delov (običajno so to različne votle oblike in odprtine) ali v primerih ko druge tehnike vidnega nadzora terjajo zelo drago razgradnjo. Poleg področja razpoznavanja in nadzora je uporaba optičnih vlaken dandanes pomembna tudi pri

the equipment's condition (the required level of reliability of the equipment during its use). Partial diagnostics refers to a determination of the condition of a particular element or a single parameter.

- **Total diagnostics** is performed for a total evaluation of the conditions of all the important parameters of the equipment conditions at hand. The objective acts in technical diagnostics are performed with instruments that measure and read out the parameter conditions, which in turn excludes subjective conclusions. Objective diagnostic acts embody three groups of condition parameters:
  - The working parameters,
  - The parameters of equipment-element damages,
  - The parameters of by-product condition.

1.1 The endoscope method for the technical diagnostics of equipment

The use of optical fibres is becoming commonplace in technical fields, for example, in the process of observing parts that are difficult to access (usually different kinds of cavities and holes) and in those cases where other techniques of visual control necessitate a very expensive disassembly process. The use of optical fibres is not only important in

postopku vzdrževanja oz. pri popravilu strojev brez nepotrebnih razstavljanj, kar naredi sam postopek bistveno bolj gospodaren.

Prvi endoskopi (s tem razumemo vse naprave za opazovanje v zaprtem prostoru) so bili oblikovani za medicinske namene. Beseda "endoskop" je grškega izvora in dobesedno pomeni "pogled od znotraj". Izrazita uporaba endoskopa se je začela z iznajdbo cistoskopa, na katerem je bil zasnovan nadaljnji razvoj moderne urologije. Zatem so bile razvite naprave imenovane "boroskopi", ki predstavljajo povezani sistem leč, opremljen s svetilko. Pri modernih videoendoskopih je omogočeno neposredno usmerjanje in snemanje opazovanega predmeta z uporabo računalniškega sistema. Dejavna uporaba elektronike je bistveno razširila področje uporabe vidnega nadzora in videosnemanja.

V večini primerov se postopki tehničnega razpoznavanja in nadzora izvajajo pri slabi osvetlitvi ali pri dnevni svetlobi. Takšne razmere še posebej niso primerne za izvajanje resnega vidnega nadzora, ker človeško oko, zaradi preslabe osvetlitve, ne more optimalno sodelovati v tem postopku, tudi če uporabimo najboljše optične inštrumente.

Človeško oko ima sposobnost učinkovitega prilagajanja različni stopnji osvetlitve. Osrednjo vlogo pri tem ima zenica, ki se lahko zoža ali razširi, odvisno od jakosti svetlobe. To omogoča, da gledamo v zelo močne izvore svetlobe pa tudi, da vidimo pri zelo šibki svetlobi ali v temi. Potreben je samo kratek čas, da se oko prilagodi na trenutno stanje ali spremembo svetlobe. Očesu je potrebno 10 do 15 minut za popolno prilagoditev pri zmerni spremembi svetlobe ter okoli 30 minut za prilagoditev na popolno temo. To je razlog, zakaj je pri delu z endoskopom treba biti pozoren na to človeško lastnost.

Drugi pomemben dejavnik, ki vpliva na delo z optičnimi sredstvi, je dnevna svetloba. Ta postavlja različne omejitve pri delu, odvisno od sredstev, ki se uporabljajo.

Prožne endoskope z optičnimi vlakni (fiberscope) uporabljamo v primerih, ko razdalja do predmeta ne presega 0,5 m.

1.2 Moderni boroskopi

Togi boroskopi (sl. 6a in b) imajo v primerjavi s fiberskopom zelo preprost optični sistem leč. Pri

the fields of diagnostics and control, but their application is currently of great significance in the process of maintenance, for example, for the repair of machines that can be completed without disassembling them, which in turn makes this process far more economical.

The first endoscopes - the meaning of this term being all equipment used for the purpose of observation in a closed space - were designed for medical purposes. The word "endoscope" has a Greek root and it can be translated as "examination from the inside". The intensive exploitation of endoscopes began with the invention of a cistoscope that set the path for the development of modern urology. Following this, the so-called boroscope was made, i.e., a system of lenses equipped with a lamp. Modern endoscopes make the direct steering and recording of an observed object possible with the use of a computer system. The widespread use of electronics has significantly broadened the fields of application of visual control and video recording.

In most cases the processes of technical diagnostics and control are performed under poor lighting conditions or during daylight. However, these conditions are not suitable for performing serious visual control, due to the fact that the human eye cannot optimally assist us in this process under poor lighting conditions, even if it possesses the best optical instrument.

The human eye has the ability to adapt to various light intensities using the pupil, which can either dilate or contract, depending on the intensity of the light. This enables us to look at very bright light sources, but also to see under very poor lighting conditions, and even in the dark. Only a certain amount of time is needed for an eye to be able to adjust to present or changing lighting conditions. The human eye needs 10–15 minutes for a total adaptation during a modest change in lighting, and around 30 minutes for an adaptation to total darkness. This is the reason why when using an endoscope one has to take the possibilities of human sight into consideration.

The second important factor that influences work with optical equipment is daylight. This sets various limitations during the work, depending on the facilities being used.

Flexible endoscopes with optical fibres (fiberscope) are used in cases when the distance to the object does not exceed 0.5 m.

1.2 Modern boroscope

Inflexible (stiff) boroscopes (Fig. 6 a, b) have a very simple optical system of lenses compared to that of

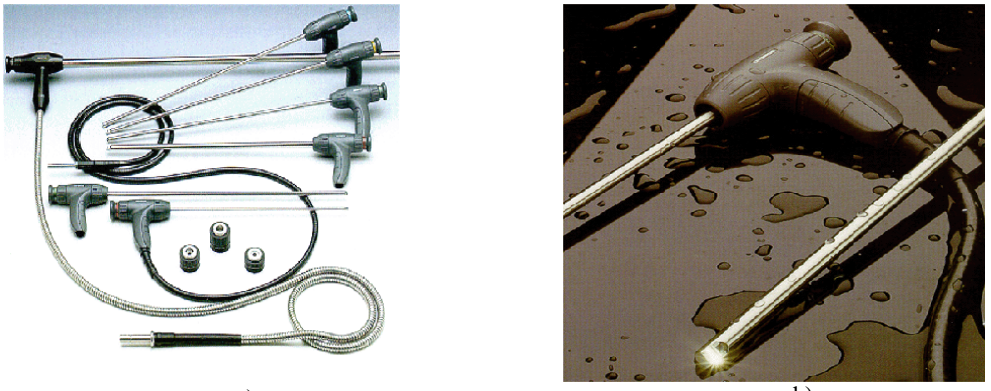

a) b)

Sl. 6. *Boroskop (a), uporaba boroskopa v nasilnem okolju (b)*
Fig. 6. *Boroscope (a), the use of a boroscope in an aggressive environment (b)*

boroskopu je slika zelo jasna. Ker se pri boroskopih ne uporablja koherentni snop optičnih vlaken, so ti nekajkrat cenejši od fiberskopa. Trdna konstrukcija in možnost krmiljenja dolžine, premera, kota in vidnega polja, kakor tudi preprostost uporabe, so naredili boroskop za zelo razširjeno sredstvo vidnega nadzora.

Zaradi trdne konstrukcije je tudi vzdrževanje boroskopov preprosto, kljub temu da so pri uporabi izpostavljeni različnim oblikam nečistoč. Pomembno je, da se po uporabi temeljito obrišejo. Boroskope lahko uporabljamo do temperatur 150 °C ([1] in [8]).

1.3 Fiberskop

Najbolj pomembna značilka fiberskopa je njegova prožnost (sl. 7 in 8), kar omogoča upogibanje brez škodljivega vpliva na sliko, ki jo prenaša. Fiberskop ima dva vira svetlobe, dve optični vlakni, prevodnika za objektiv in okular. Prevodniki svetlobe

the fiberscope. In the case of boroscopes the picture is very clear. Since the boroscopes do not use coherent sheaths of optical fibres, they are several times cheaper then fiberscopes. The firmness of its construction and the possibility of regulating its length, diameter, angle and visual field as well as its simple usage, make the boroscope a widespread tool for visual control.

Boroscopes are easy to maintain due to their firm construction, even after exposing them to dirty conditions. It is important to clean a boroscope very carefully after its use. In addition, a boroscope can be used in high temperatures up to 150ºC ([1] and [8]).

1.3 Fiberscope

The main characteristic of a fiberscope is its flexibility (Figs. 7 and 8); however, it is noteworthy that its ability to bend does not have consequences for the quality of the picture that it processes. The fiberscope has two sources of light, i.e., two fibre light conductors – a lens

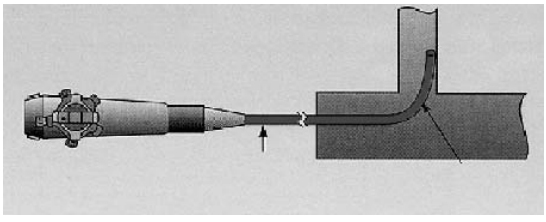

Sl. 7. *Ponazoritev prožnosti fiberskopa*
Fig. 7. *Illustration of a fiberscope's flexibility*

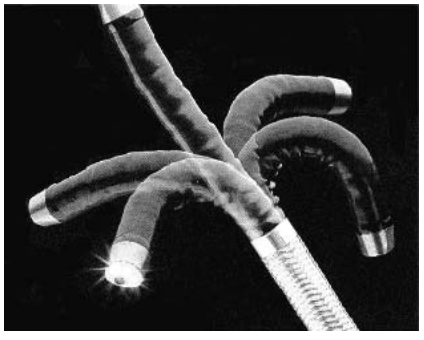

Sl. 8. *Možnosti pregleda (ocenjevanja) z vrhom (konico) fiberskopa*
Fig. 8. *Steering possibilities with the tip of the fiberscope*

za prenos slike sestoje iz približno 120.000 vlaken, premera 0,009 do 0,017 mm. Slika nastaja na visoko poliranih čelih obeh koncev svetlobnih prevodnikov za prenos slike ([1] in [8]).

Konci fiberskopa se lahko upogibajo, kar omogoča ne samo neposredni temveč tudi bočni pogled (sl. 7 in 8). Minimalni premer fiberskopa je 2 mm. Lahko ga priklopimo na TV zaslon ali monitor računalnika.

2 ENDOSKOPSKO RAZPOZNAVANJE VALJA MOTORJA

Pomen tehničnega razpoznavanja kot osnove strategije vzdrževanja glede na stanje je ponazorjen na primeru uporabe endoskopije pri vzdrževanju motorja – ugotavljanje stanja čela bata, ventila ali valja brez razstavljanja motorja. Razpoznavanje je izvedeno na ladijskih motorjih za posebne namene, pri čemer so za ta postopek pomembni številni elementi: izbrana metodologija, priprava, izbira inštrumentov, izbira mesta za izvajanje razpoznavanja, načrtovanje, prikaz rezultatov razpoznavanja, ponazorjen z endoskopskimi fotografijami ali preglednicami z opisom. Ladijski motorji, ki so predmet raziskovanja, so vgrajeni v ladje za posebne namene, zato njihove značilke v tem prispevku niso podane. Poglavitni namen prispevka je splošni prikaz primera endoskopskega razpoznavanja.

2.1 Metodologija razpoznavanja ladijskega motorja

Zanesljivo zaznavanje vzroka za prisotnost hladilne emulzije v valjih motorja ni bila mogoča brez uporabe endoskopa. Namen je bil izogniti se razstavitvi motorja z nosil, kar bi bistveno znižalo stroške popravila motorja. Pred pričetkom celotnega postopka je potrebno segreti hladilno emulzijo na 60 °C z vključitvijo obtočne črpalke za hladilno emulzijo motorja. Po 4 urah segrevanja motorja je opravljen endoskopski pregled z namenom odkriti mesto, kjer hladilna emulzija vdira v valje motorja. Da bi uspešno izvedli endoskopsko razpoznavanje je treba razdelati metodologijo za izvajanje endoskopskega nadzora. Metodologija diagnostike ladijskega motorja, kot tehnična procedura, sestoji iz naslednjih operacij ([4] in [8]):

- definiranje mesta pregleda motorja (sklopi, podsklopi, elementi, oprema motorja) na podlagi dostopne dokumentacije in pregleda motorja;

and an ocular conductor. These light conductors, whose function is the transmission of the picture, are composed of nearly 120,000 fibres, with a diameter of 0.009–0.017 mm. The picture is formed on the highly polished heads of both light conductors that transmit the picture ([1] and [8]).

The fiberscope tips are flexible, which makes a lateral view also possible (Figs. 6 and 7). The minimum diameter of a fiberscope is 2 mm. Furthermore, a fiberscope can be connected to a TV screen or a computer monitor.

2 THE ENDOSCOPIC DIAGNOSTICS OF AN ENGINE CYLINDER

The significance of technical diagnostics as a basic strategy in condition maintenance is illustrated by the use of an endoscope for the maintenance of an engine – defining the condition of a piston, valve or a cylinder without disassembly. The diagnosis was made on a ship's engine with a special assignment. There are many elements that are important for this process: the type of methodology, the preparation, the defining of the instruments, the places chosen for the diagnostic process, the planning, and the results, which are illustrated by photos or tables with a description. The ship's engine is used in special boats and its characteristics are not presented in this paper. The goal of this paper is to show examples of endoscope diagnostics in general.

2.1 Methodology of the diagnostics of a ship's engine

A reliable breakdown of the cause of the presence of a cooling emulsion in cylinders was not possible without using an endoscope. The main goal is to avoid removing the engine from its carrier, which would significantly lower the costs of repairing the engine. Prior to starting the whole procedure, it is necessary to warm up the emulsion to 60°C using a circular pump for the cooling emulsion of the engine. After four hours of warming up the engine, the endoscope examination is performed with the aim of discovering the place where the emulsion is leaking into cylinders. In order to implement the endoscope diagnostics, it is important to elaborate on the methodology for endoscope control. The methodology of the diagnostics of a ship's engine, as a technological procedure, consists of the following operations ([4] and [8]):

- Defining the place for the engine's examination (compositions, sub-compositions, elements, engine equipment) on the basis of the available documentation and an overview of the engine.

- zagotovitev dostopa endoskopske opreme na mesto, ki bo nadzorovano (skozi sedanje odprtine ali skozi na novo izdelane odprtine, upoštevajoč, da na novo izdelane odprtine ne oslabijo konstrukcije in ne motijo delovanja motorja);
- izbira najbolj ustrezne opreme in osebja za izvedbo endoskopskega nadzora;
- določanje časovnih korakov za pregled motorja;
- definiranje potrebne dokumentacije za podporo;
- analiziranje sedanjega stanja in sklepanje o tehničnem stanju dieselskega ladijskega motorja.

Priprava ladijskega motorja za endoskopski pregled vključuje množico dejavnosti, ki naj bi zagotovile dobre pogoje za nemoteno in zanesljivo izvajanje nadzora. Med temi pripravami je treba:

- zagotoviti želene razmere okolja (temperatura, tlak, vlažnost);
- pregledati tiste dele, ki bodo nadzorovani (da ne bo tujih predmetov, nesnage, iztekanja olja, goriva, hladilne emulzije);
- zagotoviti želeno stanje motorja (motor ne sme delovati, temperatura olja in hladilne emulzije pa na ustrezni ravni);
- pripraviti potrebno orodje.

Po končanih pripravah za endoskopski pregled motorja je treba določiti nadzorna mesta in poiskati najbolj ugodne poti za dostop z endoskopom. Na podlagi sklepov, ki sledijo iz analize mogočih dostopov k nadzornim mestom, se odpirajo tiste odprtine na motorju, ki so najbolj primerne za izvajanje pregleda. Izbira orodij in opreme je odvisna od: izbranih mest za preglede, konstrukcijskih rešitev odprtin za preglede in pogojev, pri katerih se bo izvajal pregled. Nadzorniki, ki izvajajo preglede morajo biti dobro seznanjeni z endoskopsko opremo (z načelom delovanja in uporabe v danih razmerah), kakor tudi s konstrukcijo in značilkami ladijskih motorjev, ki jih pregledujejo.

Zadnji korak postopka, definiranega z metodologijo pregleda ladijskega motorja, je sklepanje oz. ocena tehničnega stanja ladijskega motorja kot celotnega sistema, kakor tudi ocene stanja posameznih delov (podsklopov). Iz dobljenih rezultatov sklepamo o nadaljnji uporabi motorja oz. o potrebnem vzdrževanju, ki ga je treba izvesti takoj ali v bližnji prihodnosti.

- Ensuring access for the endoscope equipment to the places that are controlled (through already-existing openings or through boring new openings, but taking into consideration that those new openings do not jeopardise the construction and disturb the work of the engine).
- Choosing the most convenient equipment and staff that will perform the endoscope control.
- Determining the time intervals for examining the engine.
- Defining the supporting documentation.
- Analysing the present condition and making conclusions about the technical condition of the ship's diesel engine

Preparing the ship's engine for endoscope examination includes a series of activities that should provide good conditions for an undisturbed and a reliable control process. During this preparation it is necessary to:

- Provide the required environmental conditions (temperature, pressure, humidity),
- Examine those parts that will be controlled (for example, for the presence of foreign objects, dirt, oil, petrol or cooling-emulsion leakage),
- Provide the needed conditions for the engine (the engine must not be turned on and the temperature of oil and that of the cooling emulsion should be at the required level),
- Prepare the required tools.

After the preparations for the endoscope examination of the engine, it is important to determine the control places and find the best possible way for the endoscope to access them. On the basis of the conclusions drawn in the process of analysing the possible routes for accessing the control place for the examination, those openings that are the most convenient for performing the examination are selected for opening. The selection of tools depends on the following: the chosen places for the examination, the constructed solutions about openings for the examination and the conditions for performing it. The staff that performs the examination must be familiar with the endoscope equipment (principles of work and usage), as well as the construction and characteristics of the ship's engine that is being examined.

The last step in the process, defined by the examination methodology of the ship's engine, is drawing the conclusion and evaluating the technical condition of this ship's engine as an entire system as well as evaluating the technical condition of its parts. Based on the results a conclusion can be made about further exploitation of the engine as well as the necessary maintenance that should be performed either immediately or in the near future.

Preglednica 1. *Oprema za endoskopsko diagnostiko*
Table 1. *Equipment for endoscope diagnostics*

Vrsta endoskopske opreme Type of endoscope equipment	Oznaka endoskopske opreme The mark of endoscope equipment	Premer endoskopa Diameter of endoscope	Smer opazovanja Direction of oversee
vlaknoskop fiberscope	IF6C5X1-13	6,0 mm	neposredno - v vseh smereh directly – in all directions
video-endoskop video-endoscope	IV6C5	6,0 mm	neposredno - v vseh smereh directly – in all directions
video stekla video glasses	LCD stekla LCD glasses	-	-
vir svetlobe the source of light	ILV-2	-	-
boroskop boroscope	R060-063-000-50	6,0 mm	neposredno directly
boroskop boroscope	R060-063-090-50	6,0 mm	s strani laterally
računalniški zaslon computer monitor	14"	-	-
sistemski analizator system analyzer	IW-2 z opremo IW-2 with equipment	-	-

2.2 Definiranje opreme za endoskopsko razpoznavanje

Oprema, opisana v preglednici 1 se uporablja za endoskopsko razpoznavanje.

2.3 Definiranje merilnega mesta za endoskopsko razpoznavanje

Na sliki 9 je prikazan prečni prerez ladijskega motorja – predmeta raziskovanja – z nakazanim mestom vstavitve endoskopske opreme (boroskopa in vlaknoskopa) v valj motorja. Na vsakem valju je opravljeno opazovanje na definiranih mernih mestih, in to:

- čelo bata,
- puša valja,
- stična ploskev med valjem in pokrovom,
- sesalni in izpušni ventili s sedeži,
- sedež ventila,
- vodilo ventila.

Načrt endoskopskega pregleda batov in valjev, kompresorja in hladilnih naprav z merilnimi mesti ter mogočimi poškodbami je podan v preglednici 2. Ta program endoskopskega razpoznavanja, s predhodno opisano metodologijo, se lahko uporabi za ladijske motorje, ki so običajno v uporabi. Preglednica 2 prikazuje načrt pregleda za en valj.

2.2 Defining the equipment for endoscope diagnostics

The equipment described in Table 1 is used for the endoscope diagnostics.

2.3 Determining the measurement locations for endoscope diagnostics

The cross-section shows the engine – the subject of the research – with the place for inputting the endoscope equipment (boroscope and fiberscope) into the cylinder (Fig. 9). Each cylinder was separately examined at defined measuring points:

- Head of piston
- Cover of cylinder
- Connection between cylinder and head
- Suction and exhaust valve with seats
- Valve seat
- Valve guides

A plan of the diagnosis is made for each of the engine cylinders. The plan defines the objects of the diagnosis and any possible damage. The examination of the endoscope diagnostics for the piston-cylinder group, compressor and air conditioners with control places and possible damage is given in Table 2. This programme of endoscope diagnostics with previously described methodology can be applied to an engine that is used in ships. Table 2 shows a plan of the diagnostics for one cylinder.

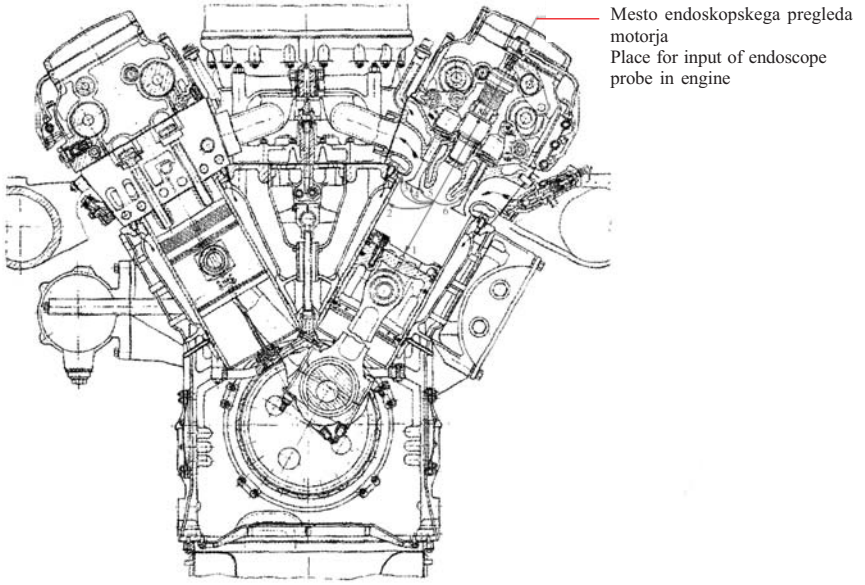

Sl. 9. *Prečni prerez motorja in mesto endoskopskega pregleda*
Fig. 9. *Cross-section of ship's engine and the place of endoscope examination*

Preglednica 2. *Endoskopsko razpoznavanje motorja – načrtovanje razpoznavanja*
Table 2. *Endoscope diagnostics of engine – planning the diagnosis*

SKUPINA BAT-VALJ IN VENTILNI MEHANIZEM PISTON-CYLINDER GROUP AND SEPARATING MECHANISM					
Objekt razpoznavanja Object of the diagnosis	**Mogoče poškodbe Possible damage**	**Objekt razpoznavanja Object of the diagnosis**	**Mogoče poškodbe Possible damage**	**Objekt razpoznavanja Object of the diagnosis**	**Mogoče poškodbe Possible damage**
čelo bata head of piston	obloge koksa deposit of coke	**puša valja surface of cylinder**	korozija corrosion	**glava valja head of the cylinder**	korozija corrosion
	razpoke fissure		vzdolžni risi longitude damages		razpoke fissure
	korozija corrosion		razpoke fissure		tesnost hermetically
	druge oblike poškodb other type of damage		žlebovi od obročkov channels of link		druge oblike poškodb other damage
			druge oblike poškodb other type of damage		
sesalni ventil intake valve	korozija corrosion	**izpušni ventil blow-out valve**	korozija corrosion	**KOMPRESOR COMPRESOR**	
	obloge koksa deposit of coke		obloge koksa deposit of coke	**kompresor compressor**	stanje difuzorja situate diffuser
	sedež ventila seat of valve		sedež ventila seat of valve		stanje lopatic rotorja situate rotor
	zračnost clearance		zračnost clearance		zračnost clearance
	gobica ventila head of valve		gobica ventila head of valve		druge oblike poškodb other damages

3 REZULTATI ENDOSKOPSKEGA RAZPOZNAVANJA

Med endoskopskim pregledom so bili pregledani vsi valji preiskovanega ladijskega motorja, da bi odkrili mogoče napake, to so: tesnost

3 RESULTS OF THE ENDOSCOPIC DIAGNOSIS

During endoscope diagnostics more cylinders of the ship's engine are checked for possible damage, including leakage of the cooling fluid, cor-

(puščanje) hladilnega sistema, korozija, mehanske poškodbe, poškodbe galvanske zaščite, deformacije, vsedline nečistoč, prisotnost tujkov itn.

V prispevku so kot ponazoritev prikazani številni posnetki stanja valjev motorja, ki so bili razpoznani po načrtu razpoznavnih opravil. Opazimo suspenzijo vode in olja v valju, korozijo čela bata ali glave motorja ter podobno (sl. 10 do 17). Ob vsakem posnetku je podan kratek opis opaženega pojava in mesto pojavljanja. Ti pojavi kažejo na določene poškodbe posameznih elementov motorja in njihovo neustreznost delovanja, npr. zračni filtri, ki ne smejo prepuščati zraka zasičenega s kapljicami morske vode, kar je pogost pojav pri delovanju ladijskih motorjev.

Rezultati endoskopskega pregleda vseh valjev motorja so podani v preglednicah, ki vsebujejo

rosion, mechanical damage, damage to the galvanic protection, deformations, the deposit of dirt and coke, the presence of extraneous objects, etc.

There are many illustrations in this paper with pictures of the condition of the engine cylinder before diagnosis, which is done according to the plan of the diagnostics tasks. It is easy to see water or oil on the cylinder, corrosion on the head of the piston and cylinder, etc (Figs. 10 to 17). We describe the situation, the place and the damage for every illustration. Those pictures show some damage to the engine elements and show possible incorrectness of other elements, such as an air filter that must not pass air full of sea water, which is very often the situation in the exploitation of this sort of engine.

The results of endoscope observations for all the engine cylinders are shown in the tables that

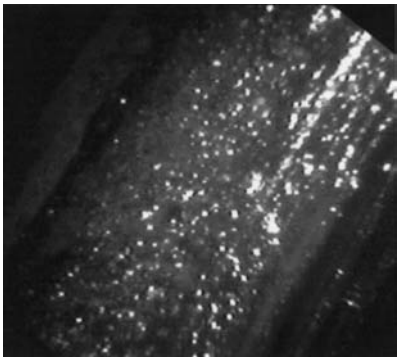

Sl. 10. *Pogled na glavo motorja (korozija zaradi vdora vode)*
Fig. 10. *View of a cylinder head at the location of the oil burner (the presence of corrosion due to water penetration)*

Sl. 11. *Površina glave motorja in odprti sesalni ventili (vidna korozija ventilov)*
Fig. 11. *The connection between the cylinder head and the surface of the cover with suction valves open (presence of corrosion on the valves)*

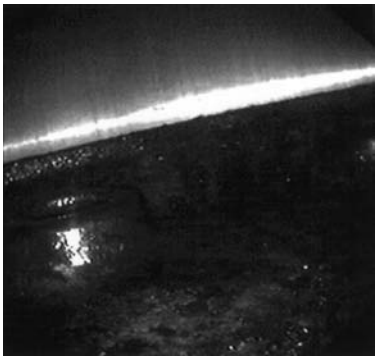

Sl. 12. *Odprt sesalni ventil in zaprt izpušni ventil (korozija glave motorja in ventila)*
Fig. 12. *Open suction valve and closed exhaust valve (presence of corrosion on the cylinder head and the valve)*

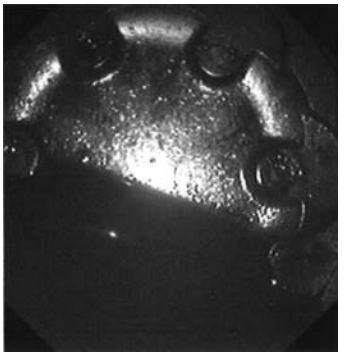

Sl. 13. *Nečistoče na čelu bata – detajl (korozija)*
Fig. 13. *Dirty piston head – detail (presence of corrosion)*

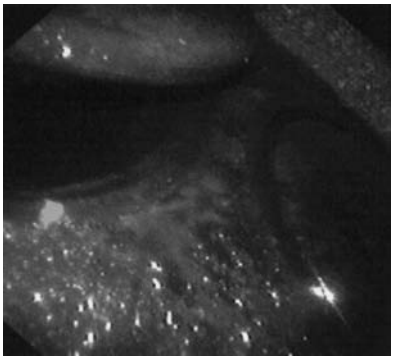

Sl. 14. *Nečistoče na čelu bata (petrolej)*
Fig. 14. *Dirty piston head with the presence of petroleum*

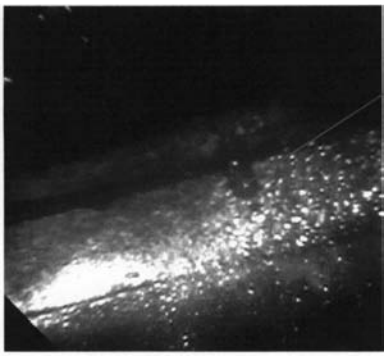

Sl. 15. *Oblikovanje kapljic vode na sestavu med glavo motorja in valjem*
Fig. 15. *Formation of water droplets on the connection between head and the cover of the cylinder*

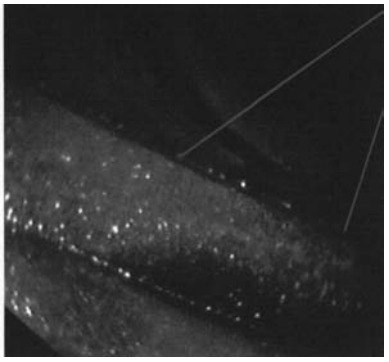

Sl. 16. *Mesto vdora vode med glavo motorja in valjem*
Fig.16. *The place of water penetration between the head and the cover of the cylinder*

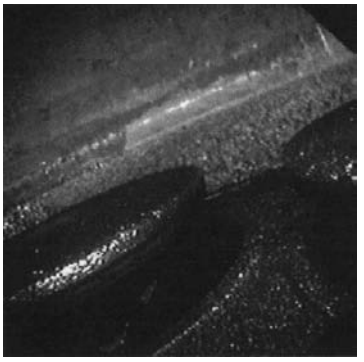

Sl. 17. *Prikaz sesalnega ventila z vidno korozijo*
Fig.17. *The appearance of suction valves with the presence of corrosion*

podatke o številu valjev, mestih merjenja, ugotovljenega stanja in sklepov operaterja. V preglednici 3 so za ponazoritev podani rezultati endoskopskega pregleda treh valjev.

Krivulja obrabe na sliki 18 prikazuje rezultat endoskopskega pregleda določenih merilnih parametrov stanja za izbrano število valjev motorja.

Grafični prikaz endoskopskega razpoznavanja kaže, da je v času zadnjega pregleda prišlo do kopičenja nezadovoljivih rezultatov. To pomeni, da je motor v stanju zmanjšane možnosti uporabe. Takšen sklep opozarja na potrebo po dejavnostih za zaustavitev motorja in popravilo ter zamenjavo delov motorja, tako tistih, ki so bili predmet pregledovanja (valji, bati itn.) kakor tudi delov, ki bi bili lahko vzrok za poškodbe valja: filtri, prečiščevalnik olja, hladilni sistem itn.

contain the number of the cylinder, the measuring location, the condition and the conclusion. Table 3 presents the results of the endoscope examination of three cylinders as an illustration in this paper.

The wearing-out curve shows the result of the endoscope diagnosis for defining the measuring condition parameters on a number of cylinders of the engine (Fig. 18).

The endoscope diagnostic graphic shows that there are many bad results about the conditions of some cylinder elements during the last examination. This means that the engine is in a condition of decreasing usage. The conclusion is that it is necessary to prepare the engine to stop working for a repair or to change some engine parts. It could be the objects of the examination (cylinder, piston, etc) or some parts that could have an influence on damage to the cylinder – filters, oil cleaners, air conditioners, etc.

Preglednica 3. *Tehnično stanje treh valjev motorja*
Table 3. *Technical condition in a number of cylinders of the engine*

Zap. število No. Cylinders	Predmet razpoznavanja Object of diagnostics	Predmet diagnostike Observed condition	Ugotovljeno stanje Conclusion
1	čelo bata head of piston	sledovi oblog traces of deposits	zadovoljivo satisfactory
	valj in glava cylinder and head	brez poškodb no damage	zadovoljivo satisfactory
	sesalni ventili suction valves	brez poškodb no damage	zadovoljivo satisfactory
	izpušni ventili exhaust valves	sledovi korozije traces of corrosion	nezadovoljivo not satisfactory
2	čelo bata head of piston	sledovi korozije traces of corrosion	nezadovoljivo not satisfactory
	valj in glava piston and head	korozija zaradi vdora vode corrosion due to water	nezadovoljivo not satisfactory
	sesalni ventili suction valves	korozija zaradi vdora vode corrosion due to penetration	nezadovoljivo not satisfactory
	izpušni ventili exhaust valves	korozija zaradi vdora vode corrosion due to water penetration	nezadovoljivo not satisfactory
3	čelo bata head of piston	brez poškodb no damage	zadovoljivo satisfactory
	valj in glava cylinder and head	brez poškodb no damage	zadovoljivo satisfactory
	sesalni ventili suction valves	sledovi korozije na gobicah traces of corrosion on "mushroom"	nezadovoljivo not satisfactory
	izpušni ventili exhaust valves	sledovi korozije na gobicah traces of corrosion on "mushroom"	nezadovoljivo not satisfactory

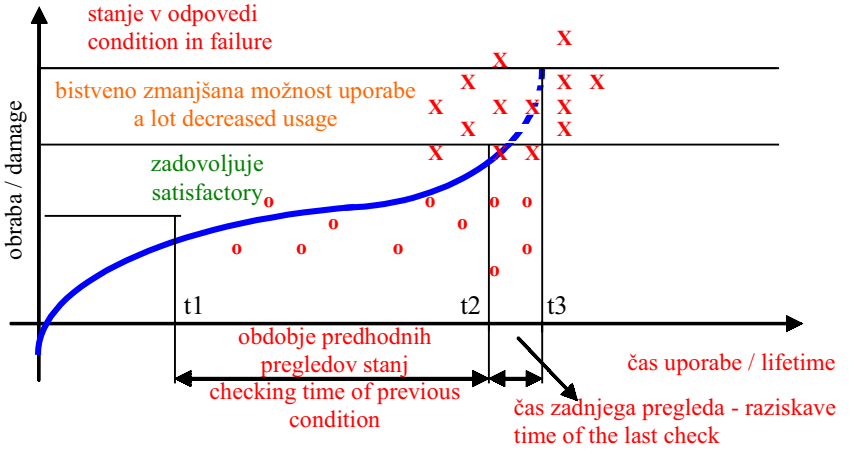

Sl. 18. *Rezultati endoskopske diagnostike*
Fig.18. *Results of endoscope diagnostics*

4 OCENJEVANJE KRITERIJEV SPREJEMLJIVOSTI NAPAK NA LADIJSKEM MOTORJU

Časovni korak pregledov se lahko določa na podlagi poznavanja konstrukcije ladijskega motorja M845 oz. delov, ki bodo razpoznavani, njihovih tehnično-tehnoloških značilk ter razmer pri delovanju. Prihodnji pregledi naj bi omogočili spremljanje poškodb posameznih delov motorja, na podlagi katerih bi lahko sprejeli kriterije

4 EVALUATION OF THE ACCEPTABILITY CRITERIA FOR DAMAGE TO THE SHIP'S ENGINE

The time intervals for the examinations can be proposed since one is familiar with the construction of the ship's engine, i.e., with those parts that need to be diagnosed, the technical and technological characteristics, and the conditions in which they work. The following examinations would enable observing the damage on the parts of the engine on the basis of which one could adopt the

sprejemljivih poškodb. Ti kriteriji so lahko v pomoč pri izdelavi etalonov za kalibracijo, ki naj bi jih uporabljali pri analizi in postopku prilagajanja kriterijev sprejemljivosti poškodb delov motorja.

Za spremljanje in prilagajanje teh kriterijev je treba vse podatke in rezultate, dobljene med endoskopskim pregledom, zapisovati v določene obrazce (liste pregledov). Kriteriji sprejemljivosti za odkrite poškodbe se definirajo s posebnim dokumentom, v katerem so podane slike poškodb in etaloni z dopustnimi kriteriji sprejemljivosti teh poškodb. Spremljajoča dokumentacija so običajno preglednice, ki vsebujejo: mesto pregleda, vrsto poškodbe, največje dopustne velikosti poškodb, kakor tudi število dopustnih napak.

Namen celovitega pregleda je ocena kriterija sprejemljivosti poškodb posameznih delov motorja, ker daje odgovor na vprašanje, v kakšnem stanju je preizkuševani motor. Na temelju ocene teh kriterijev sprejemljivosti se sprejme odločitev o nadaljnjem tehničnem saniranju poškodb in nadaljnji uporabi motorja.

Ocenitev kriterija sprejemljivosti poškodb delov motorja se lahko izvede takole:

- primerjava poškodbe z etalonom – ta kriterij predpostavlja obstoj etalona, ki je rezultat dolgotrajnega spremljanja in opazovanja razvoja poškodbe ter prirejanja mej poškodb, pri katerih motor še zadovoljivo deluje;
- primerjava poškodb s sprejetimi dopustnimi vrednostmi, podanimi v ustreznih preglednicah;
- primerjava poškodb s slikami, skicami, načrti, fotografijami in podobnimi dokumenti.

Poškodbe se pogosto ocenjuje z upoštevanjem več kriterijev, da bi se na ta način zmanjšala možnost napake.

5 SKLEPNE UGOTOVITVE

Stanje tehničnega sistema označujejo številni parametri delovnega postopka. Poudariti je treba, da vsi parametri nimajo enakega vpliva na stanje sistema. Izbira razpoznavnih parametrov, ki bodo nadzorovani, se izvaja na temelju poteka podatkov o delovanju sistema. Čeprav na tehnično razpoznavanje lahko gledamo z različnih vidikov, nobeden izmed njih ne obstaja neodvisno drug od drugega, vsaka oblika tehnične diagnostike vsebuje več vidikov. Tipični primer za to je

acceptability criteria for damage. These criteria could be helpful in the production of calibration pieces that would serve for analysis in the process of adopting the acceptability criteria for damage to the engine parts.

It is necessary to note all the data and results, acquired during endoscope examinations, in certain forms in order to follow and adopt acceptability the criteria for damage to the engine parts. The acceptability criteria for the observed damage are defined using a certain form, which contains the accompanying illustrations and calibrations with permitted acceptability criteria. The accompanying documentation usually contains tables with the place of examination, the type of damage, the maximum permitted scope of damage as well as the amount of allowed damage.

The main goal of the whole examination is the evaluation of the acceptability criteria for damage to the parts of the engine, since this answers the question about the state of the examined engine. Based on the evaluation of these acceptability criteria, a decision can be made about further technical repair and continued use.

The evaluation of the acceptability criteria for damage to parts of the engine can be performed in the following ways:

- By comparing the damage with a calibration. This criterion predicts the existence of the calibration, which is derived from a long-term follow-up and the observation of damage development and the adoption of the limits for the amount of damage with which the engine can still function properly,
- By comparing the damage with set allowed values given in tables,
- By comparing the damage with pictures, sketches, photos and other similar documents.

The evaluation of damage is, in most cases, performed using several criteria, so that a possible error could be reduced.

5 CONCLUSIONS

Many parameters of a working process characterise the condition of a technical system. However, it is important to note that not all parameters of this working process have an equal influence on the system condition. The choice of diagnostic parameters that is to be controlled is made on the basis of the history of the data about the work of a system at hand. Even though technical diagnostics can be seen from several aspects, none of them can exist independently from the others, since each type of technical diagnostics contains several other

endoskopska metoda, ki je hkrati glede na način dela - neposredna, glede na rezultate – poglobljena, glede na izvajanje – primerna. Lahko je tudi glede na uporabo občasna ali stalna, glede na obseg pa delna ali popolna.

Vlaknoskopi so posebej zanimivi zaradi svojih značilnosti. To so prilagodljivi inštrumenti, ki imajo takšno upogljivost, da ne omogočajo samo neposredni, temveč tudi bočni pogled in imajo možnost neposredne povezave z računalnikom in zaslonom, s čimer se doseže največji nadzor postopka razpoznavanja.

Med endoskopskim razpoznavanjem ladijskega motorja je mogoče nadzorovati posebne pomajkljivosti in poškodbe, to so: iztekanje hladilne tekočine, korozija, mehanske poškodbe, poškodbe galvanske zaščite, deformacije, vsedline nečistoč in koksa, kakor tudi tuje predmete.

Iz rezultatov, pridobljenih z endoskopom, poznavanja konstrukcije ladijskega motorja oz. delov, ki jih razpoznavamo, njihove tehnično-tehnološke značilnosti in razmere, v katerih obratujejo, se lahko predlagajo določene dejavnosti pri vzdrževanju ter časovni koraki za prihodnje preglede.

aspects. A typical example is the endoscope method, which is, at the same time, direct in terms of the working manner, deepening according to the results and objective according to the performance. It can also be either periodic or permanent, according to its application as well as either partial or complete according its scope.

Fibre scopes are particularly interesting because of their characteristics. They are flexible instruments that have the ability to bend, which enables not only a direct, but also a lateral view and offers the possibility of a direct connection with a computer and a monitor, which in turn allows maximum control of this diagnostic process.

During an endoscope diagnosis of a ship's engine, the control of possible defect and damage phenomena is incorporated, such as leakage of a cooling fluid, corrosion, mechanical damage, damage to galvanic protection, deformations, deposits of dirt and coke as well as the presence of extraneous objects.

On the basis of the results acquired with an endoscope and a familiarity with a ship's engine construction and its parts that are diagnosed as well as their technical and technological characteristics and the conditions in which they work, one can propose certain maintenance activities and certain time intervals for future examinations.

6 LITERATURA
6 REFERENCES

[1] Kelly, A. (1989) Maintenance and its management, *Conference Communication*, Tiford Farnham, UK.
[2] Venkatesh (2006) An introduction to total productive maintenance (TPM), www.plant – maintenance.com.
[3] Bulatović, M. (1996) Investigation of increasing the effectiveness of systems in the processing industry by prediction and prevention failures, Ph.D. thesis, *Faculty of Mechanical Engineering*, Podgorica.
[4] Technical diagnostics in function of effectiveness of technical systems (2006) Project of *Ministry of Education, Montenegro*, Podgorica.
[5] Bulatovic, M., Vukcevic, M. (2000) Incorporation of the parameters condition and probability of failures in expert system in function of technical diagnostics, *The Third World Congress on Intelligent Manufacturing Processes Systems*, Cambridge, Massachusetts, USA, June 28-30, 2000.
[6] Bulatovic, M. (2003) Expert system in function of technical diagnostics, *7th International Research/ Expert Conference " Trend in The Development of Machinery And Associated Technology" TMT 2003*, Loret de Mar, Barcelona - Spain, 15-17 September, 2003.
[7] Aronov, I.Z., Zhurtsev, M.V. (1987) Planirovanye Opredelitelnyh Ispitany na Nadyoznost i Obrabotka Rezultatov, *Politehnichesky muzey znanye*, Moskva.
[8] Šušić, J. (2006) Maintenance modelling in function of efficiency of naval ships, Master Thesis, *Faculty of Mechanical Engineering*, Podgorica.

Avtorjev naslov: prof. dr. Miodrag Bulatović
mag. Jovan Šušić
Univerza v Črni Gori
Fakulteta za strojništvo
Cetinjski put bb
81000 Podgorica, Črna Gora
bulatovm@yahoo.com

Authors' Address: Prof. Dr. Miodrag Bulatović
Mag. Jovan Šušić
University of Montenegro
Faculty of Mechanical Eng.
Cetinjski put bb
81000 Podgorica, Montenegro
bulatovm@yahoo.com

Prejeto: 12.8.2006
Received:

Sprejeto: 21.2.2007
Accepted:

Odprto za diskusijo: 1 leto
Open for discussion: 1 year

Poročila - Reports

Evropska konferenca o tribologiji - ECOTRIB 2007

Slovensko društvo za tribologijo v sodelovanju s triboloških društvoma Avstrije in Italije prireja od 12. do 15. junija 2007 v Grand hotelu Union v Ljubljani Evropsko konferenco o tribologiji - ECOTRIB 2007. Konferenca ECOTRIB je prva v seriji konferenc, ki bodo geografsko, ekonomsko in znanstveno usmerjene predvsem na področje srednje in južne Evrope in se bodo vsaki dve leti odvijale v eni od treh dežel organizatork. Letos bo konferenca ECOTRIB potekala skupaj s končno konferenco evropskega projekta COST 532: Triboscience and Tribotechnology, delovnim sestankom Marie Curie WEMESURF mreže (6. okvirni program EU), delovnim sestankom EUREKA skupine ENIWEP ter Tehničnim simpozijem Mednarodne agencije za energijo z naslovom Implementacija dogovora o naprednih materialih.

Konferenca ECOTRIB je usmerjena k perečim znanstvenim in industrijskim problemom s področja tribologije, inženiringa površine, vzdrževanja in tehnične diagnostike, kakor tudi k možnostim njihovega reševanja. Konferenca bo v obliki vabljenih predavanj mednarodno priznanih strokovnajkov, rednih predavanj ter posterjev zagotovila mednarodni forum, na katerem bodo lahko udeleženci iz industrije in raziskovalnih ustanov ter univerz predstavili zadnje izsledke raziskav in izmenjali izkušnje iz različnih področij dela.

Na konferenci, na katero je prijavljenih 225 udeležencev iz 45 držav širom sveta, bo predstavljenih 157 prispevkov, od tega 2 plenarni predavanji, 12 vabljenih predavanj, 124 govornih prispevkov in 19 posterjev. Po konferenci bodo najboljši prispevki objavljeni v mednarodnih recenziranih revijah Wear, Tribology International, Tribotest in Lubrication Science.

Konferenco ECOTRIB so finančno podprli Javna agencija za raziskovalno dejavnost Republike Slovenije, Organizacija COST ter podjetji PETROL in OLMA iz Ljubljane.

prof. dr. Jože Vižintin

Rehabilitacijski inženiring in tehnologija

Dne 16. in 17. marca 2007 so na Inštitutu republike Slovenije za rehabilitacijo potekali 18. dnevi rehabilitacijske medicine z naslovom Rehabilitacijski inženiring in tehnologija. Organizator je bil Inštitut v sodelovanju s Katedro za fizikalno in rehabilitacijsko medicino Medicinske fakultete v Ljubljani. Udeležilo se ga je veliko poslušalcev, med njimi so bili zdravniki ter drugo medicinsko in tehnično osebje. Predavali so profesorji, delovne terapevtke in mladi raziskovalci iz Slovenije, Velike Britanije, Nemčije in Italije. Udeležence je v pozdravnem govoru nagovoril minister za visoko šolstvo, znanost in tehnologijo dr. Jure Zupan. Med častnimi gosti so se pojavili direktor inštituta mag. Robert Cugelj, predsednik nacionalnega sveta invalidskih organizacij Boris Šuštaršič, dekan Medicinske fakultete v Ljubljani prof. dr. Dušan Šuput in dekan Fakultete za elektrotehniko v Ljubljani prof. dr. Tomaž Slivnik. Predavanja je povezoval predstojnik inštituta prof. dr. Črt Marinček, strokovni vodja seminarja pa je bil prof. dr. Anton Zupan. Predstavili so se tudi trije uporabniki električnih invalidskih vozičkov in prikazali nekaj funkcij, ki jih krmilijo s prstom, z brado oz. z jezikom.

Poglavitni namen seminarja je bil predstaviti najnovejše dosežke rehabilitacijskega inženiringa, ki hendikepiranim osebam v čim večji meri izboljšajo kakovost življenja. Oviranost oz. hendikep je namreč posledica prizadetosti in se kaže kot neugodje, ki izhaja iz nesposobnosti ravnati se po socialnih in ku1turnih normah. S tehničnimi pripomočki prizadetosti ne moremo omiliti ali celo odpraviti, lahko pa zelo zmanjšamo raven hendikepiranosti in odvisnosti invalidne osebe od zunanje pomoči. To lahko pri laže gibalno oviranih dosežemo s preprostejšimi rešitvami, kot so ustrezno oblikovan ročni inva1idski voziček, proteze, ortoze, bergle in hodulje. Osebe, ki v rokah ali nogah ne premorejo dovolj moči ali je zmanjšana njihova koordinacija, ali pa imajo slabo vzdržljivost, potrebujejo za samostojno gibanje električni invalidski voziček. Za

upravljanje v 80 odstotkih primerih zadostuje standardna palica za krmiljenje z roko ali z brado. Med specialne tipe krmilnih naprav uvrščamo naprave za krmiljenje z glavo, s stopalom, s srkanjem in vpihovanjem v cevko, z jezikom in ustnicami, z obračanjem oči, obrazno mimiko, z govorom itn. Z večino krmilnih naprav je mogoče prek uporabniških vmesnikov krmiliti tudi naprave, ki jih uporabljamo v bivalnem okolju. Prav to lastnost izrabljajo za izgradnjo inteligentnih domov, ki so dobili poseben pomen ob razcvetu širokopasovnih spletnih povezav. Taki domovi so tudi izjemno varni, saj se po programiranem času lahko neka naprava samodejno izklopi, kar je koristno, kadar je uporabnik dementna oseba. Žal pa se starejši uporabniki težko sprijaznijo z novimi tehnologijami.

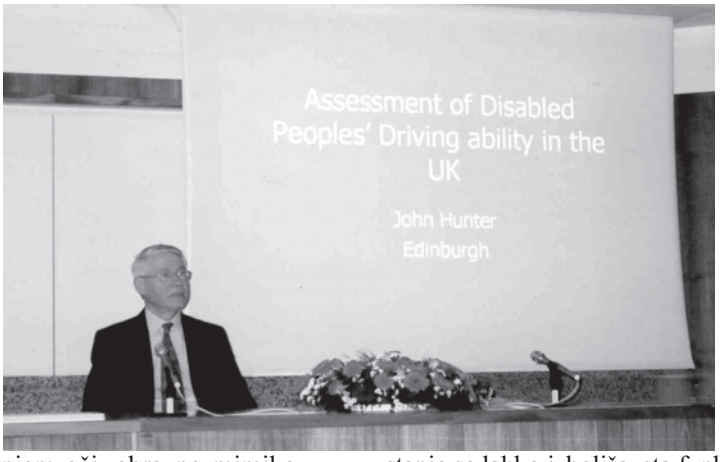

Tudi vožnja avtomobila je z uporabo prilagoditev postala dostopna celo huje gibalno oviranim. Za gibanje naprej je potreben rahel premik ročice nazaj, rahel premik naprej pa za zaviranje. Pomik ročice v levo oz. desno pomeni zavijanje v levo ali desno smer. Za vklop preostalih funkcij zadošča najmanjši gib za dotik gumba zaznavala.

Pomemben del terapije zgornjih okončin določenih pacientov, katerih zdravstveno stanje se lahko izboljša, sta funkcionalna električna stimulacija (FES) in haptični (tipalni) vmesnik. FES je metoda, pri kateri z električnimi impulzi izvabljamo funkcionalno krčenje delno ohromljenih mišic. Haptični vmesnik pa je robotska roka, povezana z računalnikom, ki jo uporabnik premika in s tem izvaja terapijo. Da bi pravilno opravljal vaje in bil motiviran, mora pacient opravljati nalogo, ki jo spremlja na monitorju. To je lahko simulacija gibanja skozi labirint (haptični vmesnik ne dopušča premika roke v smeri skozi stene labirinta), simulacija premikanja žogice iz središča do žogice na obodu in nazaj ali zlaganje sestavljanke.

mag. Dragutin Kelšin

Osebne vesti - Personal Events

Doktorat in diplome - Doctor's and Diploma Degrees

DOKTORAT

Na Fakulteti za strojništvo Univerze v Ljubljani je z uspehom zagovarjal svojo doktorsko disertacijo:

dne *6. aprila 2007*: **Tomaž Kek**, z naslovom: "Lasersko rezanje globoko vlečnega izdelka" (mentorja: prof. dr. Janez Grum, doc. dr. Roman Šturm).

S tem je navedeni kandidat dosegel akademsko stopnjo doktorja znanosti.

DIPLOMIRALI SO

Na Fakulteti za strojništvo Univerze v Ljubljani so pridobili naziv univerzitetni diplomirani inženir strojništva:

dne *25. aprila 2007*: Ivan DOVŽAN, Denis ORAČ, Damjan PAVLIČ, Alenka SAVŠEK, Igor ŠKRBEC, Miha ŠRAJ.

Na Fakulteti za strojništvo Univerze v Mariboru so pridobili naziv univerzitetni diplomirani inženir strojništva:

dne *26. aprila 2007*: Blaž BEZJAK, Amir Đambić, Aleš ELBL, Andrej VASLE.

*

Na Fakulteti za strojništvo Univerze v Ljubljani so pridobili naziv diplomirani inženir strojništva:

dne *12. aprila 2007*: Simon ARH, Matej BAJT, Boštjan DEMŠAR;

dne *16. aprila 2007*: Vinko DREV, Anton MALENŠEK.

Na Fakulteti za strojništvo Univerze v Mariboru so pridobili naziv diplomirani inženir strojništva:

dne *26. aprila 2007*: Andrej BRUMEN, Aleš MRKŠA, Igor NEDELJKO.

Pismo uredništvu - Letter to the Editorial Board

Jure Smrekar - Janez Oman - Brane Širok

Statistični pristop k analizi hladilnih sistemov s hladilnimi stolpi na naravni vlek

Strojniški vestnik 51(2005) 11, 711-723

Z veliko mero spoštovanja do pokojnega prof. dr. Branka Gašperšiča smo se odločili, da bomo odgovorili na njegov komentar, ki ga je v obliki razprave poslal na uredništvo Strojniškega vestnika. Razprava se nanaša na strokovni članek avtorjev: Jure Smrekar - Janez Oman - Brane Širok z naslovom: **Statistični pristop k analizi hladilnih sistemov s hladilnimi stolpi na naravni vlek**, ki je bil objavljen v Strojniškem vestniku.

Ker je bila profesorjeva razprava usmerjena na vsebino stavka: "Dosedanje analize delovanja hladilnih stolpov večinoma temeljijo le na poznavanju parametrov okoliškega zraka ter parametrov vstopne in izstopne hladilne vode", želimo pri odgovoru predvsem pojasniti pomen tega stavka.

Opozorili bi radi, da je v trditvi v stavku uporabljena beseda "večinoma", kar pomeni, da avtorji ne negirajo obstoj drugačnih raziskav in tudi ne raziskav, ki jih je navedel prof. Gašperšič. Pojem se predvsem nanaša na vsebine, predstavljene v člankih, ki so nastajali v zadnjih desetih do petnajstih letih.

Avtorji so v prispevku omenjeni stavek podali v kontekstu uvajanja metode diagnostike lokalnih lastnosti hladilnih stolpov, ki so v obratovanju. Omenjena metoda CPT je bila razvita v okviru Evropskega projekta OCTABAMA in pomeni nadgradnjo znanih metod, ki pri hladilnih stolpih v obratovanju temeljijo predvsem na merjenju integralnih spremenljivk postopka.

Vezano na vire, ki so navedeni v razpravi pa želimo poudariti le to, da nam je žal, da ti viri niso zavedeni v dostopnih bazah, revijah ali zbornikih iz konferenc, tako da z vsebinami teh virov nismo seznanjeni in ne moremo ocenjevati povezanosti teh vsebin z vsebino omenjenega strokovnega članka.

Jure Smrekar
prof. dr. Janez Oman
prof. dr. Brane Širok

Navodila avtorjem - Instructions for Authors

Članki morajo vsebovati:
- naslov, povzetek, besedilo članka in podnaslove slik v slovenskem in angleškem jeziku,
- dvojezične preglednice in slike (diagrami, risbe ali fotografije),
- seznam literature in
- podatke o avtorjih.

Strojniški vestnik izhaja od leta 1992 v dveh jezikih, tj. v slovenščini in angleščini, zato je obvezen prevod v angleščino. Obe besedili morata biti strokovno in jezikovno med seboj usklajeni. Članki naj bodo kratki in naj obsegajo približno 8 strani. Izjemoma so strokovni članki, na željo avtorja, lahko tudi samo v slovenščini, vsebovati pa morajo angleški povzetek.

Za članke iz tujine (v primeru, da so vsi avtorji tujci) morajo prevod v slovenščino priskrbeti avtorji. Prevajanje lahko proti plačilu organizira uredništvo. Če je članek ocenjen kot znanstveni, je lahko objavljen tudi samo v angleščini s slovenskim povzetkom, ki ga pripravi uredništvo.

VSEBINA ČLANKA

Članek naj bo napisan v naslednji obliki:
- Naslov, ki primerno opisuje vsebino članka.
- Povzetek, ki naj bo skrajšana oblika članka in naj ne presega 250 besed. Povzetek mora vsebovati osnove, jedro in cilje raziskave, uporabljeno metodologijo dela,povzetek rezulatov in osnovne sklepe.
- Uvod, v katerem naj bo pregled novejšega stanja in zadostne informacije za razumevanje ter pregled rezultatov dela, predstavljenih v članku.
- Teorija.
- Eksperimentalni del, ki naj vsebuje podatke o postavitvi preskusa in metode, uporabljene pri pridobitvi rezultatov.
- Rezultati, ki naj bodo jasno prikazani, po potrebi v obliki slik in preglednic.
- Razprava, v kateri naj bodo prikazane povezave in posplošitve, uporabljene za pridobitev rezultatov. Prikazana naj bo tudi pomembnost rezultatov in primerjava s poprej objavljenimi deli. (Zaradi narave posameznih raziskav so lahko rezultati in razprava, za jasnost in preprostejše bralčevo razumevanje, združeni v eno poglavje.)
- Sklepi, v katerih naj bo prikazan en ali več sklepov, ki izhajajo iz rezultatov in razprave.
- Literatura, ki mora biti v besedilu oštevilčena zaporedno in označena z oglatimi oklepaji [1] ter na koncu članka zbrana v seznamu literature. Vse opombe naj bodo označene z uporabo dvignjene številke[1].

OBLIKA ČLANKA

Besedilo članka naj bo pripravljeno v urejevalnilku Microsoft Word. Članek nam dostavite v elektronski obliki.

Ne uporabljajte urejevalnika LaTeX, saj program, s katerim pripravljamo Strojniški vestnik, ne uporablja njegovega formata.

Enačbe naj bodo v besedilu postavljene v ločene vrstice in na desnem robu označene s tekočo številko v okroglih oklepajih

Papers submitted for publication should comprise:
- Title, Abstract, Main Body of Text and Figure Captions in Slovene and English,
- Bilingual Tables and Figures (graphs, drawings or photographs),
- List of references and
- Information about the authors.

Since 1992, the Journal of Mechanical Engineering has been published bilingually, in Slovenian and English. The two texts must be compatible both in terms of technical content and language. Papers should be as short as possible and should on average comprise 8 pages. In exceptional cases, at the request of the authors, speciality papers may be written only in Slovene, but must include an English abstract.

For papers from abroad (in case that none of authors is Slovene) authors should provide Slovenian translation. Translation could be organised by editorial, but the authors have to pay for it. If the paper is reviewed as scientific, it can be published only in English language with Slovenian abstract, that is prepared by the editorial board.

THE FORMAT OF THE PAPER

The paper should be written in the following format:
- A Title, which adequately describes the content of the paper.
- An Abstract, which should be viewed as a mini version of the paper and should not exceed 250 words. The Abstract should state the principal objectives and the scope of the investigation, the methodology employed, summarize the results and state the principal conclusions.
- An Introduction, which should provide a review of recent literature and sufficient background information to allow the results of the paper to be understood and evaluated.
- A Theory
- An Experimental section, which should provide details of the experimental set-up and the methods used for obtaining the results.
- A Results section, which should clearly and concisely present the data using figures and tables where appropriate.
- A Discussion section, which should describe the relationships and generalisations shown by the results and discuss the significance of the results making comparisons with previously published work. (Because of the nature of some studies it may be appropriate to combine the Results and Discussion sections into a single section to improve the clarity and make it easier for the reader.)
- Conclusions, which should present one or more conclusions that have been drawn from the results and subsequent discussion.
- References, which must be numbered consecutively in the text using square brackets [1] and collected together in a reference list at the end of the paper. Any footnotes should be indicated by the use of a superscript[1].

THE LAYOUT OF THE TEXT

Texts should be written in Microsoft Word format. Paper must be submitted in electronic version.

Do not use a LaTeX text editor, since this is not compatible with the publishing procedure of the Journal of Mechanical Engineering.

Equations should be on a separate line in the main body of the text and marked on the right-hand side of the page with numbers in round brackets.

Enote in okrajšave

V besedilu, preglednicah in slikah uporabljajte le standardne označbe in okrajšave SI. Simbole fizikalnih veličin v besedilu pišite poševno (kurzivno), (npr. *v, T, n* itn.). Simbole enot, ki sestojijo iz črk, pa pokončno (npr. ms^{-1}, K, min, mm itn.).

Vse okrajšave naj bodo, ko se prvič pojavijo, napisane v celoti v slovenskem jeziku, npr. časovno spremenljiva geometrija (ČSG).

Slike

Slike morajo biti zaporedno oštevilčene in označene, v besedilu in podnaslovu, kot sl. 1, sl. 2 itn. Posnete naj bodo v ločljivosti, primerni za tisk, v kateremkoli od razširjenih formatov, npr. BMP, JPG, GIF. Diagrami in risbe morajo biti pripravljeni v vektorskem formatu, npr. CDR, AI.

Pri označevanju osi v diagramih, kadar je le mogoče, uporabite označbe veličin (npr. *t, v, m* itn.), da ni potrebno dvojezično označevanje. V diagramih z več krivuljami, mora biti vsaka krivulja označena. Pomen oznake mora biti pojasnjen v podnapisu slike.

Vse označbe na slikah morajo biti dvojezične.

Preglednice

Preglednice morajo biti zaporedno oštevilčene in označene, v besedilu in podnaslovu, kot preglednica 1, preglednica 2 itn. V preglednicah ne uporabljajte izpisanih imen veličin, ampak samo ustrezne simbole, da se izognemo dvojezični podvojitvi imen. K fizikalnim veličinam, npr. *t* (pisano poševno), pripišite enote (pisano pokončno) v novo vrsto brez oklepajev.

Vsi podnaslovi preglednic morajo biti dvojezični.

Seznam literature

Vsa literatura mora biti navedena v seznamu na koncu članka v prikazani obliki po vrsti za revije, zbornike in knjige:

[1] A. Wagner, I. Bajsić, M. Fajdiga (2004) Measurement of the surface-temperature field in a fog lamp using resistance-based temperature detectors, *Stroj. vestn.* 2(2004), pp. 72-79.

[2] Vesenjak, M., Ren Z. (2003) Dinamična simulacija deformiranja cestne varnostne ograje pri naletu vozila. *Kuhljevi dnevi '03*, Zreče, 25.-26. september 2003.

[3] Muhs, D. et al. (2003) Roloff/Matek Maschinenelemente – Tabellen, 16. Auflage. *Vieweg Verlag*, Wiesbaden.

SPREJEM ČLANKOV IN AVTORSKE PRAVICE

Uredništvo Strojniškega vestnika si pridržuje pravico do odločanja o sprejemu članka za objavo, strokovno oceno recenzentov in morebitnem predlogu za krajšanje ali izpopolnitev ter terminološke in jezikovne korekture.

Avtor mora predložiti pisno izjavo, da je besedilo njegovo izvirno delo in ni bilo v dani obliki še nikjer objavljeno. Z objavo preidejo avtorske pravice na Strojniški vestnik. Pri morebitnih kasnejših objavah mora biti SV naveden kot vir.

PLAČILO OBJAVE

Avtorji vseh prispevkov morajo za objavo plačati prispevek v višini 20,00 EUR na stiskano stran prispevka. Prispevek se zaračuna po sprejemu članka za objavo na seji Uredniškega odbora.

Units and abbreviations

Only standard SI symbols and abbreviations should be used in the text, tables and figures. Symbols for physical quantities in the text should be written in italics (e.g. *v, T, n,* etc.). Symbols for units that consist of letters should be in plain text (e.g. ms^{-1}, K, min, mm, etc.).

All abbreviations should be spelt out in full on first appearance, e.g., variable time geometry (VTG).

Figures

Figures must be cited in consecutive numerical order in the text and referred to in both the text and the caption as Fig. 1, Fig. 2, etc. Pictures may be saved in resolution good enough for printing in any common format, e.g. BMP, GIF, JPG. However, graphs and line drawings sholud be prepared as vector images, e.g. CDR, AI.

When labelling axes, physical quantities, e.g. *t, v, m,* etc. should be used whenever possible to minimise the need to label the axes in two languages. Multi-curve graphs should have individual curves marked with a symbol, the meaning of the symbol should be explained in the figure caption.

All figure captions must be bilingual.

Tables

Tables must be cited in consecutive numerical order in the text and referred to in both the text and the caption as Table 1, Table 2, etc. The use of names for quantities in tables should be avoided if possible: corresponding symbols are preferred to minimise the need to use both Slovenian and English names. In addition to the physical quantity, e.g. *t* (in italics), units (normal text), should be added in new line without brackets.

All table captions must be bilingual.

The list of references

References should be collected at the end of the paper in the following styles for journals, proceedings and books, respectively:

[1] A. Wagner, I. Bajsić, M. Fajdiga (2004) Measurement of the surface-temperature field in a fog lamp using resistance-based temperature detectors, *Stroj. vestn.* 2(2004), pp. 72-79.

[2] Vesenjak, M., Ren Z. (2003) Dinamična simulacija deformiranja cestne varnostne ograje pri naletu vozila. *Kuhljevi dnevi '03*, Zreče, 25.-26. september 2003.

[3] Muhs, D. et al. (2003) Roloff/Matek Maschinenelemente – Tabellen, 16. Auflage. *Vieweg Verlag*, Wiesbaden.

ACCEPTANCE OF PAPERS AND COPYRIGHT

The Editorial Committee of the Journal of Mechanical Engineering reserves the right to decide whether a paper is acceptable for publication, obtain professional reviews for submitted papers, and if necessary, require changes to the content, length or language.

Authors must also enclose a written statement that the paper is original unpublished work, and not under consideration for publication elsewhere. On publication, copyright for the paper shall pass to the Journal of Mechanical Engineering. The JME must be stated as a source in all later publications.

PUBLICATION FEE

For all papers authors will be asked to pay a publication fee prior to the paper appearing in the journal. However, this fee only needs to be paid after the paper is accepted by the Editorial Board. The fee is €20.00 per printed paper page.